Distribution Agreement

In presenting this thesis or dissertation as a partial fulfillment of the requirements for an advanced degree from Emory University, I hereby grant to Emory University and its agents the non-exclusive license to archive, make accessible, and display my thesis or dissertation in whole or in part in all forms of media, now or hereafter known, including display on the world wide web. I understand that I may select some access restrictions as part of the online submission of this thesis or dissertation. I retain all ownership rights to the copyright of the thesis or dissertation. I also retain the right to use in future works (such as articles or books) all or part of this thesis or dissertation.

Signature:

_____ _____

Kara L. Phipps Date

Reassortment Potential and Coinfection Dependence of Influenza A Virus is Determined through Collective Virus-Virus and Virus-Host Interactions

By
Kara L. Phipps
Doctor of Philosophy

Graduate Division of Biological and Biomedical Sciences
Microbiology and Molecular Genetics

_____
Anice Lowen, Ph.D.
Advisor

_____
Richard Compans, Ph.D.
Committee Member

_____
Eric Hunter, Ph.D.
Committee Member

_____
William Shafer, Ph.D.
Committee Member

_____
David Steinhauer, Ph.D.
Committee Member

_____
Terrence Tumpey, Ph.D.
Committee Member

Accepted:

_____
Lisa A. Tedesco, Ph.D.
Dean of the James T. Laney School of Graduate Studies

_____
Date

Reassortment Potential and Coinfection Dependence of Influenza A Virus is Determined through Collective Virus-Virus and Virus-Host Interactions

By

Kara L. Phipps
B.S., Southwest Baptist University, 2014

Advisor
Anice Lowen, Ph.D.

An abstract submitted to the Faculty of the
James T. Laney School of Graduate Studies of Emory University
in partial fulfillment of the requirements for the degree of
Doctor of Philosophy
in the Graduate Division of Biological and Biomedical Sciences
in Microbiology and Molecular Genetics
2019

Abstract

Reassortment Potential and Coinfection Dependence of Influenza A Virus is Determined through Collective Virus-Virus and Virus-Host Interactions

By
Kara L. Phipps

Influenza A virus (IAV) poses a significant threat to public health due to its constant evolution. IAVs diversify through the mutations produced by the error prone viral polymerase and gene reassortment, which occurs when two viruses co-infect the same cell and exchange gene segments. Collective interactions among coinfecting IAVs have been observed to increase genotypic diversity and productivity. However, the factors which constrain or enhance collective IAV interactions and genetic diversity potential are incompletely characterized. Segment mismatch refers to incompatibilities among gene segments and is predicted to constrain genetic diversity arising from heterologous IAV coinfections. To better understand how segment mismatch may constrain genetic exchange, this study evaluates the potential for reassortment of heterologous, representative strains of pandemic H1N1 (pH1N1) and seasonal H3N2 lineages. Results of heterologous co-infections were compared to those obtained from co-infection with homologous, genetically tagged, pH1N1 viruses. Reassortment was abundant for both, but biases for particular gene pairings were observed with heterologous IAVs. The impact of these preferences was investigated by measuring correlates of replication and viral fitness. Transmission of pH1N1/H3N2 reassortant genotypes between guinea pigs was detected, but parental H3N2 viruses dominated *in vivo*. Segment mismatch among pH1N1 and H3N2 viruses likely impact potential reassortment outcomes to constrain IAV diversification. The second study further investigates the factors which impact collective interactions among IAVs. Reassortment frequency was quantified for a panel of IAVs in multiple cell lines and relevant animal models. Dependence on IAV coinfection was found to vary with virus strain and host. The abundance of incomplete viral genomes only partially explained coinfection dependence. Rather, additional RNA quantification and viral productivity measurements revealed that viral replication is augmented by collective virus-virus interactions in a cooperative, host dependent manner. The viral polymerase was identified as the major determinant of the observed degree of reliance on coinfection. These studies together highlight the prevalence and importance of virus-virus and virus-host interactions in determining the potential for viral diversification through IAV coinfection. This work furthers our understanding of the constraints acting on IAV genetic diversification and establishes newfound importance for collective interactions in the IAV life cycle.

Reassortment Potential and Coinfection Dependence of Influenza A Virus is Determined through Collective Virus-Virus and Virus-Host Interactions

By

Kara L. Phipps
B.S., Southwest Baptist University, 2014

Advisor
Anice Lowen, Ph.D.

A dissertation submitted to the Faculty of the
James T. Laney School of Graduate Studies of Emory University
in partial fulfillment of the requirements for the degree of
Doctor of Philosophy
in the Graduate Division of Biological and Biomedical Sciences
in Microbiology and Molecular Genetics
2019

Acknowledgements

I would like to thank:

- Anice Lowen, for being a supportive mentor and leading by example in dedication and excellence.

- Ketaki Ganti, for countless conversations about science and our own beloved pets.

- The current and past Lowen Lab members: Kate Holmes, Gabrielle Delima, Meg Hockman, Nate Jacobs, Maria White, Chung-Young Lee, Camden Bair, Courtney Steger, Hui Tao, Shamika Danzy-Bedoya, and Nicolle Marshall. All have been excellent colleagues and friends.

- My family and friends at Intown Community Church and Blueprint Church, for the multitude of ways they have supported my growth as an individual throughout graduate school. Special thanks to Megan Iwan and Jason Kang for encouraging me to believe in myself and to persevere through the hardest seasons.

- My family, especially my parents, Buddy and Tammy Phipps, for their steady love and encouragement.

Table of Contents

List of Figures and Tables

Authorship Contributions

I co-first authored the publication in chapter two, which was published in *Journal of Virology* in June of 2017. I contributed by means of experimentation by generating and characterizing virus stocks and performing the heterologous single and multicycle coinfections. Data from these experiments are featured in Figures 1, 4, 5, and 6. I also measured the viral growth in parental and reassortant viruses (Figure 8). I performed data analysis for Figures 1, 7, and 8 and wrote the abstract, introduction, and methods sections of the manuscript.

I am the first author on the manuscript in chapter three. I contributed to project development, experimental design, data collection, interpretation, statistical analyses. I performed the *in vitro* coinfections and measured reassortment levels as displayed in Figure 1 A-D. I assayed viral growth and determined burst size of all viruses shown in Figure 2. I generated chimeric viruses, performed coinfections, and produced the majority of the reassortment data plotted in Figure 3. I designed the experiments and generated all data and performed statistical analyses for Figures 4-5. I designed, produced, and characterized the viruses used in Figure 6. I also generated all data in Figure 7. I wrote the original draft of the entire manuscript and participated in editing and review of the final draft.

Chapter I. Introduction

Overview

Influenza A virus (IAV) poses a significant threat to public health due to its ability to cause recurring, widespread disease. Viral evolution enables seasonal IAV strains to evade pre-existing immunity and assists in adaptation of non-human IAVs to allow transmission of novel strains in humans. Due to its segmented RNA genome, influenza viruses can diversify by two major modalities: mutation and reassortment [1-3]. Mutation produces small changes to viral genes, as dictated by the error rate of the viral polymerase. Reassortment occurs when multiple viruses infect the same cell and exchange genes and results in the formation of novel gene constellations which differ from either parental virus [4]. Incompatibilities among gene segments at the RNA or protein level are known as "segment mismatch" and are important in determining the overall genetic diversity which may be produced from a reassortment event [5]. While viral diversity exists within the two IAV subtypes which currently circulate in humans, a much greater number of subtypes circulate in non-human hosts, with wild waterfowl being the primary reservoir [6, 7]. Hosts at the human-animal interface, such as poultry and swine, pose a risk for the introduction, adaptation, and transmission of novel IAVs in humans [8-11]. Pandemics occur when a novel strain achieves sustained human-to-human transmission on a global scale. While pandemic events have great consequences, their occurrences are relatively rare due to host differences which present barriers to replication and transmission [9, 12, 13]. Further studies of the factors which contribute to viral diversification and host adaptation among IAVs are needed to achieve a greater understanding of the circumstances which lead to the emergence of epidemic and pandemic strains. Collective interactions among coinfecting viruses, of which reassortment is one type, have been observed to alter infection dynamics and viral diversity. A number of

studies support a role for collective interactions among IAVs to yield productive infection [14-18]. However, the conditions which dictate the prevalence and degree of reliance on collective interactions are currently unknown.

This work identifies constraints of genotypic diversification by demonstrating the impact of segment mismatch on the reassortment potential and fitness of reassortant genotypes arising from heterologous coinfection with divergent IAV subtypes. The second study reveals that IAVs exhibit a dependence on collective interactions which varies with virus strain and host and identifies the viral polymerase as a major determinant of coinfection dependence and viral diversification. These new insights underline the importance of virus-virus as well as virus-host interactions in determining the potential for viral diversification through coinfection. This work provides a greater understanding of the constraints acting on IAV diversification and will be useful for future evolutionary and molecular studies and could inform more accurate estimation of the evolutionary capacity of IAVs [15-18].

Influenza as a significant threat to public health

Influenza viruses pose a threat to public health due to their ability to evolve to adapt to new hosts and evade pre-existing immunity. IAVs are a subset of the viruses belonging to the family *Orthomyxoviridae* which contains segmented, negative sense RNA viruses. Four types of influenza viruses have been identified: A, B, C, and D [19, 20]. Influenza A virus (IAV) and influenza B viruses (IBV) circulate seasonally in humans and cause a significant disease burden. Influenza C virus (ICV) infection is primarily limited to children and causes only mild disease [2]. Though influenza D virus (IDV) has demonstrated the capacity to replicate in a human culture system, detection of IDV infection has been limited to bovine and porcine hosts, and thus, the virus is not a considered a major threat to humans [19, 21]. IBVs are largely limited to

infection in humans [11, 22]. IBVs can be further classified by whether they originate from the Victoria or Yamagata lineage [2]. Of the influenza virus types, IAVs are responsible for the greatest disease burden in humans. IAVs occupy a wide range of hosts and thus can cause occasional pandemics in addition to seasonal disease [9, 23]. IAVs are further classified by subtypes, which are referred to by the identity of the viral surface glycoproteins, hemagglutinin (HA) and neuraminidase (NA). 18 different HA types and 11 different NA types have been identified, but only two subtypes, H1N1 and H3N2, currently circulate in humans [6, 7, 24-26].

Evolution of IAVs includes both antigenic drift and genetic shift. Antigentic drift refers to gradual changes due to selection on mutations produced by the error prone viral polymerase. The viral HA is the major antigenic target and can explore a relatively wide sequence range; and evolution of this protein is the primary reason for seasonal immune escape [27-29]. Genetic shift is accomplished through gene reassortment, which occurs when multiple influenza viruses of the same type coinfect the same cell in the same host and exchange gene segments. Genetic shift can result in the incorporation of a novel HA subtype, but the incorporation of other gene segments may also result in significant advances in other important properties, such as replication and antiviral resistance [30-32]. Viral evolution through both antigenic drift and genetic shift contributes to re-emergence and seasonal epidemics and necessitates constant surveillance and annual vaccine reformulation [26]. Current antiviral therapies include neuraminidase inhibitors and adamantanes. These treatments have limited utility as antiviral resistance to adamantanes has become widespread and neuraminadase inhibitors possess a short time window of efficacy, even when the viral strain is susceptible [31]. In addition to the burden of seasonal influenza, antigenically novel IAV strains from non-human hosts can occasionally lead to pandemics. Global spread of novel IAVs in humans occurred in 1918, 1957, 1968, and most recently in

2009. The 1918 pandemic strain is suggested to have originated from the host species crossover of an avian strain, however, it is unclear whether it was directly transmitted to humans or through an intermediate mammalian host [33-35]. The 1918 strain continued to circulate as a seasonal H1N1 lineage until it incorporated three genes from an avian IAV strain and formed a novel H2N2 strain which gave rise to another pandemic in 1957. A similar event occurred in 1968 when reassortment with an avian IAV produced a novel H3N2 strain [36, 37]. The seasonal H1N1 lineage reemerged in the human population in 1977 and began cocirculating seasonally along with the H3N2 subtype [38-40]. The most recent pandemic occurred in 2009 when an H1N1 subtype containing genes from human, avian, and swine IAVs spread among the human population. This new H1N1 replaced the seasonal H1N1 lineage [4, 41]. Given than IAVs exhibit seasonal emergence of vaccine escape, the potential for zoonoses, and treatment options are limited, there is a need for research which can improve our understanding of how IAV evolves.

Influenza A virus host range

Influenza viruses occupy a wide host range, including both avian and mammalian species. This broad range supports substantial viral genetic diversity and provides opportunity for host-species transfers. While only two IAV subtypes, H1N1 and H3N2, currently circulate in humans, other host species harbor multiple subtypes [2]. Nearly all IAV subtypes can be found in wild waterfowl, such as ducks and geese, which comprise the primary reservoir of IAV [6, 7]. Stable lineages of IAV also circulate in human, swine, horses, dogs, and bats [10, 11, 25]. Occasionally, IAVs exhibit the ability to overcome host restriction to infect non-native hosts. The precise frequency of IAV cross-species transfers is unknown, however, transfer events involving wild birds, poultry, swine, horses, dogs, and humans have been reported [11, 42, 43]. Spillover IAV

transfer from wild birds into poultry has facilitated the establishment of IAV in domestic bird populations and zoonoses, and while uncommon, have been observed with avian IAVs H5N1, H7N9, and H9N2 [44-46]. These human-avian zoonoses present heightened concern for the occurrence of future pandemics because if sufficient host adaptation occurs, as may happen through mutation or reassortment between human and non-human IAV strains, the criteria for a pandemic strain will be met.

Influenza A virus life cycle

Viral infection, by definition, is a coordinated process involving viral and host factors. Though much is known about the identity and nature of host interactions, IAV viral-host interactions are incompletely characterized. The first stage of the viral life cycle begins with attachment of the viral surface glycoprotein, HA, to sialic acid on the host cell surface. Tropism varies between humans and avian species [47, 48]. The primary site of infection in humans is in the upper respiratory tract, while the gastrointestinal tract serves as the major site of replication in birds [48]. The affinity and specificity of avian and human IAVs often differs by the identity of terminal sialic acid structure. Avian IAVs typically favor a α2,3 linkage to galactose; human IAVs frequently exhibit a preference for α2, 6 linkages [47]. Human adapted IAVs often acquire mutations which enable them to better utilize α2,6 linked sialic acids [13] [49]. Following receptor binding, the virion is endocytosed. In the early endosome, pH changes result in acidification of the viral capsid through the M2 ion channel. Acidification causes the release of the viral genome from the outer layer of the viral capsid, which is comprised of the viral matrix protein, M1 [50, 51]. In the late endosome, further reduction in internal pH results in a conformational change in HA, which triggers the fusion of viral and endosomal membranes [52, 53]. Following fusion, viral genes, are released into the cytoplasm [54]. Each viral RNA gene

segment is associated with multiple nucleoprotein (NP) monomers. Electrostatic interactions among NP proteins lead to vRNPs adopting a coiled structure with the terminii forming a panhandle like structure [55]. Conservation of 3' and 5' terminii enables base pairing of the viral promoter, which is associated with a heterotrimeric viral polymerase, comprised of viral proteins PB2, PB1 and PA [56, 57]. These components: viral RNA, NP, and the viral polymerase comprise each viral nucleoprotein (vRNP) [58]. Many host factors have been identified as being able to bind vRNPs, but despite this, little is known about how the coordination of the passage of vRNPs through the cytoplasm [59-61]. Entry of vRNPs into the nucleus is an active process for vRNPs, which must partner with cellular importins [62, 63].

Viral transcription and replication take place in the nucleus and the regulation of these processes is still poorly understood. Primary transcription begins with the action of the "*cis*" or "resident" polymerase which is associated with the vRNP upon entry. During transcription, IAVs exploit cellular mRNAs to perform cap snatching. Association of the viral polymerase with cellular RNA polymerase II at its C terminal domain brings the viral polymerase close to cellular RNAs which the PB2 protein then binds. The PA subunit functions as an endonuclease and cleaves mRNAs just downstream of the 5' cap following binding [64, 65]. The short, capped RNAs are then used as primers for viral mRNA transcription by the PB1 subunit, which catalyzes the synthesis of RNAs. Upon reaching the poly-uracil stretch near the 5' end of the vRNA, the polymerase stutters to produce a poly-A tail [66]. Two viral mRNAs, M and NS, undergo additional modifications and are spliced via cellular proteins in the nucleus [67, 68]. The spliced form of M produces the M2 mRNA. The NS transcript is spliced to produce either the nuclear export protein, NEP, or NS1, which participates in many functions, but is primarily known as an interferon antagonist [69]. Viral mRNAs are exported to the cytoplasm where they

are translated by cellular ribosomes. Nuclear localization signals are found on M1 and NEP, as well as the proteins which contribute to vRNPs (PB2, PB1, PA, and NP), and direct the newly formed proteins back to the nucleus where they can further contribute to the replication cycle [70-73].

The mechanism or mechanism(s) which control the transition of the viral polymerase action from transcription to genomic replication are not well understood. As a negative sense virus, IAVs must generate an intermediate template which is complementary to the viral RNA. This complementary RNA (cRNA) is needed as an antisense template for the production negative sense, genomic RNAs. Unlike transcription, replication is a primer independent process. The *cis* polymerase initiates replication at the 3' end of the viral RNA and synthesizes the anti-sense copy. The cRNA copy of a gene differs from mRNA in that it does not contain a 5' cap and does include the 5' UTR. cRNAs associate with NP and form a double helical structure similar to that of genomic vRNPs [74-76]. A number of mechanisms have been proposed to mediate the switch between mRNA and cRNA production. The relative proportions of viral RNA species (vRNA, mRNA, and cRNA), accumulation of NP, and the production of short viral RNAs that resemble the vRNA termini have all been implicated in the control of cRNA or vRNA synthesis [77-80]. In addition to interactions among viral RNAs and viral proteins, a number of host factors have also been implicated in regulation of viral transcription and replication [81]. The presence of a newly synthesized, or "*trans*" polymerase, is required for the synthesis of vRNA from cRNA [82, 83]. This new polymerase does not need to be catalytically active in order for vRNA synthesis to occur, which indicates it may be "*trans*-activating" rather than *trans*-acting [74]. The host factors, ANP32A and ANP32B, promote replication of the vRNA from cRNA through molecular interactions involving PB2 [84, 85]. The genomic viral RNAs associate with NP

monomers during replication and the addition of a polymerase complex produces a new vRNP complex [66, 78].

vRNPs are bound by M1 and NEP and exported from the nucleus via the Crm1 pathway [86, 87]. Once in the cytoplasm, the GTP-ase Rab11 is able to interact with RNPs and direct their transport by recycling endosomes to the apical cell surface [88, 89]. Genome packaging for IAV has been determined to be a selective process involving terminal regions of each gene segment [90-92]. The precise details regarding the location and identity of these packaging signals is a major area of study and current literature supports that selective packaging is mediated by RNA-RNA interactions among segments [5, 93, 94]. Indeed, electron microscopy studies have indicated that the full complement of viral genes is packaged with >90% fidelity [95]. Fluorescent labeling of vRNPs leaving the nucleus indicates that vRNPs become organized and associate during transit from the nucleus [90, 96]. HA, NA, and M2 proteins traverse the Golgi complex where they are modified before being targeted to the cell surface [97-101]. Once at the cell surface, HA and NA bind to M1 proteins, which are associated with vRNPs. Viral proteins HA, NA, M1, and M2 are implicated in viral budding [102-105]. M2 concentrates at the neck of budding virions and mediates scission [106]. Release from the host cell is facilitated by the receptor destroying enzyme, NA, which cleaves sialic acids on the cell surface and frees the virion from the cell surface [107-109].

Evolution of influenza A viruses

Influenza virus evolution occurs through selection of mutations which arise from the action of the error prone viral polymerase, as well as gene reassortment [4]. RNA viruses possess a high mutation rate due to their lack of proofreading ability. Estimation for the mutation rate of IAV predicts 2-3 mutations will arise per genome [66, 110]. Reassortment can generate rapid changes

in the viral genome, allow coupling of advantageous mutations, and lead to the loss of deleterious mutations within a gene constellation [32]. In the field, reassortment has been seen to facilitate the spread of antiviral resistance and the production of novel epidemic strains [30, 31, 111]. Reassortment between viruses adapted to different host species can give rise to chimeric viruses with increased potential for cross-species transfer due to combination of novel and human-adapted components in a single genotype. This mechanism underlied the emergence of the 1957, 1968, and 2009 pandemic strains, which carried genes from IAVs adapted to human and non-human hosts [12, 13].

Segment mismatch

While reassortment between two distinct IAVs results in 256 theoretical genotype combinations, reassortment potential between divergent strains can be limited by negative epistatic interactions of physical and functional properties of gene segments which have not coevolved [112]. This phenomenon is broadly known as “segment mismatch” and may occur at the RNA or protein level. RNA level mismatches are mainly attributed to differences in RNA-RNA interactions among segments during assembly [91, 94, 113, 114]. Mismatch at this level results in preferential packaging of segments and limits the number of potential genotypes [5, 113, 115]. Protein-level mismatches refer to functional incompatibilities and can result in reduction of viral fitness. Protein mismatch has been documented for the two major viral surface proteins, HA and NA, as well as viral polymerase components. Introduction of HA and NA from divergent strains by reassortment can lead to suboptimal HA and NA cooperativity and projects poor fitness. Because HA binds cellular sialic acids for viral entry while NA cleaves sialic acids to allow release upon viral budding, imbalance in HA binding and NA cleavage can lead to poor viral attachment or, alternatively, inefficient release during viral budding and thus has been shown to

result in virus attenuation [116, 117]. The viral polymerase, comprised of proteins from PB1, PB2, and PA gene segments, presents another opportunity for protein incompatibilities. Previous studies have suggested polymerase component mismatch would lead to a limitation of reassortment outcomes or attenuation of progeny [118]. The sources and degree to which segment mismatch limits reassortment potential are an important aspect of predicting whether an epidemiologically significant strain may be formed. For example, H5Nx and H7N9 viruses have produced sporadic infections from spillover transmission of the virus to humans [45, 119]. If either of these HA subtypes became adapted to replication in humans, the strain would be a high risk for pandemic potential. In a recent paper by White et al., divergence in RNA packaging signals demonstrated that the incorporation of the HA of H5 and H7 subtypes into a human H3N2 background is disfavored by RNA packaging signal mismatch [93]. Segment mismatch among viral gene segments or viral proteins is also important in determining viral diversity which may be produced from a coinfection as the number of viable gene constellations can be significantly reduced by negative epistasis. For instance, if only two segments from divergent IAVs exhibit strong mismatch, the theoretical number of 256 different genotypes which may be expected to arise out of a coinfection will be reduced by half to 128 potential genotypes. Thus, identification of the sources of segment mismatch as well as the degree to which such incompatibilities impact viral fitness is important when considering reassortment potential of divergent IAVs.

Collective interactions among viruses

Collective interactions are an important aspect to consider for understanding and predicting viral infection outcomes. The term “collective interactions” used here broadly defines interactions which occur among viruses and viral components when viruses concurrently infect the same cell

and impact the viral life cycle in an appreciable way. Collective interactions among viruses are diverse and may lead to differences in viral production, kinetics, and genetic diversity [120-122]. Viruses may be helper dependent, meaning they are reliant on collective interactions to complete their viral life cycle. Another form of dependence on coinfection can be found in viruses that require multiple infection for viral production. Examples of coinfection dependent viruses are found in both animal and plant kingdoms [122]. For instance, Hepatitis D virus is dependent on coinfection with Hepatitis B virus to enable viral budding [123]. Multiple virus families, which are mainly found in plants, package their genes in separate virions, and coinfection is required for the full genome to be delivered [1]. Viruses can exhibit competitive collective interactions. One such example is superinfection exclusion, which occurs when the presence of an initial virus reduces the likelihood of a subsequent infection with a similar virus. Superinfection exclusion may result from indirect changes to the host cell upon infection or through the direct action of a virus, such the bacteriophage P1 sim protein which interferes with nucleic acid injection of a superinfecting phage [122, 124]. The propagation of interfering (DI) particles is also a form of collective interaction. Examples of defective viral genomes are found in positive and negative sense RNA viruses, though their existence was first discovered in IAVs [125-127]. Defective genes contain internal deletions or other major errors which prevent function, and thus, their replication depends on complementation by a replication competent virus.

A wide range of viruses utilize various strategies to facilitate high multiplicity, localized infection [121]. Cell-to-cell spread, either by the fusion of adjacent cells or intercellular connections, has been observed for HIV, Measles virus, respiratory syncytial virus, parainfluenza viruses, and influenza viruses, among others [120, 121, 128]. The delivery of multiple viruses via extracellular vesicles has been reported for enteroviruses, noroviruses, and rotatviruses [121,

129]. Aggregates of viruses, either formed by clustering of the viruses alone or attachment to a bacterial surface, also facilitate high multiplicity of infection [130]. The number of mechanisms and taxa of viruses which facilitate the spread of collective units of virus points to potential advantages for coinfection and relevance for future studies.

Studies have shown multiplicity of infection (MOI) can affect the kinetics, efficiency, and diversity arising from viral infections. Dose dependent cooperation was observed with vesicular stomatitis virus (VSV): transcription and replication levels were enhanced with increasing multiplicity of infection [131]. Faster kinetics of viral production were seen with high MOI infection of polio virus [121]. Similarly, increasing the MOI of an H3N2 IAV strain *in vitro* revealed that increasing MOI led to faster replication kinetics [18]. Increasing the MOI of HIV *in vitro* was found to lead to earlier viral gene production [120]. Plaque formation, in some cases, can be aided by co-infection [132]. There is also evidence that cooperation can occur at the protein level in IAVs as transfecting in viral proteins can rescue the function of a temperature sensitive mutant under non-permissive conditions [133]. Indeed, the practice of supplying IAV proteins in *trans* is commonly employed to enhance virus production from IAV rescue [134-136]. Vaccinia virus exhibits enhanced infectivity when secondary infection occurs in cells which are already expressing viral proteins [137]. Coinfection of multiple variants can also enhance genetic diversification as it provides opportunity for recombination [138]. Overall, these observations indicate that collective interactions among co-infecting viral particles can impact key properties of infection of many viruses.

Coinfection dependence among influenza viruses

Multiple studies have provided evidence that IAV particles frequently rely on collective interactions for productive infection to occur, though concerted efforts to understand how MOI

impacts IAV infection are currently lacking. Under low multiplicity conditions, IAVs often express only a subset of the viral proteins, as detected by flow cytometry [17]. In contrast, under high multiplicity conditions, all assayed viral proteins are readily detectable. When cells extracted from infected animals were probed for viral proteins, they likewise showed that not all infected cells contained detectable levels of each viral protein [16, 17]. Fonville et al. provided additional support for a requirement of multiple infection for productive IAV infection through experimental and computational studies. A computational simulation of IAV coinfection was used to predict reassortment levels given the assumption that each viral particle led to a productive infection and all infected cells produced equivalent numbers of viral progeny. Experimental data from an *in vitro* coinfection revealed that reassortment and coinfection levels were much higher than predicted by the simulation and indicated that progeny production is concentrated in coinfected cells [15]. Building on this study, Jacobs et al. found by careful analysis of IAV production at the single-cell level that IAV particles often fail to replicate the full viral genome [18]. Therefore, productive infection of IAV often required genetic complementation through co-infection. Kaverin et al. also indicated that coinfection could boost viral production by the observing that greater numbers of plaque forming units (PFU) were recoverable from cells coinfected with a temperature sensitive virus at a nonpermissible temperature than when the same amount of virus was used to inoculate naïve cells [139]. This result suggested that a cooperative interaction, such as gene complementation, led to increased productivity. Importantly, the virus stocks used in studies by Jacobs et al. and Kaverin et al. were tested to ensure low defective RNA content, and thus these findings represent a phenotype of replication competent IAVs. These observations also indicate that the phenotype of MOI dependence likely extends to all contexts of IAV infection.

Host dependent barriers to infection

Potential mechanisms for inefficiencies in the viral life cycle which may lead to a dependence on collective interactions are diverse. Many of these inefficiencies are likely exacerbated in the case of host species crossover. Avian and mammalian IAVs are known to exhibit host adaptive differences in receptor preference, pH of fusion, NA stalk length, and polymerase activity [9, 13]. Multiple stages in the viral life cycle pose a host dependent barrier to infection. Receptor binding specificities are known to influence attachment preferences among avian and mammalian cells and can result in differences in infectivity [140, 141]. As IAVs replicate in the nucleus, the nuclear membrane also poses a barrier to infection. The import of vRNPs through the nuclear pore complex by importin α and β is impacted by host specific IAV adaptations [132, 142-145]. IAVs containing mammalian adaptation signatures in PB2 (E627K, D701N) and NP (N319K) have been shown to enhance importin-α interactions and import in mammalian, but not avian cells, by differentially favoring of importin-α isoforms [62, 63, 143, 146, 147]. Cytosolic restriction factors also act on the incoming vRNP to prevent nuclear entry or to dampen early life cycle events such as transcription and replication. MxA is a host factor which specifically interferes with the interaction between NP and PB2 proteins and reduces both replication activity and vRNP transport to the nucleus in a host specific manner [60, 148-153]. The innate immune sensor, RIG-I, has also been shown to directly interfere with vRNPs prior to nuclear entry [154, 155]. The host factor TRIM22 targets the viral nucleoprotein (NP), which coats incoming vRNPs and is essential for their nuclear import, and tags it for proteasomal degradation [61]. MOV10 is another host factor which specifically interferes with vRNP delivery to the nucleus [156]. Polymerase activity certainly is affected by host background. Over thirty different host factors have been identified to effect viral polymerase function in some way, with likely more remaining

to be identified. These host factors act on multiple processes involving the viral polymerase including nuclear import, transcription initiation, post translational modifications of viral proteins, assembly of the polymerase complex, and export [49, 81]. As is expected, the host background plays a role in determining the nature and efficiency of these virus-host interactions. Avian adapted IAVs are restricted in polymerase activity in mammalian cells due to poor interaction with mammalian ANP32A, and require compensatory mutations, such as PB2 E627K, for replication to occur effectively [84, 85, 157]. In conclusion, differences in adaptive features of IAVs lead to various incompatibilities or inefficiencies when infecting alternative host species. While the compatibility of viral and host factors can be acquired through adaptive mutations or reassortment with adapted strains, the impact of collective interactions on viral production efficiency has not been closely studied. It may be plausible to anticipate the efficiency of affected viral life cycle events could be influenced by viral protein and gene dose. For example, interfering host factors may be competitively inhibited by a large number of incoming viral proteins when viruses infect at high multiplicity. Increasing gene dosage through multiple infection could enable complementation of segments which would otherwise have been absent due to inefficiency in vRNP delivery.

Introduction to thesis project

The first aim of this dissertation was to evaluate the reassortment potential between human seasonal IAV strains representative of the pH1N1 and H3N2 subtypes currently co-circulating. By comparing reassortment levels between homologous and heterologous strains, we were able to measure the impact of segment mismatch on reassortment frequency. Studies of viral replication, polymerase activity, *and in vivo* transmission of chimeric viruses revealed consequences of segment mismatch on progeny fitness. Overall, reassortment between

heterologous viruses was found to be efficient, however, biased reassortment patterns and fitness defects among reassortant genotypes likely limits the number of reassortant genotypes which arise out of reassortment events involving pH1N1 and H3N2 viruses in nature. This finding reveals that segment compatibility dynamics can limit the effective diversity of reassortment events.

The second aim of this dissertation was to investigate factors determining coinfection dependence of IAVs. We found that coinfection and reassortment levels varied with virus-host pairings. Coinfection led to enhanced RNA replication in a host dependent manner. In particular, an H9N2 virus tested displayed a near-absolute dependence on coinfection for replication. Chimeric viruses containing selected components of the H9N2 strain revealed that this phenotype was mainly due to the viral polymerase. Quantification of incomplete viral genomes demonstrated a partial need for complementation. Together, these results indicated the H9N2 strain benefitted from some additional means of cooperation through coinfection which involved the viral polymerase. This study indicated that collective interactions among coinfecting IAV virions could serve to augment the efficiency of viral infection. Reliance on coinfection for efficient viral replication could lead to enhanced diversity through reassortment and other virus-virus interactions.

This work centers on the factors and conditions which facilitate and limit IAV diversification through collective interactions, with particular attention to reassortment potential. The second chapter provides concrete results which support that functional incompatibilities among gene segments can limit viral diversification through gene reassortment. Further studies of reassortment patterns at the population and molecular levels to characterize reassortment potential among strains of interest. The third chapter demonstrates that dependence of IAVs on

coinfection and collective interactions, including reassortment, differs with virus strain and host species. The viral polymerase was found to play a major role in dictating the phenotype of coinfection dependence. This finding provides rationale for further study of the functions of the viral polymerase and how differences in fidelity, activity, and processivity may impact coinfection dependence. Together, these studies identify important features of IAV evolution, and could be informative for furthering understanding and predicting evolutionary dynamics on a population level.

References

1. McDonald, S.M., et al., *Reassortment in segmented RNA viruses: mechanisms and outcomes.* Nat Rev Microbiol, 2016. **14**(7): p. 448-60.

2. Fields, B.N., D.M. Knipe, and P.M. Howley, *Fields virology*. 2013, Philadelphia: Wolters Kluwer Health/Lippincott Williams & Wilkins.

3. Lyons, D.M. and A.S. Lauring, *Mutation and Epistasis in Influenza Virus Evolution.* Viruses, 2018. **10**(8).

4. Steel, J. and A.C. Lowen, *Influenza A virus reassortment.* Curr Top Microbiol Immunol, 2014. **385**: p. 377-401.

5. White, M.C., J. Steel, and A.C. Lowen, *Heterologous Packaging Signals on Segment 4, but Not Segment 6 or Segment 8, Limit Influenza A Virus Reassortment.* J Virol, 2017. **91**(11).

6. Dugan, V.G., et al., *The evolutionary genetics and emergence of avian influenza viruses in wild birds.* PLoS Pathog, 2008. **4**(5): p. e1000076.

7. Webster, R.G., et al., *EVOLUTION AND ECOLOGY OF INFLUENZA-A VIRUSES.* Microbiological Reviews, 1992. **56**(1): p. 152-179.

8. Lee, J.H., et al., *Evaluation of the zoonotic potential of a novel reassortant H1N2 swine influenza virus with gene constellation derived from multiple viral sources.* Infect Genet Evol, 2015. **34**: p. 378-93.

9. Cauldwell, A.V., et al., *Viral determinants of influenza A virus host range.* J Gen Virol, 2014. **95**(Pt 6): p. 1193-210.

10. Manz, B., M. Schwemmle, and L. Brunotte, *Adaptation of avian influenza A virus polymerase in mammals to overcome the host species barrier.* J Virol, 2013. **87**(13): p. 7200-9.

11. Parrish, C.R., P.R. Murcia, and E.C. Holmes, *Influenza virus reservoirs and intermediate hosts: dogs, horses, and new possibilities for influenza virus exposure of humans.* J Virol, 2015. **89**(6): p. 2990-4.

12. Schrauwen, E.J. and R.A. Fouchier, *Host adaptation and transmission of influenza A viruses in mammals.* Emerg Microbes Infect, 2014. **3**(2): p. e9.

13. Taubenberger, J.K. and J.C. Kash, *Influenza virus evolution, host adaptation, and pandemic formation.* Cell host & microbe, 2010. **7**(6): p. 440-451.

14. Te Velthuis, A.J.W., et al., *Mini viral RNAs act as innate immune agonists during influenza virus infection.* Nat Microbiol, 2018. **3**(11): p. 1234-1242.

15. Fonville, J.M., et al., *Influenza Virus Reassortment Is Enhanced by Semi-infectious Particles but Can Be Suppressed by Defective Interfering Particles.* PLoS Pathog, 2015. **11**(10): p. e1005204.

16. Brooke, C.B., et al., *Influenza A virus nucleoprotein selectively decreases neuraminidase gene-segment packaging while enhancing viral fitness and transmissibility.* Proc Natl Acad Sci U S A, 2014. **111**(47): p. 16854-9.

17. Brooke, C.B., et al., *Most influenza a virions fail to express at least one essential viral protein.* J Virol, 2013. **87**(6): p. 3155-62.

18. Jacobs, N.T., et al., *Incomplete influenza A virus genomes occur frequently but are readily complemented during localized viral spread.* Nat Commun, 2019. **10**(1): p. 3526.

19. Su, S., et al., *Novel Influenza D virus: Epidemiology, pathology, evolution and biological characteristics.* Virulence, 2017. **8**(8): p. 1580-1591.

20. Zambon, M.C., *Epidemiology and pathogenesis of influenza.* J Antimicrob Chemother, 1999. **44 Suppl B**: p. 3-9.

21. Holwerda, M., et al., *Determining the Replication Kinetics and Cellular Tropism of Influenza D Virus on Primary Well-Differentiated Human Airway Epithelial Cells.* Viruses, 2019. **11**(4): p. 377.

22. Osterhaus, A., et al., *Influenza B virus in seals.* Science, 2000. **288**(5468): p. 1051-1053.

23. Baigent, S.J. and J.W. McCauley, *Influenza type A in humans, mammals and birds: determinants of virus virulence, host-range and interspecies transmission.* Bioessays, 2003. **25**(7): p. 657-671.

24. Kandeil, A., et al., *Isolation and Characterization of a Distinct Influenza A Virus from Egyptian Bats.* 2019. **93**(2): p. e01059-18.

25. Tong, S., et al., *A distinct lineage of influenza A virus from bats.* Proceedings of the National Academy of Sciences of the United States of America, 2012. **109**(11): p. 4269-4274.

26. Petrova, V.N. and C.A. Russell, *The evolution of seasonal influenza viruses.* Nat Rev Microbiol, 2018. **16**(1): p. 47-60.

27. Lee, J.M., et al., *Deep mutational scanning of hemagglutinin helps predict evolutionary fates of human H3N2 influenza variants.* Proc Natl Acad Sci U S A, 2018. **115**(35): p. E8276-e8285.

28. Doud, M.B. and J.D. Bloom, *Accurate Measurement of the Effects of All Amino-Acid Mutations on Influenza Hemagglutinin.* Viruses, 2016. **8**(6).

29. Heaton, N.S., et al., *Genome-wide mutagenesis of influenza virus reveals unique plasticity of the hemagglutinin and NS1 proteins.* Proceedings of the National Academy of Sciences of the United States of America, 2013. **110**(50): p. 20248-20253.

30. Nelson, M.I., et al., *Multiple reassortment events in the evolutionary history of H1N1 influenza A virus since 1918.* PLoS Pathog, 2008. **4**(2): p. e1000012.

31. Nelson, M.I., et al., *The origin and global emergence of adamantane resistant A/H3N2 influenza viruses.* Virology, 2009. **388**(2): p. 270-8.

32. Ince, W.L., et al., *Reassortment complements spontaneous mutation in influenza A virus NP and M1 genes to accelerate adaptation to a new host.* J Virol, 2013. **87**(8): p. 4330-8.

33. Worobey, M., G.Z. Han, and A. Rambaut, *Genesis and pathogenesis of the 1918 pandemic H1N1 influenza A virus.* Proc Natl Acad Sci U S A, 2014. **111**(22): p. 8107-12.

34. Gibbs, M.J. and A.J. Gibbs, *Molecular virology: was the 1918 pandemic caused by a bird flu?* Nature, 2006. **440**(7088): p. E8; discussion E9-10.

35. Taubenberger, J.K., et al., *Characterization of the 1918 influenza virus polymerase genes.* Nature, 2005. **437**(7060): p. 889-93.

36. Wendel, I., et al., *The avian-origin PB1 gene segment facilitated replication and transmissibility of the H3N2/1968 pandemic influenza virus.* J Virol, 2015. **89**(8): p. 4170-9.

37. Kawaoka, Y., S. Krauss, and R.G. Webster, *Avian-to-human transmission of the PB1 gene of influenza A viruses in the 1957 and 1968 pandemics.* Journal of virology, 1989. **63**(11): p. 4603-4608.

38. Nakajima, K., U. Desselberger, and P. Palese, *Recent human influenza A (H1N1) viruses are closely related genetically to strains isolated in 1950.* Nature, 1978. **274**(5669): p. 334-9.

39. Kung, H.C., et al., *Influenza in China in 1977: recurrence of influenzavirus A subtype H1N1.* Bulletin of the World Health Organization, 1978. **56**(6): p. 913-918.

40. Zakstelskaja, L.J., et al., *Influenza in the USSR in 1977: recurrence of influenzavirus A subtype H1N1.* Bulletin of the World Health Organization, 1978. **56**(6): p. 919-922.

41. Zhang, Y., et al., *Key Molecular Factors in Hemagglutinin and PB2 Contribute to Efficient Transmission of the 2009 H1N1 Pandemic Influenza Virus.* Journal of Virology, 2012. **86**(18): p. 9666-9674.

42. Worobey, M., G.Z. Han, and A. Rambaut, *A synchronized global sweep of the internal genes of modern avian influenza virus.* Nature, 2014. **508**(7495): p. 254-7.

43. Nelson, M.I. and A.L. Vincent, *Reverse zoonosis of influenza to swine: new perspectives on the human-animal interface.* Trends in Microbiology, 2015. **23**(3): p. 142-153.

44. Gao, R., et al., *Human infection with a novel avian-origin influenza A (H7N9) virus.* N Engl J Med, 2013. **368**(20): p. 1888-97.

45. Abdel-Ghafar, A.N., et al., *Update on avian influenza A (H5N1) virus infection in humans.* N Engl J Med, 2008. **358**(3): p. 261-73.

46. Pusch, E.A. and D.L. Suarez, *The Multifaceted Zoonotic Risk of H9N2 Avian Influenza.* Veterinary sciences, 2018. **5**(4): p. 82.

47. Connor, R.J., et al., *Receptor specificity in human, avian, and equine H2 and H3 influenza virus isolates.* Virology, 1994. **205**(1): p. 17-23.

48. Couceiro, J.N., J.C. Paulson, and L.G. Baum, *Influenza virus strains selectively recognize sialyloligosaccharides on human respiratory epithelium; the role of the host cell in selection of hemagglutinin receptor specificity.* Virus Res, 1993. **29**(2): p. 155-65.

49. Long, J.S., et al., *Host and viral determinants of influenza A virus species specificity.* Nat Rev Microbiol, 2019. **17**(2): p. 67-81.

50. Pinto, L.H., L.J. Holsinger, and R.A. Lamb, *Influenza virus M2 protein has ion channel activity.* Cell, 1992. **69**(3): p. 517-28.

51. Matlin, K.S., et al., *Infectious entry pathway of influenza virus in a canine kidney cell line.* J Cell Biol, 1981. **91**(3 Pt 1): p. 601-13.

52. Cross, K.J., et al., *Composition and functions of the influenza fusion peptide.* Protein Pept Lett, 2009. **16**(7): p. 766-78.

53. Harrison, S.C., *Viral membrane fusion.* Nat Struct Mol Biol, 2008. **15**(7): p. 690-8.

54. Martin, K. and A. Helenius, *Transport of incoming influenza virus nucleocapsids into the nucleus.* J Virol, 1991. **65**(1): p. 232-44.

55. Compans, R.W., J. Content, and P.H. Duesberg, *Structure of the ribonucleoprotein of influenza virus.* J Virol, 1972. **10**(4): p. 795-800.

56. Desselberger, U., et al., *The 3' and 5'-terminal sequences of influenza A, B and C virus RNA segments are highly conserved and show partial inverted complementarity.* Gene, 1980. **8**(3): p. 315-28.

57. Robertson, J.S., *5' and 3' terminal nucleotide sequences of the RNA genome segments of influenza virus.* Nucleic Acids Res, 1979. **6**(12): p. 3745-57.

58. Eisfeld, A.J., G. Neumann, and Y. Kawaoka, *At the centre: influenza A virus ribonucleoproteins.* Nat Rev Microbiol, 2015. **13**(1): p. 28-41.

59. Cros, J.F. and P. Palese, *Trafficking of viral genomic RNA into and out of the nucleus: influenza, Thogoto and Borna disease viruses.* Virus Res, 2003. **95**(1-2): p. 3-12.

60. Xiao, H., et al., *The human interferon-induced MxA protein inhibits early stages of influenza A virus infection by retaining the incoming viral genome in the cytoplasm.* J Virol, 2013. **87**(23): p. 13053-8.

61. Di Pietro, A., et al., *TRIM22 Inhibits Influenza A Virus Infection by Targeting the Viral Nucleoprotein for Degradation.* Journal of Virology, 2013. **87**(8): p. 4523-4533.

62. Pumroy, R.A., et al., *Molecular determinants for nuclear import of Influenza A PB2 by importin α isoforms 3 and 7.* Structure (London, England : 1993), 2015. **23**(2): p. 374-384.

63. Resa-Infante, P. and G. Gabriel, *The nuclear import machinery is a determinant of influenza virus host adaptation.* Bioessays, 2013. **35**(1): p. 23-7.

64. Dias, A., et al., *The cap-snatching endonuclease of influenza virus polymerase resides in the PA subunit.* Nature, 2009. **458**(7240): p. 914-8.

65. Yuan, P., et al., *Crystal structure of an avian influenza polymerase PA(N) reveals an endonuclease active site.* Nature, 2009. **458**(7240): p. 909-13.

66. Te Velthuis, A.J. and E. Fodor, *Influenza virus RNA polymerase: insights into the mechanisms of viral RNA synthesis.* Nat Rev Microbiol, 2016. **14**(8): p. 479-93.

67. Lamb, R.A., C.J. Lai, and P.W. Choppin, *Sequences of mRNAs derived from genome RNA segment 7 of influenza virus: colinear and interrupted mRNAs code for overlapping proteins.* Proc Natl Acad Sci U S A, 1981. **78**(7): p. 4170-4.

68. Lamb, R.A. and C.J. Lai, *Sequence of interrupted and uninterrupted mRNAs and cloned DNA coding for the two overlapping nonstructural proteins of influenza virus.* Cell, 1980. **21**(2): p. 475-85.

69. Hale, B.G., et al., *The multifunctional NS1 protein of influenza A viruses.* J Gen Virol, 2008. **89**(Pt 10): p. 2359-76.

70. Nath, S.T. and D.P. Nayak, *Function of two discrete regions is required for nuclear localization of polymerase basic protein 1 of A/WSN/33 influenza virus (H1 N1).* Mol Cell Biol, 1990. **10**(8): p. 4139-45.

71. Jones, I.M., P.A. Reay, and K.L. Philpott, *Nuclear location of all three influenza polymerase proteins and a nuclear signal in polymerase PB2.* Embo j, 1986. **5**(9): p. 2371-6.

72. Mukaigawa, J. and D.P. Nayak, *Two signals mediate nuclear localization of influenza virus (A/WSN/33) polymerase basic protein 2.* J Virol, 1991. **65**(1): p. 245-53.

73. Nieto, A., et al., *Complex structure of the nuclear translocation signal of influenza virus polymerase PA subunit.* J Gen Virol, 1994. **75 (Pt 1)**: p. 29-36.

74. York, A., et al., *Isolation and characterization of the positive-sense replicative intermediate of a negative-strand RNA virus.* Proc Natl Acad Sci U S A, 2013. **110**(45): p. E4238-45.

75. Beaton, A.R. and R.M. Krug, *Transcription antitermination during influenza viral template RNA synthesis requires the nucleocapsid protein and the absence of a 5' capped end.* Proc Natl Acad Sci U S A, 1986. **83**(17): p. 6282-6.

76. Hay, A.J., et al., *Transcription of the influenza virus genome.* Virology, 1977. **83**(2): p. 337-55.

77. Olson, A.C., E. Rosenblum, and R.D. Kuchta, *Regulation of influenza RNA polymerase activity and the switch between replication and transcription by the concentrations of the vRNA 5' end, the cap source, and the polymerase.* Biochemistry, 2010. **49**(47): p. 10208-15.

78. Turrell, L., et al., *The role and assembly mechanism of nucleoprotein in influenza A virus ribonucleoprotein complexes.* Nat Commun, 2013. **4**: p. 1591.

79. Perez, J.T., et al., *A small-RNA enhancer of viral polymerase activity.* J Virol, 2012. **86**(24): p. 13475-85.

80. Chua, M.A., et al., *Influenza A virus utilizes suboptimal splicing to coordinate the timing of infection.* Cell Rep, 2013. **3**(1): p. 23-9.

81. Peacock, T.P., et al., *Host Determinants of Influenza RNA Synthesis.* Annu Rev Virol, 2019.

82. Resa-Infante, P., et al., *The influenza virus RNA synthesis machine: advances in its structure and function.* RNA Biol, 2011. **8**(2): p. 207-15.

83. Jorba, N., R. Coloma, and J. Ortin, *Genetic trans-complementation establishes a new model for influenza virus RNA transcription and replication.* PLoS Pathog, 2009. **5**(5): p. e1000462.

84. Long, J.S., et al., *Species difference in ANP32A underlies influenza A virus polymerase host restriction.* Nature, 2016. **529**(7584): p. 101-4.

85. Staller, E., et al., *ANP32 proteins are essential for influenza virus replication in human cells.* J Virol, 2019.

86. Chaimayo, C., et al., *Selective incorporation of vRNP into influenza A virions determined by its specific interaction with M1 protein.* Virology, 2017. **505**: p. 23-32.

87. Huang, S., et al., *A second CRM1-dependent nuclear export signal in the influenza A virus NS2 protein contributes to the nuclear export of viral ribonucleoproteins.* J Virol, 2013. **87**(2): p. 767-78.

88. de Castro Martin, I.F., et al., *Influenza virus genome reaches the plasma membrane via a modified endoplasmic reticulum and Rab11-dependent vesicles.* Nat Commun, 2017. **8**(1): p. 1396.

89. Momose, F., et al., *Apical transport of influenza A virus ribonucleoprotein requires Rab11-positive recycling endosome.* PLoS One, 2011. **6**(6): p. e21123.

90. Chou, Y.Y., et al., *One influenza virus particle packages eight unique viral RNAs as shown by FISH analysis.* Proc Natl Acad Sci U S A, 2012. **109**(23): p. 9101-6.

91. Hutchinson, E.C., et al., *Genome packaging in influenza A virus.* J Gen Virol, 2010. **91**(Pt 2): p. 313-28.

92. Muramoto, Y., T. Noda, and Y. Kawaoka, *[Selective packaging mechanism for influenza A virus]*. Tanpakushitsu Kakusan Koso, 2006. **51**(11): p. 1596-601.

93. White, M.C., et al., *H5N8 and H7N9 packaging signals constrain HA reassortment with a seasonal H3N2 influenza A virus.* Proc Natl Acad Sci U S A, 2019.

94. Fournier, E., et al., *Interaction network linking the human H3N2 influenza A virus genomic RNA segments.* Vaccine, 2012. **30**(51): p. 7359-67.

95. Nakatsu, S., et al., *Complete and Incomplete Genome Packaging of Influenza A and B Viruses.* MBio, 2016. **7**(5).

96. Majarian, T.D., R.F. Murphy, and S.S. Lakdawala, *Learning the sequence of influenza A genome assembly during viral replication using point process models and fluorescence in situ hybridization.* PLoS Comput Biol, 2019. **15**(1): p. e1006199.

97. Steinhauer, D.A., et al., *Deacylation of the hemagglutinin of influenza A/Aichi/2/68 has no effect on membrane fusion properties.* Virology, 1991. **184**(1): p. 445-8.

98. Veit, M., et al., *Site-specific mutagenesis identifies three cysteine residues in the cytoplasmic tail as acylation sites of influenza virus hemagglutinin.* J Virol, 1991. **65**(5): p. 2491-500.

99. Veit, M., et al., *The M2 protein of influenza A virus is acylated.* J Gen Virol, 1991. **72 (Pt 6)**: p. 1461-5.

100. Veit, M. and M.F. Schmidt, *Timing of palmitoylation of influenza virus hemagglutinin.* FEBS Lett, 1993. **336**(2): p. 243-7.

101. Sugrue, R.J., R.B. Belshe, and A.J. Hay, *Palmitoylation of the influenza A virus M2 protein.* Virology, 1990. **179**(1): p. 51-6.

102. Chutiwitoonchai, N. and Y. Aida, *NXT1, a Novel Influenza A NP Binding Protein, Promotes the Nuclear Export of NP via a CRM1-Dependent Pathway.* Viruses, 2016. **8**(8).

103. Chen, B.J., et al., *Influenza virus hemagglutinin and neuraminidase, but not the matrix protein, are required for assembly and budding of plasmid-derived virus-like particles.* J Virol, 2007. **81**(13): p. 7111-23.

104. Ali, A., et al., *Influenza virus assembly: effect of influenza virus glycoproteins on the membrane association of M1 protein.* J Virol, 2000. **74**(18): p. 8709-19.

105. Gomez-Puertas, P., et al., *Influenza virus matrix protein is the major driving force in virus budding.* J Virol, 2000. **74**(24): p. 11538-47.

106. Rossman, J.S., et al., *Influenza virus M2 protein mediates ESCRT-independent membrane scission.* Cell, 2010. **142**(6): p. 902-13.

107. Riegger, D., et al., *The nucleoprotein of newly emerged H7N9 influenza A virus harbors a unique motif conferring resistance to antiviral human MxA.* J Virol, 2015. **89**(4): p. 2241-52.

108. Palese, P. and R.W. Compans, *Inhibition of influenza virus replication in tissue culture by 2-deoxy-2,3-dehydro-N-trifluoroacetylneuraminic acid (FANA): mechanism of action.* J Gen Virol, 1976. **33**(1): p. 159-63.

109. Palese, P., et al., *Characterization of temperature sensitive influenza virus mutants defective in neuraminidase.* Virology, 1974. **61**(2): p. 397-410.

110. Pauly, M.D., M.C. Procario, and A.S. Lauring, *A novel twelve class fluctuation test reveals higher than expected mutation rates for influenza A viruses.* Elife, 2017. **6**.

111. Holmes, E.C., et al., *Whole-genome analysis of human influenza A virus reveals multiple persistent lineages and reassortment among recent H3N2 viruses.* PLoS Biol, 2005. **3**(9): p. e300.

112. White, M.C. and A.C. Lowen, *Implications of segment mismatch for influenza A virus evolution.* J Gen Virol, 2018. **99**(1): p. 3-16.

113. Gerber, M., et al., *Selective packaging of the influenza A genome and consequences for genetic reassortment.* Trends Microbiol, 2014. **22**(8): p. 446-55.

114. Gavazzi, C., et al., *An in vitro network of intermolecular interactions between viral RNA segments of an avian H5N2 influenza A virus: comparison with a human H3N2 virus.* Nucleic Acids Res, 2013. **41**(2): p. 1241-54.

115. Baker, S.F., et al., *Influenza A and B virus intertypic reassortment through compatible viral packaging signals.* J Virol, 2014. **88**(18): p. 10778-91.

116. Gen, F., et al., *Attenuation of an influenza A virus due to alteration of its hemagglutinin-neuraminidase functional balance in mice.* Arch Virol, 2013. **158**(5): p. 1003-11.

117. Wagner, R., M. Matrosovich, and H.D. Klenk, *Functional balance between haemagglutinin and neuraminidase in influenza virus infections.* Rev Med Virol, 2002. **12**(3): p. 159-66.

118. Li, C., et al., *Compatibility among polymerase subunit proteins is a restricting factor in reassortment between equine H7N7 and human H3N2 influenza viruses.* J Virol, 2008. **82**(23): p. 11880-8.

119. To, K.K., et al., *The emergence of influenza A H7N9 in human beings 16 years after influenza A H5N1: a tale of two cities.* Lancet Infect Dis, 2013. **13**(9): p. 809-21.

120. Boullé, M., et al., *HIV Cell-to-Cell Spread Results in Earlier Onset of Viral Gene Expression by Multiple Infections per Cell.* PLoS pathogens, 2016. **12**(11): p. e1005964-e1005964.

121. Sanjuán, R. and M.-I. Thoulouze, *Why viruses sometimes disperse in groups?(†).* Virus evolution, 2019. **5**(1): p. vez014-vez014.

122. DaPalma, T., et al., *A systematic approach to virus-virus interactions.* Virus Res, 2010. **149**(1): p. 1-9.

123. Rizzetto, M., *Hepatitis D: thirty years after.* J Hepatol, 2009. **50**(5): p. 1043-50.

124. Kliem, M. and B. Dreiseikelmann, *The superimmunity gene sim of bacteriophage P1 causes superinfection exclusion.* Virology, 1989. **171**(2): p. 350-5.

125. Von Magnus, P., *Incomplete forms of influenza virus.* Adv Virus Res, 1954. **2**: p. 59-79.

126. von, M.P., *Propagation of the PR8 strain of influenza A virus in chick embryos. II. The formation of incomplete virus following inoculation of large doses of seed virus.* Acta Pathol Microbiol Scand, 1951. **28**(3): p. 278-93.

127. Manzoni, T.B. and C.B. López, *Defective (interfering) viral genomes re-explored: impact on antiviral immunity and virus persistence.* Future virology, 2018. **13**(7): p. 493-503.

128. Cifuentes-Munoz, N., R.E. Dutch, and R. Cattaneo, *Direct cell-to-cell transmission of respiratory viruses: The fast lanes.* PLoS Pathog, 2018. **14**(6): p. e1007015.

129. Santiana, M., et al., *Vesicle-Cloaked Virus Clusters Are Optimal Units for Inter-organismal Viral Transmission.* Cell Host Microbe, 2018. **24**(2): p. 208-220.e8.

130. Andreu-Moreno, I. and R. Sanjuan, *Collective Infection of Cells by Viral Aggregates Promotes Early Viral Proliferation and Reveals a Cellular-Level Allee Effect.* Curr Biol, 2018. **28**(20): p. 3212-3219.e4.

131. Timm, C., A. Gupta, and J. Yin, *Robust kinetics of an RNA virus: Transcription rates are set by genome levels.* Biotechnol Bioeng, 2015. **112**(8): p. 1655-62.

132. Aguilera, E.R., et al., *Plaques Formed by Mutagenized Viral Populations Have Elevated Coinfection Frequencies.* MBio, 2017. **8**(2).

133. Krystal, M., et al., *Expression of the three influenza virus polymerase proteins in a single cell allows growth complementation of viral mutants.* Proc Natl Acad Sci U S A, 1986. **83**(8): p. 2709-13.

134. Zhou, B. and D.E. Wentworth, *Influenza A virus molecular virology techniques.* Methods Mol Biol, 2012. **865**: p. 175-92.

135. Hoffmann, E., et al., *A DNA transfection system for generation of influenza A virus from eight plasmids.* 2000. **97**(11): p. 6108-6113.

136. Fodor, E., et al., *Rescue of influenza A virus from recombinant DNA.* J Virol, 1999. **73**(11): p. 9679-82.

137. Stiefel, P., et al., *Cooperative Vaccinia Infection Demonstrated at the Single-Cell Level Using FluidFM.* Nano Letters, 2012. **12**(8): p. 4219-4227.

138. Erickson, A.K., et al., *Bacteria Facilitate Enteric Virus Co-infection of Mammalian Cells and Promote Genetic Recombination.* Cell Host Microbe, 2018. **23**(1): p. 77-88.e5.

139. Kaverin, N.V., L.I. Kolomietz, and I.A. Rudneva, *Incomplete influenza virus: partial functional complementation as revealed by hemadsorbing cell count test.* J Virol, 1980. **34**(2): p. 506-11.

140. Maines, T.R., et al., *Effect of receptor binding domain mutations on receptor binding and transmissibility of avian influenza H5N1 viruses.* Virology, 2011. **413**(1): p. 139-147.

141. Matrosovich, M., J. Stech, and H.D. Klenk, *Influenza receptors, polymerase and host range.* Rev Sci Tech, 2009. **28**(1): p. 203-17.

142. Flatt, J.W. and U.F. Greber, *Misdelivery at the Nuclear Pore Complex-Stopping a Virus Dead in Its Tracks.* Cells, 2015. **4**(3): p. 277-96.

143. Gabriel, G., et al., *Differential use of importin-alpha isoforms governs cell tropism and host adaptation of influenza virus.* Nat Commun, 2011. **2**: p. 156.

144. Hudjetz, B. and G. Gabriel, *Human-like PB2 627K influenza virus polymerase activity is regulated by importin-alpha1 and -alpha7.* PLoS Pathog, 2012. **8**(1): p. e1002488.

145. Hudjetz, B. and G. Gabriel, *Human-like PB2 627K Influenza Virus Polymerase Activity Is Regulated by Importin-α1 and -α7.* PLoS Pathogens, 2012. **8**(1): p. e1002488.

146. Sediri, H., et al., *Adaptive mutation PB2 D701N promotes nuclear import of influenza vRNPs in mammalian cells.* Eur J Cell Biol, 2015. **94**(7-9): p. 368-74.

147. Resa-Infante, P., et al., *The Host-Dependent Interaction of α-Importins with Influenza PB2 Polymerase Subunit Is Required for Virus RNA Replication.* PLoS ONE, 2008. **3**(12): p. e3904.

148. Ciminski, K., et al., *Human MxA is a potent interspecies barrier for the novel bat-derived influenza A-like virus H18N11.* Emerg Microbes Infect, 2019. **8**(1): p. 556-563.

149. Deeg, C.M., et al., *In vivo evasion of MxA by avian influenza viruses requires human signature in the viral nucleoprotein.* J Exp Med, 2017. **214**(5): p. 1239-1248.

150. Dornfeld, D., et al., *Eurasian Avian-Like Swine Influenza A Viruses Escape Human MxA Restriction through Distinct Mutations in Their Nucleoprotein.* J Virol, 2019. **93**(2).

151. Gotz, V., et al., *Influenza A viruses escape from MxA restriction at the expense of efficient nuclear vRNP import.* Sci Rep, 2016. **6**: p. 23138.

152. Turan, K., et al., *Nuclear MxA proteins form a complex with influenza virus NP and inhibit the transcription of the engineered influenza virus genome.* Nucleic Acids Res, 2004. **32**(2): p. 643-52.

153. Zimmermann, P., et al., *The viral nucleoprotein determines Mx sensitivity of influenza A viruses.* J Virol, 2011. **85**(16): p. 8133-40.

154. Li, W., et al., *Interactions between the influenza A virus RNA polymerase components and retinoic acid-inducible gene I.* J Virol, 2014. **88**(18): p. 10432-47.

155. Weber, M., et al., *Influenza virus adaptation PB2-627K modulates nucleocapsid inhibition by the pathogen sensor RIG-I.* Cell Host Microbe, 2015. **17**(3): p. 309-19.

156. Zhang, J., et al., *Host Protein Moloney Leukemia Virus 10 (MOV10) Acts as a Restriction Factor of Influenza A Virus by Inhibiting the Nuclear Import of the Viral Nucleoprotein.* J Virol, 2016. **90**(8): p. 3966-80.

157. Long, J.S., et al., *Species specific differences in use of ANP32 proteins by influenza A virus.* Elife, 2019. **8**.

Chapter II. Seasonal H3N2 and 2009 pandemic H1N1 influenza A viruses reassort efficiently but produce attenuated progeny

Kara L. Phipps[1], Nicolle Marshall[1], Hui Tao[1], Shamika Danzy[1], Nina Onuoha[1], John Steel[1] and Anice C. Lowen[1]*

[1]Department of Microbiology and Immunology, Emory University School of Medicine, Atlanta, Georgia, USA

*Address correspondence to Anice C. Lowen, anice.lowen@emory.edu

K.L.P. and N.M. contributed equally to this work.

The work of this chapter was published in the Journal of Virology in 2017.

Citation:

Phipps, K. L., Marshall, N., Tao, H., Danzy, S., Onuoha, N., Steel, J., & Lowen, A. C. (2017). Seasonal H3N2 and 2009 Pandemic H1N1 Influenza A Viruses Reassort Efficiently but Produce Attenuated Progeny. *Journal of virology*, *91*(17), e00830-17. doi:10.1128/JVI.00830-17

Abstract

Reassortment of gene segments between coinfecting influenza A viruses (IAV) facilitates viral diversification and has significant epidemiological impact on seasonal and pandemic influenza. Since 1977, human IAVs of H1N1 and H3N2 subtypes have cocirculated with relatively few documented cases of reassortment. We evaluated the potential for viruses of the 2009 pandemic H1N1 (pH1N1) and seasonal H3N2 lineages to reassort under experimental conditions. Results of heterologous coinfections with pH1N1 and H3N2 viruses were compared to those obtained following coinfection with homologous, genetically tagged, pH1N1 viruses as a control. High genotype diversity was observed among progeny of both coinfections; however, diversity was more limited following heterologous coinfection. Pairwise analysis of genotype patterns revealed that homologous reassortment was random while heterologous reassortment was characterized by specific biases. pH1N1:H3N2 reassortant genotypes produced under single-cycle coinfection conditions showed a strong preference for homologous PB2-PA combinations and general preferences for the H3N2 NA, pH1N1 M, and the H3N2 PB2 except when paired with the pH1N1 PA or NP. Multicycle coinfection results corroborated these findings and revealed an additional preference for the H3N2 HA. Segment compatibility was further investigated by measuring chimeric polymerase activity and growth of selected reassortants in human tracheobronchial epithelial cells. In guinea pigs inoculated with a mixture of viruses, parental H3N2 viruses dominated but reassortants also infected and transmitted to cage mates. Taken together, our results indicate that strong intrinsic barriers to reassortment between seasonal H3N2 and pH1N1 viruses are few, but that the reassortants formed are attenuated relative to parental strains.

Importance

The genome of IAV is relatively simple, comprising eight RNA segments, each of which typically encodes one or two proteins. Each viral protein carries out multiple functions in coordination with other viral components and the machinery of the cell. When two IAV coinfect a cell, they can exchange genes through reassortment. The resultant progeny viruses often suffer fitness defects due to suboptimal interactions among divergent viral components. The genetic diversity generated through reassortment can facilitate the emergence of novel outbreak strains. Thus, it is important to understand the efficiency of reassortment and the factors that limit its potential. The research described here offers new tools for studying reassortment between two strains of interest, and applies those tools to viruses of the 2009 pandemic H1N1 and seasonal H3N2 lineages, which currently cocirculate in humans and therefore have the potential to give rise to novel epidemic strains.

Introduction

The multipartite genome of influenza A virus (IAV) allows the exchange of gene segments in cells coinfected with multiple variant viruses [1]. This process of horizontal gene transfer is termed reassortment and, together with polymerase error, is an important source of viral genetic diversity [2]. Reassortment of IAVs adapted to distinct host species has played a prominent role in the emergence of pandemic strains [3, 4]. This type of reassortment, involving highly divergent viruses, brings about large shifts in genotype and phenotype, which can facilitate host species transfers [5]. In addition, reassortment between cocirculating human IAVs is an important source of genetic diversity in the evolution of seasonal influenza viruses [6-11]. In this case, reassortment among related strains can act as a catalyst of viral evolution by allowing point mutations on

differing segments to be brought together in a combinatorial manner. Multiple beneficial mutations can thereby be merged within a single genotype, alleviating clonal interference and facilitating the emergence of novel variants [6, 12]. This mechanism is thought to have led to widespread resistance to adamantanes within the human H3N2 lineage when a resistance mutation on the M segment was coupled with an HA gene encoding an antigenically novel hemagglutinin [7].

IAVs of H1N1 and H3N2 subtypes have cocirculated in humans since 1977 [13, 14]. Prior to 2009, seasonal H3N2 viruses cocirculated with H1N1 viruses of the 1918 lineage. Since 2009, this same H3N2 lineage has cocirculated with viruses derived from the 2009 pandemic. The endemicity of two distinct IAV lineages within the global human population has created the opportunity for coinfection and therefore reassortment between them. Such reassortment has not, however, been detected frequently. Occasional case reports have documented heterosubtypic coinfection in humans, and reassortment was confirmed in a subset of these reports [15-24]. Over the past 40 years, few H1N1:H3N2 reassortant viruses have achieved sustained transmission in humans and none have remained prevalent over multiple seasons [25, 26]. In contrast, the two major lineages of influenza B virus, Victoria and Yamagata, have exhibited frequent reassortment in humans since their divergence in the 1970s [27, 28]. Moreover, intrasubtype reassortment within both H1N1 and H3N2 lineages has given rise to multiple epidemiologically significant strains [6-11, 29]. These examples indicate that circulation within human hosts does not preclude coinfection and reassortment of influenza viruses and therefore that the rarity with which H1N1/H3N2 reassortant viruses are detected is likely due to evolutionary constraints acting on their heterologous reassortment.

Reassortment between two IAVs that differ in all eight segments can give rise to 256 distinct genotypes. When two divergent strains reassort, however, the diversity generated is often limited

by epistasis among gene segments [30]. Negative epistatic interactions arising during IAV reassortment are termed “segment mismatch” and may occur at the RNA or protein levels. RNA level mismatches are thought to arise due to sequence divergence in packaging or other cis-acting signals. Incompatibilities among noncognate RNA packaging signals results in preferential incorporation of homologous segment groupings during assembly and can strongly bias the formation of reassortant genotypes [31-33]. Protein level mismatches result from suboptimal physical or functional interactions among viral proteins. In contrast to mismatch during genome packaging, incompatibilities among viral proteins are not manifested until after a reassortant virus is formed and goes on to infect another cell. An example of protein mismatch commonly observed is an imbalance between hemagglutinin (HA) and neuraminidase (NA) functions [34-36]. HA binds cellular sialic acids for viral entry while NA cleaves sialic acids to allow release at the end of the viral life cycle [37]. HA/NA imbalance can therefore lead to poor viral attachment or aggregation at the cell surface [35, 38]. The trimeric viral polymerase, comprised of proteins encoded on the PB2, PB1, and PA gene segments, presents another opportunity for protein incompatibilities. Polymerase complexes that derive components from divergent IAV strains are often associated with reduced polymerase activity and/or attenuated viral growth [39-42]. Due to the myriad of ways that IAV proteins and functions are interconnected throughout the viral life cycle, the phenomenon of segment mismatch is complex and has been difficult to address in a quantitative or systematic way [43].

Herein, we aimed to identify the sources of constraint acting on reassortment between viruses of the seasonal H3N2 and 2009 pandemic H1N1 (pH1N1) lineages. To accomplish this aim, we used a novel strategy in which the genotypes emerging from heterologous coinfection with influenza A/Panama/2007/99 (H3N2) virus and an A/NL/602/2009 (H1N1)-like virus were compared to

those observed following homologous coinfection with two closely related pH1N1 viruses. We furthermore employed a comprehensive pairwise analysis of gene segments to systematically identify biases in reassortment. Our results reveal that heterologous coinfections yielded high levels of reassortment, but that genotype diversity was lower than seen with the homologous control coinfection. Pairwise analysis of genotype patterns corroborated this observation: homologous reassortment was found to occur randomly, whereas heterologous coinfection was characterized by both subtle and pronounced biases. The functional and fitness implications of several of the segment preferences detected were evaluated by measuring chimeric polymerase activity and by assessing the growth of selected reassortant viruses in human tracheobronchial epithelial (HTBE) cells. Finally, given that many reassortant gene combinations were detected with high frequency and associated with relatively minor fitness defects in monoculture, we tested the potential for H3N2/pH1N1 reassortants to compete with parental strains in vivo. Inoculation of guinea pigs with a diverse mixture of H3N2/pH1N1 reassortant viruses demonstrated that, while the parental H3N2 virus dominated infection, reassortant genotypes were also successfully propagated within the primary host and transmitted to contact animals.

Results

Reassortment between H3N2 and pH1N1 viruses yielded a high diversity of viral genotypes.

We reported previously that reassortment between a tagged version of A/Panama/2007/99 virus (Pan/99wt-His) and a highly homologous variant of the same strain (Pan/99var-HAtag) is efficient, with up to 95% of viruses generated through MDCK cell coinfection carrying reassortant genotypes [44, 45]. We also saw that reassortment levels declined with decreasing infectious dose [44, 45]. Here, we have built on these earlier findings to design a novel and quantitative means of

evaluating reassortment efficiency for two heterologous IAVs. Namely, we evaluated reassortment over a wide range of doses to ensure that reassortment and coinfection readouts were not saturated, we measured infection levels to control for variation in effective multiplicity of infection (MOI), and we compared reassortment observed with heterologous viruses to the levels observed following coinfection with homologous "wildtype" (wt) and "variant" (var) viruses of the pH1N1 background. Reassortment between these two variants of the same strain served as a control, indicative of baseline reassortment. Taken together, this approach enables quantitative analysis of reassortment efficiency for a relevant pairing of heterologous IAVs, and allows meaningful interpretation of these data by comparison to the control data set.

To evaluate reassortment efficiency, coinfections with homologous and heterologous viruses were performed in MDCK cells and limited to a single round of infection. The homologous coinfection included pH1N1wt-HAtag plus pH1N1var-HIS viruses as coinfection partners. The heterologous coinfection included pH1N1wt-HAtag and Pan/99wt-His viruses. As described in the Materials and Methods section, the pH1N1 viruses used herein are based on, but not identical to, the A/NL/602/2009 (H1N1) strain. These viruses were chosen in part for practical reasons based on the reagents available and, although these particular isolates did not cocirculate, because they are representative of their respective, cociruclating, human lineages. For simplicity, pH1N1wt-HAtag and Pan/99wt-His viruses are here referred to as pH1N1 and H3N2, respectively. Following coinfection, clonal isolates from cell culture supernatants were obtained by plaque assay and genotyped. Based on this experimental design, reassortant gene constellations that do not form or do not support plaque formation are not detected. The levels of reassortment observed are represented in **Figure 1** as a diversity index, which is equivalent to the number of unique genotypes identified in a sample divided by the number of isolates screened [46]. This diversity index is

plotted against the percentage of cells that expressed both viral HA proteins on the cell surface, as detected by flow cytometry. Enumeration of HA expressing cells was used to monitor the effective MOI. Inclusion of this parameter in the analysis ensures that any differences in reassortment between two coinfections are not due to differing MOIs.

The diversities of genotypes detected following homologous (pH1N1wt-HAtag plus pH1N1var-HIS) and heterologous (pH1N1 plus H3N2) coinfections was comparable over the lower dosage ranges tested, indicating that reassortment occurs readily between pH1N1 and H3N2. As the percentage of cells that were dually HA positive increased beyond 20%, however, diversity levels attained following heterologous coinfection appeared restricted (**Figure 1**). Curve fitting and nonlinear regression confirmed that the homologous and heterologous data sets differed significantly. Specifically, following log-log transformation to linearize the data, the slope of the homologous diversity index was found to increase at a greater rate ($p=0.003$). The difference between curves at high levels of infection suggests that fewer reassortant genotypes are viable following heterologous coinfection compared than after homologous coinfection.

Pairwise analysis of gene segments for the identification of bias in reassortment outcomes.

While diversity indices observed following pH1N1 plus H3N2 virus coinfection indicated that appreciable reassortment occurred, the diversity index calculation employed does not allow evaluation of genotype patterns. To identify and quantify biases in reassortment, a more detailed analysis is necessary. One approach would be to test whether all 256 possible genotypes are equally represented among progeny viruses. A more technically feasible approach is to evaluate whether, for a given pair of gene segments, all four possible genotypes are equally represented. For example, when considering PB2 and PB1 segments following infection with parental viruses A and B,

progeny viruses could carry AA, AB, BA or BB genotypes. If reassortment is random, $PB2_A$ carrying viruses would be expected to be 50% AA and 50% AB, while $PB2_B$ carrying viruses would be 50% BA and 50% BB. Performing such an analysis for all pairwise combinations of segments allows detection of favored and disfavored combinations, as well as preferences for particular segments regardless of the gene constellation. To display the results in an easily interpretable fashion, we generated scatterplots for each of the eight segments. Each plot contains seven data points corresponding to the remaining seven segments. To illustrate how this works, we will continue the example given above. On the x axis of the PB2 plot, viruses with $PB2_A$ are analyzed and the proportion with an AA combination of PB2 and PB1 is plotted. Thus, if the PB1 data point is at 0.7 on the horizontal axis, the homologous AA combination occurred in 70% of reassortant viruses and the heterologous AB combination was present in 30%. On the y axis of the same plot, viruses with $PB2_B$ are examined and the proportion with a BB combination of PB2 and PB1 is plotted. Thus, if the PB1 data point is at 0.7 on the vertical axis, the homologous BB combination was preferred. When data are plotted in this way, one obtains a graphical representation in which segment linkages, or the lack thereof, can be easily identified. Interpretations assigned to different regions of the two-dimensional plot are shown in **Figure 2**. Importantly, if reassortment is random, all data points are expected to fall in the middle of the plot, at 0.5 on each axis.

To apply this pairwise analysis to pH1N1wt-HAtag plus pH1N1var-HIS and pH1N1 plus H3N2 virus pairings, we used genotype data obtained from triplicate coinfections performed at the highest MOI tested in **Figure 1** (i.e., corresponding to the three rightmost data points for each combination of parental viruses). Even at these high MOIs, an appreciable proportion of infected cells were infected with only one parental virus. We therefore excluded parental genotypes from

our analyses to avoid biasing results toward homologous combinations. To support a robust analysis, at least 100 clonal isolates per replicate were screened. Following exclusion of parental viruses and any viruses for which one or more segments could not be typed, 54 to71 viral genotypes per replicate remained. Pairwise analysis was performed separately for each replicate and then average results were calculated. As detailed in the following sections, results revealed that reassortment between pH1N1wt-HAtag and pH1N1var-HIS viruses occurred randomly, while reassortment between pH1N1 and H3N2 viruses was characterized by strong pairwise linkages involving PB2 and PA segments and several less pronounced preferences for particular segments or segment combinations.

Homologous reassortment between pH1N1wt-HAtag and pH1N1var-HIS viruses occurred randomly.

Results of pairwise genotype analysis for pH1N1wt-HAtag plus pH1N1var-HIS virus reassortment are displayed in **Figure 3**. On all eight graphs the seven data points fall near the midpoint (0.5, 0.5), revealing that genetic exchange between these homologous parental viruses occurred randomly. This observation indicates that coinfecting viral genomes mix freely within the cell at a stage of the viral life cycle that precedes segment bundling [47-49]. These results also give a valuable reference for comparison when analyzing data obtained from heterologous coinfection.

Heterologous reassortment between pH1N1 and H3N2 viruses was non-random.

In contrast to results obtained with pH1N1wt-HAtag plus pH1N1var-HIS viruses, results of pairwise genotype analyses for pH1N1 plus H3N2 virus reassortment revealed evidence of systematic bias in segment assortment. **Figure 4** shows the results obtained when coinfections

were performed under single-cycle conditions, as were used for pH1N1wt-HAtag plus pH1N1var-HIS coinfection. In addition, we evaluated the genotypes detected following heterologous coinfection performed under conditions that allowed for a second cycle of infection; results of these analyses are shown in **Figure 5**. The scatterplots show visually that a number of data points deviate from the center of the graph for pH1N1 plus H3N2 reassortment. To test whether these apparent biases in reassortment were statistically significant, we used the data obtained from pH1N1wt-HAtag plus pH1N1var-HIS reassortment as a reference for comparison. Specifically, the proportions of reassortant viruses that carried a homologous segment pairing ("proportion homologous") were compared using Student's *t*-test. Triplicate results for a given pairwise combination from pH1N1 plus H3N2 coinfection were compared to the full data set (triplicate results of all 112 pairings combined) from the pH1N1wt-HAtag plus pH1N1var-HIS coinfection. Results of these analyses that were common under single-cycle and multicycle conditions are described in the following sections. In general, the outcomes observed under the two coinfection conditions were similar, as indicated by a strong correlation between the data sets (**Figure 6**). Two exceptions were noted, however. Under multicycle conditions, the H3N2 HA segment was favored in pairings with both H3N2 and pH1N1 segments, although the former were not found to be significant (**Table 1**). Conversely, both HA segments were detected with approximately equal frequency under single-cycle conditions. In addition, under single-cycle conditions the H3N2 PB1 was slightly favored in several pairwise combinations, but multicycle conditions showed that the pH1N1 and H3N2 PB1 segments assorted randomly.

Viruses combining the pH1N1 PB2 and H3N2 PA segments were detected rarely.

The PB2 scatterplots in **Figures 4 and 5** show that, among viruses with the pH1N1 PB2 segment, ~95% also carried the pH1N1 PA segment (p=0.011). Similarly, as visible on the PA scatterplots, nearly all reassortant viruses carrying the H3N2 PA also possessed the H3N2 PB2 (p=0.031). These strong biases suggest that the combination of the pH1N1 PB2 with the H3N2 PA was essentially nonfunctional. The relationship was not reciprocal, however: the PA scatterplots reveal that the pH1N1 PA was paired with PB2 from either parental strain with approximately the same frequency (p=0.804). Among viruses with the H3N2 PB2, the homologous PA was preferred but not required, with 71% or 60% of viruses carrying the H3N2 PA under single-cycle and multicycle conditions, respectively. This trend did not reach statistical significance (P=0.058).

PB2 and NA segments from H3N2 virus were favored among reassortant viruses.

Data points in the lower right portion of each scatterplot within **Figures 4 and 5** indicate a preference for the H3N2 -derived segment, regardless of whether the partner segment in the pairwise analysis was of H3N2 or pH1N1 virus origin. Under both single and multi cycle conditions, the NA data point was found in this region of all graphs. Statistical analysis indicated significance for most, but not all, pairings compared to the control data set (**Table 1**). Thus, the proportion of pH1N1 segments that coassorted with the homologous NA was lower than expected while the proportion of H3N2 segments that coassorted with the homologous NA was higher, than expected based on the results of homologous reassortment between pH1N1wt-HAtag and pH1N1var-HIS viruses.

The PB2 data point also typically fell in the lower right quadrant, with two exceptions: on the PA and NP plots, the PB2 point is at the center-right. Thus, the H3N2 PB2 was preferred over the pH1N1 PB2 in all pairwise combinations under both single and multicycle conditions, except with

pH1N1 PA and NP. Viruses with pH1N1 PA or NP carried either PB2 with approximately the same frequency. With few exceptions, preferences for the H3N2 PB2 were statistically significant ($P<0.05$; **Table 1**).

The M segment of the pH1N1 background was compatible with all H3N2 segments and preferred in several pairwise combinations with segments of pH1N1 and H3N2 origin.

Under both single and multicycle conditions, most of the data points generated through pairwise analysis tended to fall on the right half or in the lower-right region of the scatterplots. These patterns reflect biases favoring H3N2 segments together with another H3N2 segment (right side) or together with segments of either strain origin (lower right). The M segment was an exception to this generalization. On a number of plots, the M segment data point fell into the upper half of the graph or into the upper left quadrant, indicating preferences for the pH1N1 M segment over the H3N2 M segment (**Figures 4 and 5**). Compared to the control data set, the pH1N1 M segment was significantly preferred in several pairings under multicycle conditions. Under single-cycle conditions, preference for the pH1N1 M segment reached significance only in the pairwise analysis with the H3N2 PB1 segment (**Table 1**).

Activities of chimeric polymerase complexes suggest that interactions at the protein level underlie reassortment patterns observed among PB2, PB1, PA and NP segments.

To investigate whether observed reassortment patterns involving pH1N1 and H3N2 PB2, PB1, PA and NP segments could be attributed to functions of the encoded proteins in replication and transcription of viral RNAs, we evaluated the activities of wild-type and chimeric polymerase complexes in a minireplicon assay. The PB2, PB1, PA and NP proteins of pH1N1 and H3N2

viruses were coexpressed in all possible combinations with a virus-like segment encoding firefly luciferase. *Renilla* expression was used as an internal control for transfection efficiency. The average results of three independent experiments, each with 3 technical replicates, are presented in **Figure 7**. The wild-type H3N2 polymerase complex supported higher luciferase activity than the wild-type pH1N1 complex by ~20-fold ($P<0.0001$, unpaired *t*-test), and this difference mapped to the PB2 segment. To allow differences not attributable to PB2 to be visualized more easily, data are therefore presented in two separate graphs: polymerase complexes that include the H3N2 PB2 are shown in **Figure 7A** and those that include the pH1N1 PB2 are shown in **Figure 7B**. These data sets offered the following insights into the compatibility of pH1N1 and H3N2 polymerase components.

Introduction of the heterologous PB1 segment into either strain background did not reduce polymerase activity, consistent with the observation that this segment assorted randomly between pH1N1 and H3N2 viruses under multicycle coinfection conditions. In contrast, introduction of any other H3N2 segment(s) together with the pH1N1 PB2 markedly reduced activity. Notably, combination of the H3N2 PA segment with PB2, PB1 and NP from pH1N1 virus was unfavorable. This finding offers a mechanistic explanation for the observation that reassortant viruses with pH1N1 PB2 and H3N2 PA segments were detected rarely: low viral fitness likely resulted from poor polymerase function given this combination of PB2 and PA proteins. Finally, the H3N2 PB2 protein supported higher luciferase activity than the pH1N1 PB2 protein even when paired with polymerase components derived from the pH1N1 virus, a result which likely maps to the difference in the PB2 627 domain between these viruses [50] and is consistent with the general preference for H3N2 PB2 segment observed in our reassortment data set.

Growth in HTBE cell cultures revealed attenuation of reassortant genotypes.

With the aim of testing whether patterns of reassortment observed in MDCK cell coinfection were likely to extend to a coinfected human host, we generated selected reassortant viruses by reverse genetics and evaluated their growth phenotypes in primary, differentiated, HTBE cells (**Figure 8**). We attempted to rescue 14 genotypes, including the parental control viruses. Twelve were recovered successfully, while H3N2 virus carrying the pH1N1 PB2 and pH1N1 virus with the H3N2 PA were not. The H3N2:pH1N1 PB2 virus was not rescued in three independent attempts. The pH1N1:H3N2 PA virus rescue yielded a small number of plaques, but we were unsuccessful in amplifying these plaque isolates despite multiple attempts under various conditions. We concluded that these two reassortant genotypes are effectively nonviable, consistent with the results of our pairwise analyses (**Figures 4 and 5**).

For those reassortant genotypes that were recovered by reverse genetics, growth analyses in HTBE cells revealed that introduction of pH1N1 PB1, HA or M segments into the H3N2 virus background reduced viral fitness in this system (**Figure 8A**). By comparison, pairwise analyses of reassortant genotypes, which showed that the pH1N1 M segment was compatible with all H3N2 segments under both single and multicycle conditions, and that HA and PB1 segments of the two strain backgrounds exchanged freely under single and multicycle conditions, respectively. This apparent difference between growth and reassortment analyses may reflect the fact that plaque isolates genotyped in our reassortment assay were selected at random, regardless of plaque size. In addition, parental isolates were excluded from the pairwise analysis of genotypes but are included for comparison in the growth analyses. A more extreme fitness defect was seen with introduction of the pH1N1 PA into the H3N2 background. This gene constellation lowered viral yields by $>10^4$-fold at the 48 and 72 h time points relative to the H3N2wt control. Parallel introduction of pH1N1

PA and PB2 proteins into the H3N2 background yielded an intermediate phenotype, with 50-100-fold lower titers compared to H3N2wt virus observed in HTBE cells (**Figure 8A**). Although reassortant viruses with the H3N2 PB2 tended to carry the homologous PA (**Figure 4**), this association was neither strong nor significant, making the severity of the growth defects observed for the H3N2:pH1N1 PA and H3N2:pH1N1 PB2 plus PA viruses unexpected. Importantly, however, pairwise reassortment analyses cannot capture epistatic interactions involving more than two genes. Minireplicon and reassortment data suggest that inclusion of the pH1N1 NP together with pH1N1 PB2 and PA segments may improve viral growth to levels comparable to that of the H3N2wt strain.

Again in the pH1N1 background, the recombinant wild-type strain exhibited the most robust growth (**Figure 8B**). Single gene reassortants in which the H3N2 PB1, HA or NA segment was introduced showed about 10-fold lower growth in HTBE cells. As noted above, detection of reassortant viruses following coinfection required only that such viruses form visible plaques. The growth data are therefore consistent with reassortment results, which suggested that these three H3N2 segments would be compatible with the pH1N1 background. Introduction of the H3N2 PB2 alone, or together with the H3N2 PA, into the pH1N1 background reduced viral titers by ~100-1000-fold at the 24, 48, and 72 h time points relative to the titer of pH1N1wt control (**Figure 8B**). In contrast, the reassortment and minireplicon data sets suggested that inclusion of the H3N2 PB2 would be favorable in the pH1N1 background. This apparent discrepancy might be attributable to higher order interactions among segments: the compatibility of H3N2 genes with the pH1N1 background may be dependent on a genetic context that involves more than two genes and therefore cannot be detected through pairwise genotype analyses. In addition, higher polymerase

activity, as seen with the H3N2 PB2 in the pH1N1 background, may not be optimal for viral growth.

pH1N1:H3N2 reassortant viruses were detected in inoculated and contact guinea pigs following the introduction of a diverse coinfection supernatant into guinea pigs.

As a second means of gauging the relevance of reassortment patterns observed in MDCK cell culture, we evaluated the potential for pH1N1:H3N2 reassortant viruses to propagate within and transmit between guinea pigs. To this end, three guinea pigs were inoculated intranasally with a highly diverse mixture of viruses obtained following single-cycle coinfection of MDCK cells. Namely, the supernatant from the first replicate of our coinfection experiments described above was used as the inoculum. This sample had a diversity index = 0.83; the genotypes detected are shown in **Figure 9A**. A relatively high dose of $1x10^5$ PFU per guinea pig was used to avoid stochastic reduction of viral diversity upon inoculation. The viral genotypes detected in nasal wash samples obtained from inoculated animals on days 1, 2 and 3 post-inoculation revealed that the H3N2wt genotype dominated the infection but did not render reassortant variants undetectable (limit of detection = 5% frequency in the population). In particular, reassortant viruses carrying the pH1N1 M segment formed an appreciable proportion of the viral population in all three inoculated animals, with up to 43% of M segments sampled of pH1N1 origin (**Figure 9**). Transmission to each of the three contact guinea pigs was first detected on day 2 postinoculation (day 1 postexposure). Analysis of viruses isolated from these early positive samples again indicated a fitness advantage for the H3N2wt strain, but also revealed reassortant viruses in contact guinea pigs (**Figure 9**). Although reassortment in contact animals, rather than transmission of reassortant viruses, could formally account for the detection of nonparental genotypes in the

contacts, our prior data on the kinetics of reassortment in guinea pigs strongly suggest that transmission of reassortant viruses occurred [46, 51]. Overall, the results of this experiment suggest that the pH1N1 virus and pH1N1:H3N2 reassortants are marginally less fit than the H3N2 parental virus when placed in direct competition.

Discussion

The observation that reassortment involving two divergent IAVs proceeds nonrandomly has been documented numerous times [33, 41, 52-62]. The biases that characterize heterologous reassortment are indicative of epistatic interactions among gene segments: favored genotypes are typically those that do not break positive interactions by combining segments that have diverged at relevant loci. Put another way, negative epistatic interactions, or instances of "segment mismatch," constrain viral diversification through reassortment. Despite early recognition of this phenomenon, and its importance in the evolution of pandemic and epidemic IAVs, segment mismatch has rarely been examined in a systematic way. Here we offer two innovations designed to make evaluations of heterologous reassortment more informative.

First, we show that IAV reassortment occurs randomly in the absence of segment mismatch, by evaluating the diversity of genotypes generated through reassortment of two highly similar IAVs. (While we previously reported that homologous reassortment was highly efficient [45], analysis of these earlier data to test for randomness was not performed.) This observation reveals that additional constraints on IAV reassortment in coinfected cells are negligible. It furthermore enables rigorous identification of epistatic interactions in heterologous reassortment by providing a baseline for comparison.

Second, we introduced pairwise analysis of gene segments as a means of detecting nonrandom reassortment outcomes. Specifically, for each of the 16 segments present in a coinfection, we determined the proportion of reassortant viruses that carried each of the other segments from the same parental strain. The strengths of this approach include (i) that it is comprehensive, so that any pairwise biases present in the data set should not be overlooked; (ii) that the method can be applied to smaller data sets, since any two segments can form a maximum of only four different genotypes; and (iii) that the resultant data can be visualized easily. An important limitation of a pairwise genotype analysis is that epistatic interactions involving three or more segments may not be apparent. While the strategy used here could potentially be expanded to allow the identification of higher order interactions, a large number of viruses would need to be sampled to give this approach appropriate power (since the number of possible genotypes increases exponentially with the number of segments analyzed).

To demonstrate the utility of these two methodologies, and with the aim of identifying constraints acting on the reassortment of cocirculating human IAVs, we evaluated the outcomes of reassortment between viruses of the pH1N1 and seasonal H3N2 lineages. Our results revealed that this pairing of parental viruses allowed robust diversification through reassortment in MDCK cell culture. When full viral genotypes (rather than pairwise combinations), were considered, the diversity detected following heterologous reassortment was marginally restricted compared to that seen with homologous reassortment. Pairwise analysis allowed the detection of a number of subtle biases, as well as a potent negative interaction involving the pH1N1 PB2 and the H3N2 PA.

Incompatibility among the three polymerase segments and NP from divergent strains has often been noted in the literature [39-41, 55, 60, 63-65]. Our own polymerase reconstitution data, and those of others, suggest that these mismatches arise at the protein level and result in reduced

polymerase activity [39-41, 64, 65]. Indeed, a previous in-depth analysis of the heterologous $PB2_{pH1N1}$ / PA_{H3N2} pairing revealed impaired replication-initiation relative to the full pH1N1 polymerase complex, which mapped largely to PA_{H3N2} residues 184N and 383N [40]. The relatively free exchange of PB1 segments between pH1N1 and H3N2 viruses seen here is likely due to the fact that they are closely related: the PB1 segment of the pH1N1 lineage is derived from the human seasonal H3N2 lineage [66, 67]. In contrast to a number of reports in which heterologous HA/NA combinations have been found to yield viruses with fitness defects [34-36, 68, 69], we did not note negative interactions between pH1N1 and H3N2 virus HA and NA genes. While this finding may be attributable in part to the use of MDCK cells, the phenotypes of selected reassortant viruses in HTBE cells indicate that heterologous HA/NA combinations did not exert a major fitness cost in this setting as well.

Despite the observation that pronounced biases in pH1N1:H3N2 reassortment were limited, multicycle growth analyses of selected reassortants in HTBE cells, revealed a clear advantage of parental genotypes. In vivo, inoculation of guinea pigs with a diverse mixture of reassortant viruses, indicated that the H3N2 parental strain in particular was predominant. These results are consistent with only sporadic detection of pH1N1:H3N2 reassortant viruses within the human population, despite their cocirculation over an 8-year period. The observed phenotypes in HTBE cells and guinea pigs underline the fact that minor fitness defects can be highly significant when amplified over many rounds of viral replication, and when multiple variant viruses are in direct competition. For this reason, the magnitude of epistatic effects acting on IAV reassortment is expected to be less important than whether an epistatic interaction is positive or negative. The subtle biases in pH1N1:H3N2 reassortment noted herein may therefore play a major role in limiting the success of intersubtypic reassortant viruses within the human population.

Despite often complex linkages among gene segments, genetic exchange between diverse IAV lineages has been documented repeatedly in nature [6, 8, 10, 11, 70-73]. In these cases, selection pressures imposed by the host environment might favor a reassortant virus, thereby offsetting fitness defects due to segment mismatch. In addition, frequent errors in RNA replication allow incompatibilities among viral proteins or packaging signals to be alleviated through post-reassortment adaptive changes [36, 74, 75]. With these concepts in mind, it is notable that several reassortant genotypes were detected in guinea pigs with mixed pH1N1:H3N2 infection, and transmitted to cage mates. These data imply that similar reassortants could be sufficiently fit to achieve sustained spread in humans if changing selection pressures reduce competition from parental viruses. Indeed, the prevalence of reassortant viruses incorporating the pH1N1 M segment in global swine populations suggests that the strong representation of this segment in our in vivo study may be indicative of its potential to penetrate the human H3N2 lineage [76-78].

In sum, we offer a rigorous means of evaluating the potential for heterologous reassortment to give rise to fit influenza virus variants. We furthermore show that genetic exchange between representative strains of pH1N1 and seasonal H3N2 lineages yields a diverse range of reassortant genotypes, but that these reassortants are attenuated relative to the parental strains. We propose that the observed fitness defects are likely to be highly significant on an epidemiological scale, but also could be overcome through reduced competition from parental strains and/or mutation of mismatched gene segments.

Materials and Methods

Cells

Madin-Darby canine kidney (MDCK) cells (a kind gift of Peter Palese, Icahn School of Medicine at Mount Sinai) were maintained in minimal essential medium (MEM; Gibco) supplemented with 10% fetal bovine serum and penicillin-streptomycin. 293T cells (ATCC CRL-3216) were maintained in Dulbecco's minimal essential medium (Gibco) supplemented with 10% fetal bovine serum. Human tracheobronchial epithelial (HTBE) cells from a single donor were acquired from Lonza and were amplified and differentiated into air-liquid interface cultures as recommended by Lonza and described by Danzy et al. [79].

Viruses

All viruses used in this work were generated using reverse genetics techniques [80]. The rescue system for A/Panama/2007/99 (H3N2) [Pan/99] virus was initially described in reference 81, and that for A/Netherlands/602/2009 (H1N1) [NL/09] virus was a gift of Ron Fouchier (Erasmus Medical Center) [81]. The passage history of Pan/99 virus includes egg passage, as it previously served as a vaccine strain, while the NL/09 virus was derived from a primary human specimen prior to the cloning of the viral cDNA to generate the reverse genetics system [81]. The Pan/99wt_His virus was described previously [45] and is modified from the wild-type Pan/99 sequence through the inclusion of a HIS epitope tag plus GGGS linker at the N terminus of the HA protein (inserted after the signal peptide). The pH1N1wt_HAtag and pH1N1var_His viruses carry similarly modified HA genes, with the HA tag or His tag, respectively, plus a GGGS linker inserted at the N terminus of the NL/09 HA protein. These two viruses also carry PB2, PB1, PA, NP, M and NS gene segments of the NL/09 strain. Due to the unusually low neuraminidase activity associated with the NL/09 NA protein [82], we replaced the NL/09 NA segment with that of

influenza A/CA/04/2009 (H1N1) virus. The NL/09 and A/CA/04/2009 NA proteins differ by two amino acids. These two substitutions were found to increase the growth rate of the resultant pH1N1 viruses relative to the unmodified NL/09 strain (data not shown), which was important for allowing detection of pH1N1 genes in the context of coinfection with Pan/99 virus. In addition to the His tag and linker inserted into the HA protein, the pH1N1var_His virus carries a single synonymous mutation per segment relative to the pH1N1wt_HAtag virus, as follows: PB2 C273T, PB1 T288C, PA C360T, HA C305T, NP A351G, NA G336A, M G295A, and NS C341T. These eight silent mutations act as genetic markers for determining the parental origin of gene segments following the isolation of progeny viruses from coinfected cells.

To evaluate the growth of selected H3N2:pH1N1 reassortant viruses in HTBE cells, viruses were generated by reverse genetics using the appropriate pPOL1 Pan/99 and pHW NL/09 plasmids. Where the pH1N1 NA segment was included, the pPOL1 CA/04/09 NA plasmid was used. Support plasmids encoding WSN PB2, PB1, PA or NP proteins in pCAGGS were included in rescue transfections as needed. This set of viruses did not include variant mutations or epitope tags.

Pan/99wt-His virus was cultured in 9-11 day old embryonated chicken eggs incubated at 33^{o}C. All other viruses were grown in MDCK cells incubated at 33^{o}C. Since the presence of defective interfering RNAs in the context of coinfection could result in misleading preferences for segments of a certain parental origin, care was taken to limit their accumulation. Viruses were cultured at a low MOI and maintained at a low passage number (passaged once or twice following rescue or plaque purification in MDCK cells). The levels of defective interfering segments derived from PB2, PB1 and PA segments of all virus stocks used in coinfection were assessed by droplet digital PCR as described in reference [83] and found to be minimal.

Coinfection with homologous or heterologous virus pairs

MDCK cells were seeded at $4x10^5$ cells/well in 6 well dishes 18-24 h prior to infection. Appropriate viruses were combined at high titer and then serially diluted in phosphate-buffered saline (PBS) to achieve a range of MOIs (10, 6, 3, 1, 0,6, 0.3, or 0.1 PFU/cell). The ratio of HA positive cells detected by flow cytometry was used to optimize the proportion of each virus used in a mixture. Namely, a 1:1 ratio of HA tag-positive cells to His tag-positive cells following a single-cycle of replication in the presence of NH_4Cl was sought. In terms of PFU titer, the ratios used were 1:1 (pH1N1wt_HAtag and pH1N1var_His) for homologous coinfections and 5:1 (pH1N1wt_HAtag and Pan/99wt_His, respectively) for heterologous coinfections. Triplicate wells were inoculated at each MOI. Inoculation was performed on ice and dishes were incubated at 4˚C for 45-50 min to allow attachment. After removal of the inoculum, cells were washed three times with cold PBS and then warm virus medium (MEM supplemented with 3% bovine serum albumin and penicillin-streptomycin) was added. After 3 h of incubation at 33˚C, virus medium was changed to either i) virus medium supplemented with 1 M NH_4Cl for single-cycle growth or ii) virus medium supplemented with 1 μg/mL trypsin for multicycle growth. Cells were harvested and supernatant was collected at 24 h postinfection.

Determination of infection levels based on HA surface expression

To enumerate infected cells, surface expression of HIS and HA epitope tags was detected by flow cytometry. This method was previously described in detail [45]. The percentage of cells that were positive for both epitope tags is expressed as a percentage of cells dually HA positive in **Figure 1**.

Determination of reassortment levels

The following protocol was used to characterize the diversity of viral genotypes present in supernatants from cell culture coinfections and in nasal washes from guinea pigs. Plaque assays were performed in 10 cm cell culture dishes to isolate viral clones. For pH1N1 plus H3N2

coinfection samples, where plaque size was heterogeneous, all plaques on a dish were marked while holding the dish up to the light. The plate was then placed on a surface (where plaque size is not visible) and 5 ml serological pipets were used to collect the agar plugs overlaying plaques selected at random. Each agar plug was dispensed into 160 µl PBS. RNA was extracted from these 160 µl samples using the ZR-96 Viral RNA Kit (Zymo Research) and eluted in 40 water. Reverse transcription was performed with Maxima RT (ThermoFisher) according to the manufacturer's protocol. After 1:4 dilution in water, each cDNA was combined with segment specific primers and Precision Melt Supermix (Bio-Rad) and analyzed by qPCR followed by high resolution melt (HRM) analysis in a CFX384 Touch Real-Time PCR Detection System (Bio-Rad). Primers used to differentiate the gene segments of pH1N1wt-His and pH1N1var-HAtag viruses amplify an ~100 bp region of each gene segment, which contains the site at which a single nucleotide change was introduced into the pH1N1var-HAtag virus. Primers used to differentiate the gene segments of pH1N1 and H3N2 viruses bind to sequences conserved between these two strains and amplify an ~100 bp region that differs by at least one nucleotide between the two strains (**Table 2**). The sequence differences in these amplicons confer differences in melting properties to the cDNA, which is the basis of the HRM genotyping method. Thus, Precision Melt Analysis software (Bio-Rad) was used to determine the parental virus origin of each gene segment based on melting properties of the cDNAs. The HRM genotyping method is also described in references [44, 45, 84]. The HA and NA segments of pH1N1 and H3N2 viruses did not contain conserved regions of sufficient length to allow for the design of common primers. For this reason, HA and NA segments in samples derived from heterologous coinfection were genotyped by conventional qPCR with strain-specific primers. The sequences of all primers used for genotyping are given in **Table 1**. For each coinfection supernatant or guinea pig nasal wash sample analyzed in this way, at least 17 and

typically up to 21 plaque isolates were analyzed. To generate data used in pairwise analysis, this sample number was increased.

Pairwise analysis of gene segments

As a means of detecting bias in reassortment outcomes, a pairwise analysis of segments incorporated into reassortant progeny viruses was performed. The genotype tables included as **Data Set S1 in the supplemental material** report the raw data used. An R script was written to perform the following functions on each of the replicate data sets and then compute and plot the average and standard deviation of the triplicate values. The coinfecting parental viruses, and the segments they carry, were designated "0" and "1." The script first identified all reassortant viruses with PB2 of type 0 and then determined what proportion of those viruses also carried segment$_i$ of type 0 (where segment$_i$ represents each of the other segments). This step yielded a set of seven "proportion homologous" values for PB2 from virus 0. Similarly, the proportion of viruses with PB2 of type 1 that also carried segment$_i$ of type 1 was then calculated. This process was repeated for all segments, giving seven "proportion homologous" values for each of the 16 segments examined (eight from virus 0 and eight from virus 1). These results were plotted on a set of eight scatterplots, with proportion homologous from virus 0 on the x axis and proportion homologous from virus 1 on the y axis.

Statistical analyses of these data were also performed in R. Unpaired Student's *t*-tests were used to evaluate whether proportion homologous values observed following heterologous coinfection differed significantly from those observed following homologous coinfection. Since all possible pairwise combinations resulting from homologous coinfection were functionally homologous, the full set of 336 proportion homologous values (8 segments x 2 viruses x 7 segment$_i$ x 3 replicates = 336) was included in these *t*-tests as the comparator for each set of three proportion homologous

values obtained from heterologous coinfection. The correspondence between results obtained from the heterologous coinfections performed under single-cycle and multicycle conditions was assessed in R using Pearson's product moment correlation coefficient.

Polymerase reconstitution assay

293T cells were seeded at $1.5x10^5$ cells per well in 24 well dishes and incubated for 18-24 h at 37˚C. Cells were then transfected with X-treme Gene 9 transfection reagent (Roche) and 500 ng of each plasmid in Opti-MEM. Each well received six plasmids, as follows: pPOL1 NP luc (encoding, in the negative sense, firefly luciferase flanked by the NP untranslated regions of influenza A/WSN/1933 virus), pRL-TK (encoding *Renilla* luciferase under the control of a thymidine kinase promoter), pCAGGS PB2, pCAGGS PB1, pCAGGS PA, and pCAGGS NP. Plasmids encoding the viral polymerase components carried genes from either Pan/99 or NL/09, as indicated in **Figure 7**. Transfections were incubated at 37˚C for 24 h. Following incubation, medium was removed from cells and Dual-Glo® luciferase assay reagent (Promega) was added and incubated for 20 min at room temperature. Lysate aliquots of 100 µl from each reaction were added in triplicate to a 96 well plate (Costar) and firefly luminescence was read using a microplate reader (Biotek® Synergy H1 Hybrid Reader). Stop & Glo® substrate (Promega) was then added and incubated for 20 min at room temperature. Following incubation, *Renilla* luciferase luminescence was measured as above. The ratio of firefly to *Renilla* luciferase readouts was calculated for each sample and expressed as normalized polymerase activity. Three technical replicates were included in each transfection, and the experiment was performed on three different days.

Viral growth in HTBE cells

Human tracheobronchial epithelial (HTBE) cells (Lonza) at least 4 weeks after differentiation into air-liquid interface cultures were used to assess virus growth. Immediately prior to infection, mucus was aspirated and the cell monolayer was washed three times with PBS. Cells were then inoculated with virus diluted in PBS to an MOI of 0.001 PFU/cell and incubated for 1 h at 33˚C. Subsequently, the inoculum was removed and cell monolayer was washed three times with PBS. To sample virus, 200 μL PBS was added to each well and incubated for 30 min before collection. Samples were taken at 1, 12, 24, 48, and 72 h post infection. Virus growth was quantified by plaque assay.

Viral growth and transmission in guinea pigs

Female, Hartley strain, guinea pigs weighing 300 to 350 g were obtained from Charles River Laboratories. Prior to inoculation or nasal lavage, animals were sedated with a mixture of ketamine (30 mg/kg) and xylazine (4 mg/kg). Virus used for inoculation was a cell culture supernatant derived from single-cycle coinfection with Pan/99wt-His and pH1N1wt -HAtag viruses. This supernatant was diluted in PBS to allow intranasal inoculation of guinea pigs with $1x10^5$ PFU in a 300 μL volume. One contact guinea pig was introduced into the same cage with each of the inoculated animals at 24 h post-inoculation. Nasal wash samples were collected as described previously [85], with PBS as the collection fluid. Animals were housed in a Caron 6040 environmental chamber set to 10ºC and 20% RH throughout the seven-day exposure period and lids were left off of the cages during this time to ensure environmental control within the cages [86].

Acknowledgements

We would like to thank Seema Lakdawala for helpful discussion. This work was supported in part by the National Institutes of Health under R01AI099000 to ACL and the Centers of Excellence for Influenza Research and Surveillance (CEIRS) contract HHSN272201400004C to ACL and JS. KLP is currently supported by the National Institute of Allergy and Infectious Diseases of the National Institutes of Health under Award Number T32AI106699. The content is solely the responsibility of the authors and does not necessarily represent the official views of the National Institutes of Health.

Figures and tables

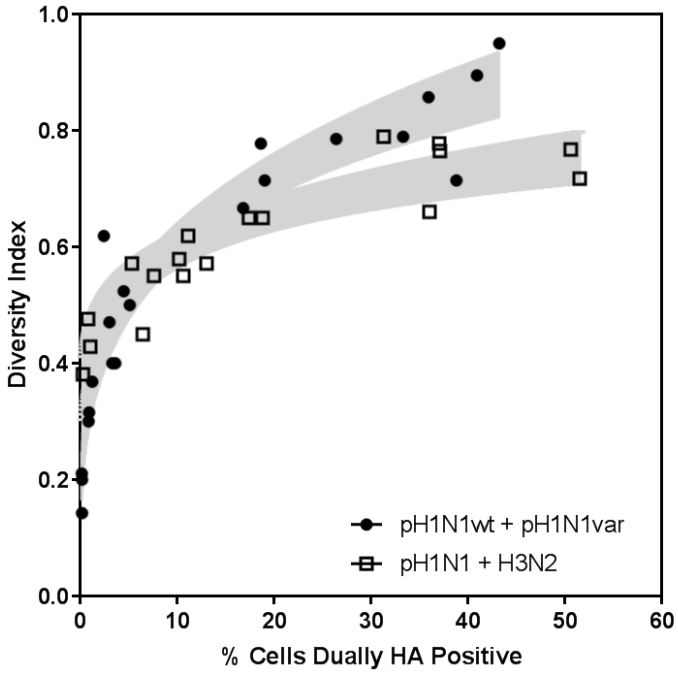

Figure 1. ***Diversity of genotypes generated through pH1N1 plus H3N2 reassortment is comparable to that produced by homologous reassortment.***

Coinfections were performed in MDCK cells over a wide range of MOIs with pH1N1wt-HAtag and pH1N1var-His viruses (closed circles) or pH1N1wt-HAtag and H3N2wt-His viruses (open squares). Infections were limited to a single cycle. Infected cells were enumerated at 24 h postinfection by flow cytometry targeting the His and HA epitope tags. The percentage of cells expressing both epitope tags on the cell surface is plotted on the x axis. The parental origin of each gene segment was determined for plaque isolates from each coinfection culture. The diversity index, plotted on the y axis, is equal to the number of different genotypes identified divided by the number of isolates screened. Each data point resulted from the screening of 17 to 21 plaque isolates, with the exception of the three

rightmost data points of each data set, which had 54 to 71 plaque isolates. The curve fits displayed for each data set were determined by nonlinear regression analysis in Prism. Shaded regions define the 95% confidence bands. To evaluate whether the two data sets differ significantly, log-log transformation was used to linearize the data and slopes were determined. The slopes were 0.25 for homologous coinfection and 0.14 for heterologous coinfection ($P = 0.0003$).

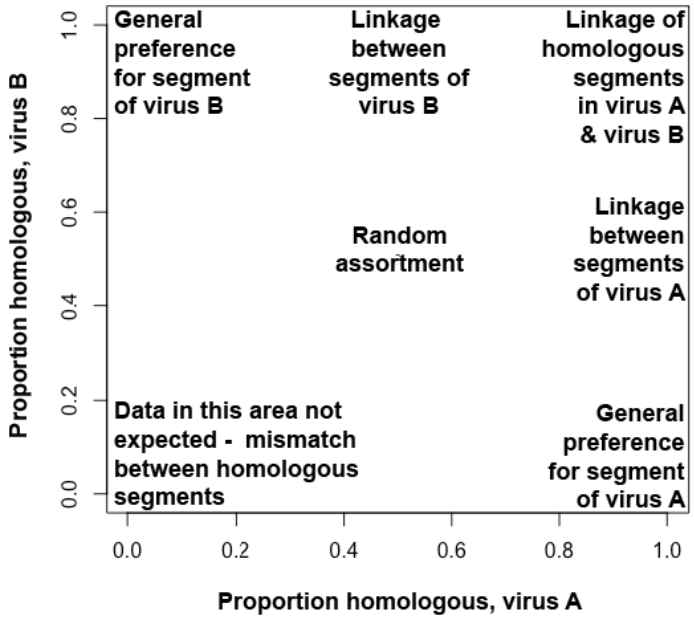

Figure 2. ***Pairwise analysis can reveal whether a given segment exchanges freely between viruses, is subject to specific pairwise linkages, or is generally favored or disfavored irrespective of gene constellation.***

Segments incorporated into reassortant progeny viruses were subjected to a pairwise analysis, and a scatterplot was generated for each of the eight segments. Data points corresponding to each of the other seven segments ($segment_i$) were plotted. The coinfecting viruses are here termed virus A and virus B. On the PB2 scatterplot, for example, the viruses carrying the PB2 of virus A are analyzed on the x axis and the viruses carrying the PB2 of virus B are analyzed on the y axis. On both axes, the proportion of viruses that carry the homologous combination of PB2 and $segment_i$ (AA or BB) is plotted. The interpretation of data points present in each area of the graph is indicated.

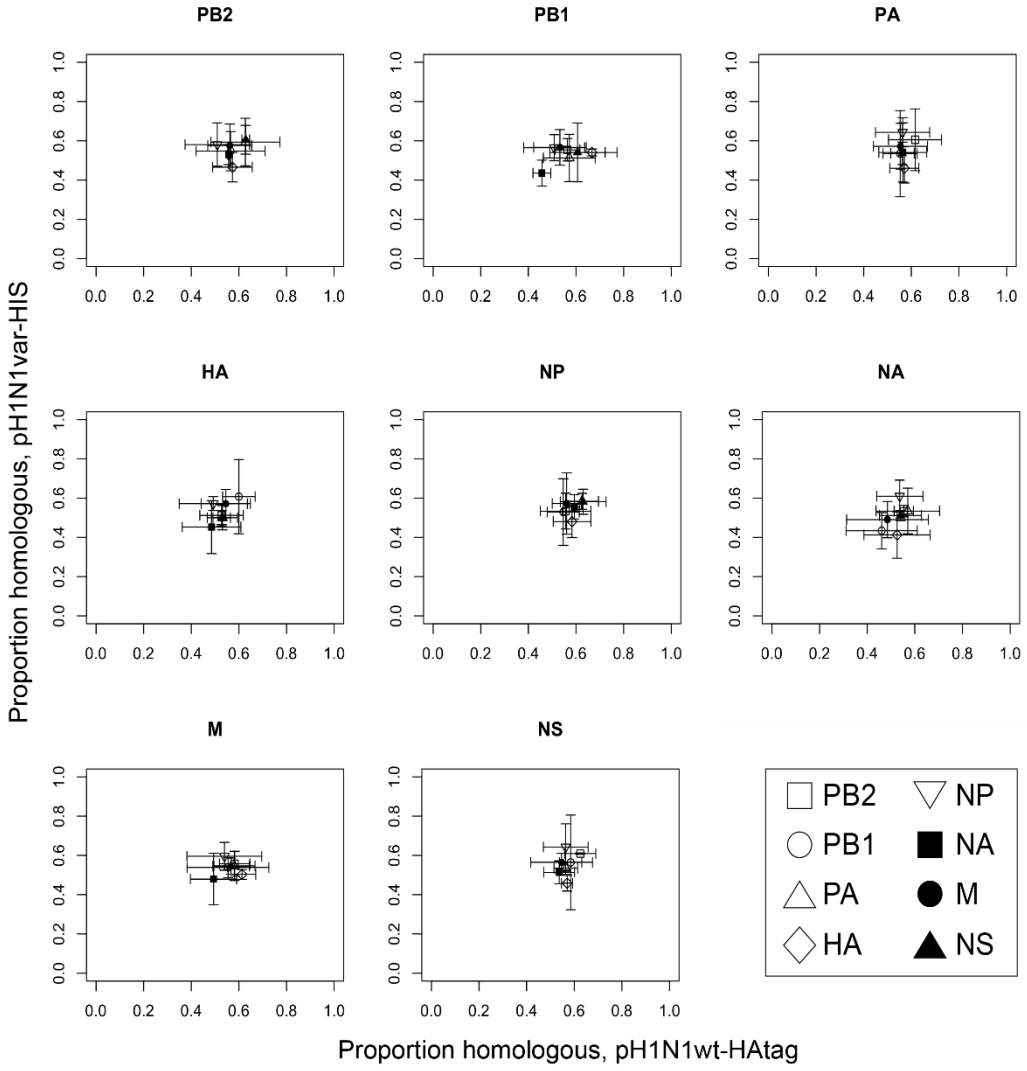

Figure 3. ***Pairwise analysis of segments incorporated into reassortant progeny indicates that reassortment between pH1N1wt-HAtag and pH1N1var-His viruses is random.***

The segment analyzed in each scatterplot is indicated above the plot area. On each graph, viruses with the indicated segment from pH1N1wt-HAtag are analyzed on the horizontal axis and viruses with the indicated segment from pH1N1var-His virus are analyzed on the vertical axis. The seven data points indicate the frequency with which homologous pairwise combinations were observed between the segment indicated at the top of the plot and segment$_i$

(as outlined in the legend to Fig. 2). Averages of results from three replicate coinfections are plotted, and error bars indicate standard deviations.

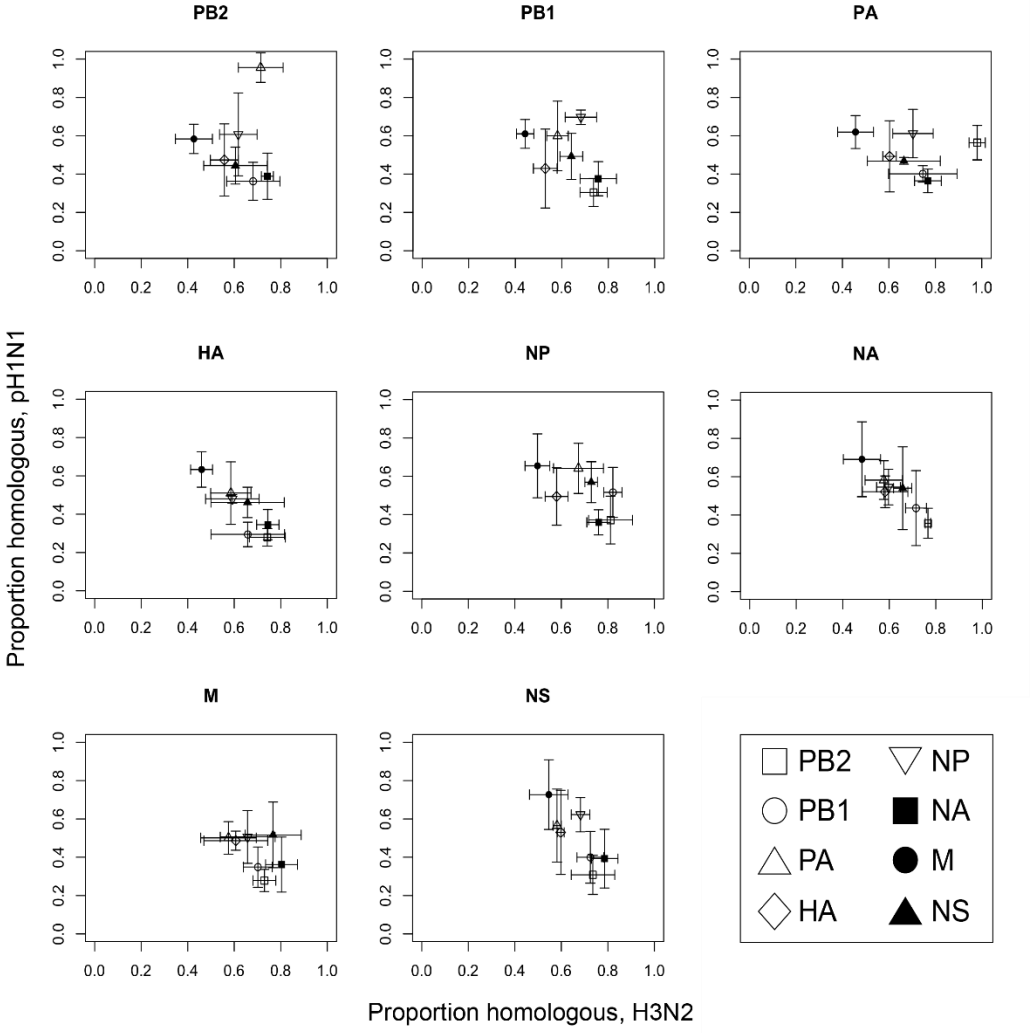

Figure 4. ***Pairwise analysis of segments incorporated into reassortant progeny following a single cycle of replication reveals biases in reassortment between pH1N1 and H3N2 viruses.*** Here, coinfections were performed in the absence of trypsin and with the addition of ammonium chloride at 3 h postinfection. Released virus was sampled at 24 h postinfection. The segment analyzed in each scatterplot is indicated above the plot area. On each graph,

viruses with the indicated segment from H3N2 virus are analyzed on the horizontal axis and viruses with the indicated segment from pH1N1 virus are analyzed on the vertical axis. The seven data points indicate the frequency with which homologous pairwise combinations were observed between the segment indicated at the top of the plot and segment$_i$ (as outlined in the legend to Fig. 2). Averages of results from three replicate coinfections are plotted, and error bars indicate standard deviations.

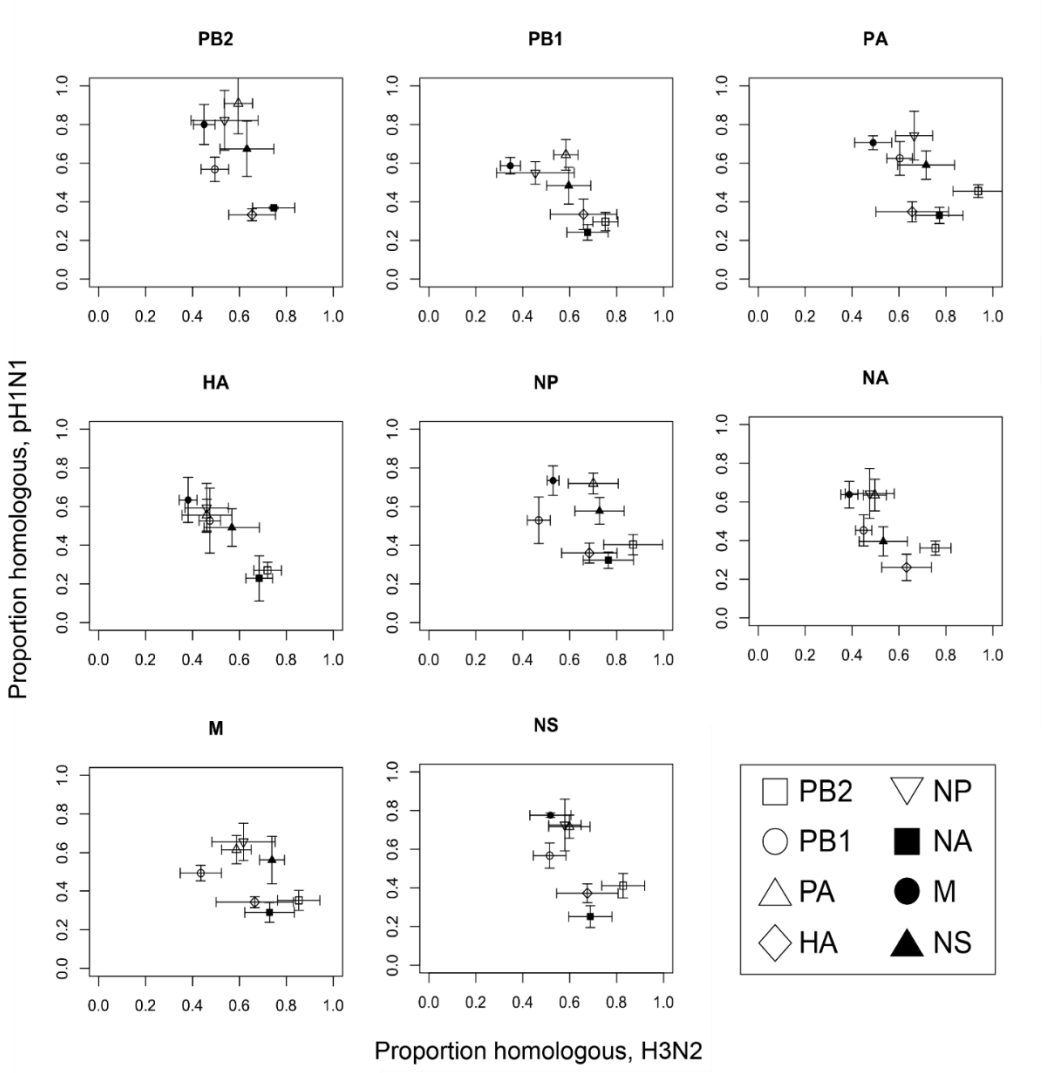

Figure 5. ***Pairwise analysis of segments incorporated into reassortant progeny following multiple rounds of replication reveals biases in reassortment between pH1N1 and H3N2 viruses.***

Here, coinfections were performed in the presence of trypsin and without the addition of ammonium chloride. Released virus was sampled at 24 h postinfection. The segment analyzed in each scatterplot is indicated above the plot area. On each graph, viruses with the indicated segment from H3N2 virus are analyzed on the horizontal axis and viruses with the indicated segment from pH1N1 virus are analyzed on the vertical axis. The seven data points indicate

the frequency with which homologous pairwise combinations were observed between the segment indicated at the top of the plot and segment$_i$ (as outlined in the legend to Fig. 2). Averages of results from three replicate coinfections are plotted, and error bars indicate standard deviations.

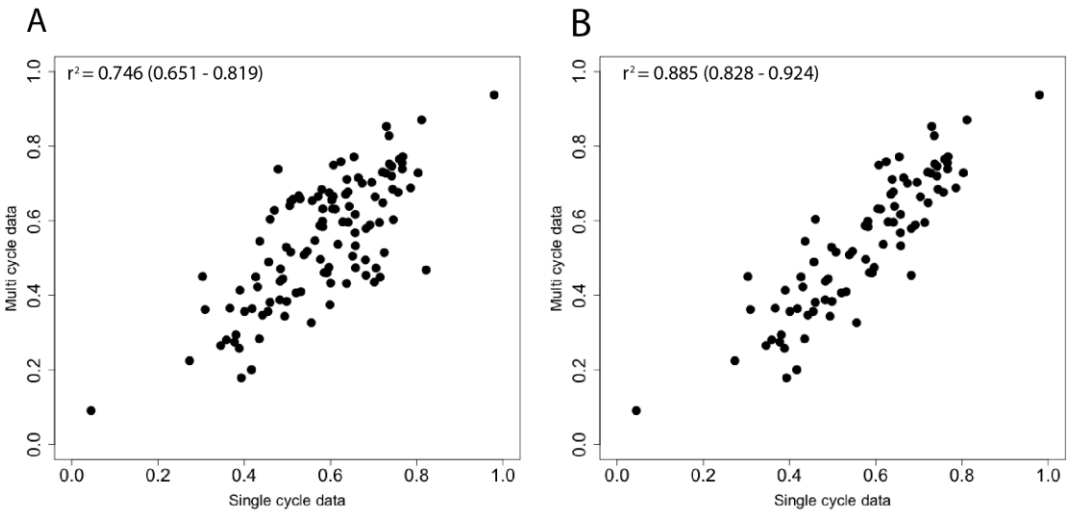

Figure 6. ***Results of single-cycle and multicycle coinfections with pH1N1 plus H3N2 viruses are well correlated.***

Correlation between full data sets was obtained from pairwise analysis of gene segments present in reassortant progeny viruses produced under single-cycle and multicycle conditions. The Pearson correlation coefficient, with 95% confidence interval, is indicated.

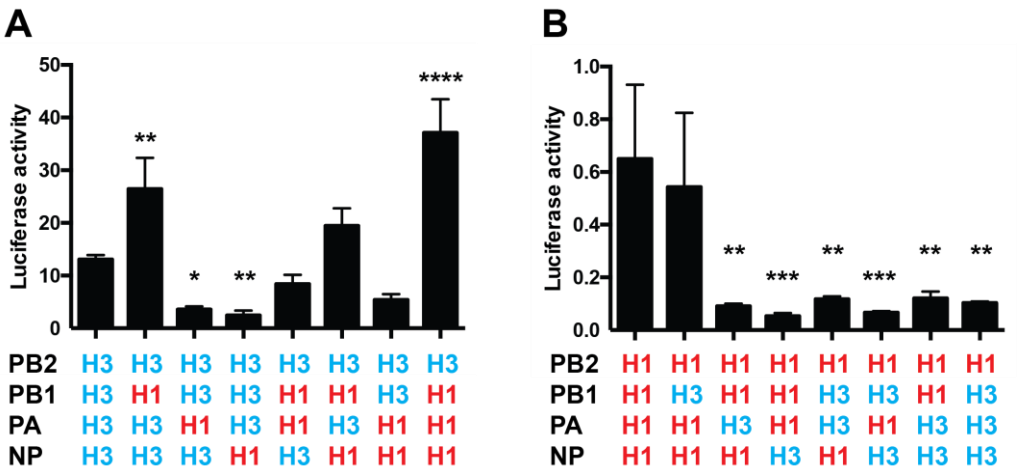

Figure 7. ***Activities of chimeric viral polymerase complexes in a minireplicon assay reflect reassortment patterns observed among PB2, PB1, PA, and NP segments***.

Viral polymerase complexes, comprising PB2, PB1, PA, and NP proteins plus a firefly luciferase reporter template flanked by the NP untranslated regions of WSN virus, were reconstituted by transient transfection of 293T cells. An expression vector encoding *Renilla* luciferase was included as a control for transfection efficiency, and firefly luciferase activity was normalized to *Renilla* luciferase activity to yield the values plotted. Each bar represents the average result of nine replicates derived from three transfections. Error bars represent standard deviations. One-way analysis of variance (ANOVA) with multiple comparisons was used to evaluate significance relative to the wild-type parental genotype plotted on the same graph. Samples displayed in panels A and B were run in parallel. The strain origin of each viral protein is indicated below the *x* axis, with H3 representing H3N2 and H1 representing pH1N1. (A) Activity of polymerase complexes with the H3N2 PB2; (B) activity of polymerase complexes with the pH1N1 PB2. *, $P < 0.05$; **, $P < 0.01$, ***, $P < 0.001$; ****, $P < 0.0001$.

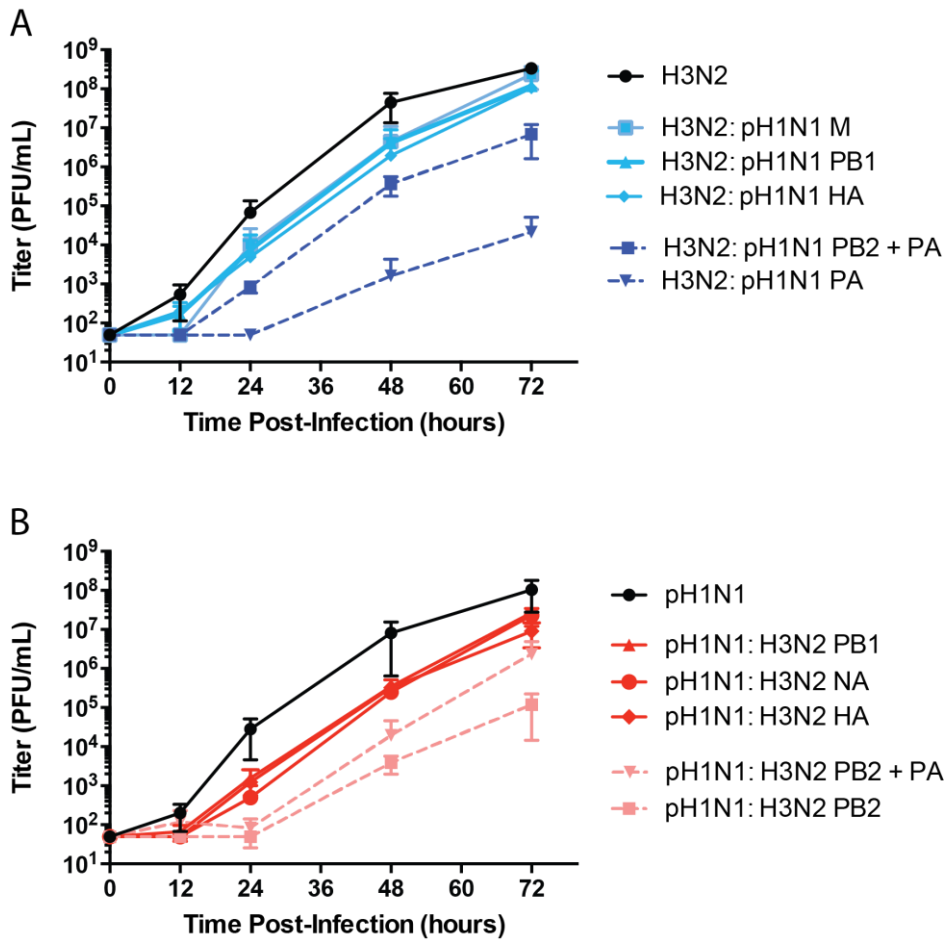

Figure 8. ***Growth in HTBE cells revealed attenuation of certain reassortant genotypes.***

Triplicate wells of fully differentiated HTBE cells were inoculated with the indicated viruses at an MOI of 0.001 PFU/cell and incubated at 33°C. Viral titers present in apical samples collected at the indicated time points were determined by a plaque assay on MDCK cells. The mean result of three replicates is plotted, with the standard deviation indicated by an error bar. (A) Growth of viruses with H3N2-derived PB2 in HTBE cells; (B) growth of viruses with pH1N1-derived PB2 in HTBE cells.

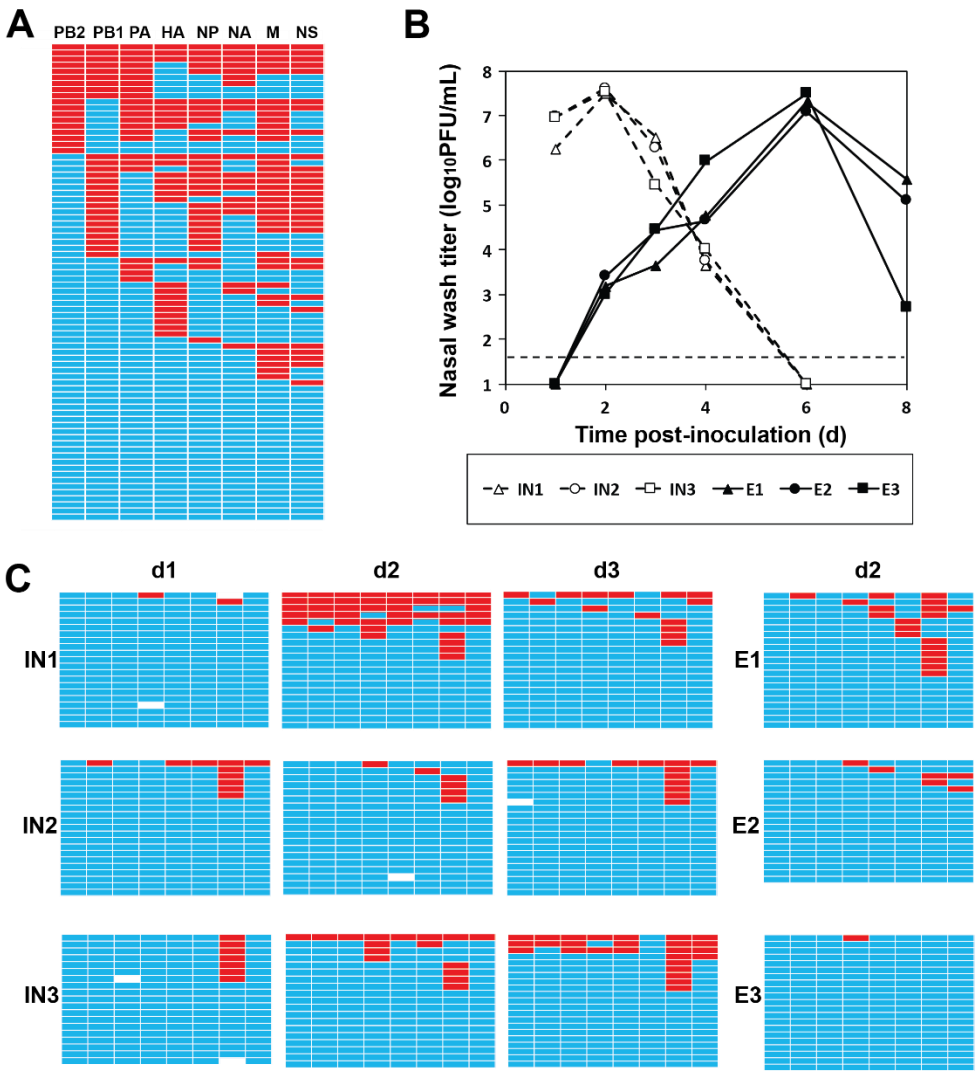

Figure 9. ***Reassortant viruses were detected in inoculated and contact guinea pigs following inoculation with a diverse population of viruses derived from pH1N1:H3N2 coinfection***.

Three guinea pigs were inoculated intranasally with 1 x 10^5 PFU of virus derived from a single-cycle coinfection in MDCK cells. At 24 h postinoculation, one naive guinea pig was placed in the same cage with each inoculated animal. (A) Viral genotypes detected in the inoculum included both parental gene constellations and a diverse set of reassortant viruses. Gene segments are identified above each column. Each row represents an individual plaque isolate derived from the coinfection supernatant. Turquoise, H3N2 origin; red, pH1N1 origin.

(B) Viral titers detected in nasal washes of inoculated (IN) and exposed (E) animals. Dashed lines represent inoculated animals, and solid lines represent contacts. A horizontal dashed line indicates the limit of detection (50 PFU/ml). (C) Viral genotypes detected in inoculated and exposed guinea pigs. Viral gene segments are represented schematically by eight colored bars arranged horizontally: PB2, PB1, PA, HA, NP, NA, M, and NS segments are shown from left to right. Turquoise indicates H3N2, red represents pH1N1, and white bars signify segments that could not be typed. The 18 to 21 viral isolates genotyped from each nasal lavage sample are grouped together. The guinea pig from which viruses were collected is indicated on the left. Time after inoculation is indicated in days above each column.

Table 1. P values associated with proportion homologous data[1]

		PB2	PB1	PA	HA	NP	NA	M	NS
Single-cycle coinfection	pH1N1 PB2	-	0.081	**0.011**	0.558	0.689	0.147	0.522	0.199
	pH1N1 PB1	**0.027**	-	0.680	0.418	**0.017**	0.076	0.295	0.499
	pH1N1 PA	0.804	**0.022**	-	0.648	0.483	**0.032**	0.292	**0.005**
	pH1N1 HA	**0.008**	**0.019**	0.719	-	**0.017**	**0.045**	0.255	0.194
	pH1N1 NP	0.131	0.702	0.346	0.592	-	**0.036**	0.389	0.779
	pH1N1 NA	**0.049**	0.421	0.631	0.620	0.945	-	0.336	0.947
	pH1N1 M	**0.013**	0.080	0.431	0.158	0.642	0.151	-	0.775
	pH1N1 NS	0.054	0.194	0.898	0.894	0.291	0.219	0.232	-
	Pan99 PB2	-	0.183	0.096	0.835	0.281	**0.003**	0.114	0.554
	Pan99 PB1	**0.029**	-	0.348	0.570	0.074	**0.043**	**0.032**	0.080
	Pan99 PA	**0.001**	0.147	-	0.073	0.089	**0.020**	0.172	0.329
	Pan99 HA	**0.048**	0.356	0.546	-	0.589	**0.017**	0.077	0.358
	Pan99 NP	**0.040**	**0.005**	0.182	0.399	-	**0.017**	0.233	**0.004**
	Pan99 NA	**1.01E-6**	**0.020**	0.618	0.619	0.249	-	0.284	**0.034**
	Pan99 M	**0.021**	**0.049**	0.741	0.544	0.252	**0.022**	-	0.088
	Pan99 NS	0.073	**0.031**	0.065	**0.010**	**0.024**	**0.017**	0.954	-
Multicycle coinfection	pH1N1 PB2	-	0.661	0.058	**0.004**	0.093	**1.15E-19**	0.051	0.272
	pH1N1 PB1	**0.009**	-	0.174	**0.041**	0.993	**0.004**	0.269	0.356
	pH1N1 PA	**0.031**	0.271	-	**0.019**	0.118	**0.009**	**0.013**	0.434
	pH1N1 HA	**0.006**	0.840	0.905	-	0.608	**0.041**	0.332	0.412
	pH1N1 NP	**0.037**	0.799	**0.029**	**0.021**	-	**0.009**	0.050	0.554
	pH1N1 NA	**0.009**	0.175	0.207	**0.017**	0.334	-	0.151	0.070
	pH1N1 M	**0.019**	0.136	0.254	**0.004**	0.194	**0.010**	-	0.870
	pH1N1 NS	0.062	0.684	**0.038**	**0.022**	0.150	**0.010**	**9.62E-07**	-
	Pan99 PB2	-	0.248	0.318	0.210	0.893	0.062	0.059	0.338
	Pan99 PB1	**0.020**	-	0.364	0.311	0.423	0.128	**0.012**	0.481
	Pan99 PA	**0.024**	0.230	-	0.357	0.127	0.061	0.319	0.142
	Pan99 HA	**0.035**	0.098	0.286	-	0.237	0.051	**0.012**	0.812
	Pan99 NP	**0.047**	0.100	0.132	0.186	-	0.072	0.296	0.098
	Pan99 NA	**0.031**	**0.031**	0.202	0.308	0.342	-	**0.013**	0.806
	Pan99 M	**0.027**	0.153	0.409	0.347	0.477	0.098	-	**0.022**
	Pan99 NS	**0.033**	0.482	0.436	0.238	0.530	0.120	0.601	-

[1]Values <0.05 are in bold face font and indicate that proportion homologous values obtained from pH1N1 plus H3N2 coinfection were significantly different from those observed following pH1N1wt plus pH1N1var coinfection (Student's *t* test).

Table 2. Primers used to genotype progeny isolated from mixed infections

Parental virus pairing	Primer name	Primer sequence
pH1N1wt plus pH1N1var	NL PB2 247 F	GGACAAACCCTCTGGAGCAA
	NL PB2 315 R	TACGGCCAGAGGTGATACCA
	NL PB1 225 F	CCCGATTGATGGACCACTACC
	NL PB1 311 R	TCAAGGAAAGCCATAGCCTCT
	NL PA 313 F	ACAACAGGGGTAGAGAAGCC
	NL PA 410 R	ATGTGGACTTCCCTCCGTGT
	NL HA 282 F	TGTGAATCACTCTCCACAGCA
	NL HA 361 R	CCTGGGTAACACGTTCCATTG
	NL NP 309 F	CCCTAAGAAAACAGGAGGACCC
	NL NP 411 R	TTGGCGCCAAACTCTCCTTA
	NL NA 293 F	CTGCCCTGTTAGTGGATGGG
	NL NA 368 R	GACAAACACATCCCCCTTGG
	NL M 256 F	ACGCTTTGTCCAAAATGCCC
	NL M 364 R	CTTGGCCCCATGGAACGTTA
	NL NS 320 F	GTCACGAGACTGGTTCATGC
	NL NS 389 R	CTGGTCCAATCGCACGCAAA
pH1N1 plus H3N2	P99 NL PB2 101 F	GTGGACCATATGGCCATAAT
	P99 NL PB2 187 R	TCATTGCCATCATCCARTTCAT
	P99 NL PB1 809 F	TTTGCGAAAAGCTTGAACAG
	P99 NL PB1 912 R	TGTGTCTTGTGAATTAGTCATCATC
	P99 NL PA 601 F	CAGTCCGAAAGAGGCGAAG
	P99 NL PA 755 R	CCCTCAATGCAGCCGTTC
	P99 NL NP 161 F	CTACATCCAAATGTGCACTG
	P99 NL NP 270 R	CTTCTCTCATCAAAAGCAGA
	P99 NL M 145 F	GGCTCTCATGGAATGGCTAA
	P99 NL M 258 R	CGTCTACGCTGCAGTCCTC
	P99 NL NS 539 F	TGAGGATGTCAAAAATGCA
	P99 NL NS 639 R	TTCTCCAAGCGAATCTCTGT
	P99 HA 802 F	ATTGCTCCTCGGGGTTACTT
	P99 HA 926 R	GGTTTGTCATTGGGAATGCT
	P99 NA 408 F	ATCAATTTGCCCTTGGACAG
	P99 NA 517 R	TGGAACACCCAACTCATTCA
	NL HA 345 F	GGAACGTGTTACCCAGGAGA
	NL HA 459 R	GATTGGGCCATGAACTTGTC
	NL NA 296 F	CCCTGTTAGTGGATGGGCTA
	NL NA 397 R	GGGGAGCATGATATGAATGG

References

1. Desselberger U, Nakajima K, Alfino P, Pedersen FS, Haseltine WA, Hannoun C, et al. Biochemical evidence that "new" influenza virus strains in nature may arise by recombination (reassortment). Proc Natl Acad Sci U S A. 1978;75(7):3341-5.

2. Scholtissek C. Molecular evolution of influenza viruses. Virus Genes. 1995;11(2-3):209-15.

3. Taubenberger JK, Kash JC. Influenza Virus Evolution, Host Adaptation, and Pandemic Formation. Cell Host & Microbe. 2010;7(6):440-51.

4. Schrauwen EJ, Fouchier RA. Host adaptation and transmission of influenza A viruses in mammals. Emerging microbes & infections. 2014;3(2):e9.

5. Ma EJ, Hill NJ, Zabilansky J, Yuan K, Runstadler JA. Reticulate evolution is favored in influenza niche switching. Proc Natl Acad Sci U S A. 2016;113(19):5335-9.

6. Holmes EC, Ghedin E, Miller N, Taylor J, Bao Y, St George K, et al. Whole-genome analysis of human influenza A virus reveals multiple persistent lineages and reassortment among recent H3N2 viruses. PLoS Biol. 2005;3(9):e300.

7. Nelson MI, Simonsen L, Viboud C, Miller MA, Holmes EC. The origin and global emergence of adamantane resistant A/H3N2 influenza viruses. Virology. 2009;388(2):270-8.

8. Nelson MI, Viboud C, Simonsen L, Bennett RT, Griesemer SB, St George K, et al. Multiple reassortment events in the evolutionary history of H1N1 influenza A virus since 1918. PLoS Pathog. 2008;4(2):e1000012.

9. Rambaut A, Pybus OG, Nelson MI, Viboud C, Taubenberger JK, Holmes EC. The genomic and epidemiological dynamics of human influenza A virus. Nature. 2008;453(7195):615-9.

10. Simonsen L, Viboud C, Grenfell BT, Dushoff J, Jennings L, Smit M, et al. The genesis and spread of reassortment human influenza A/H3N2 viruses conferring adamantane resistance. Mol Biol Evol. 2007;24(8):1811-20.

11. Westgeest KB, Russell CA, Lin X, Spronken MIJ, Bestebroer TM, Bahl J, et al. Genome-wide Analysis of Reassortment and Evolution of Human Influenza A(H3N2) Viruses Circulating between 1968 and 2011. Journal of Virology. 2014;88(5):2844-57.

12. Ince WL, Gueye-Mbaye A, Bennink JR, Yewdell JW. Reassortment complements spontaneous mutation in influenza A virus NP and M1 genes to accelerate adaptation to a new host. J Virol. 2013;87(8):4330-8.

13. Young JF, Desselberger U, Palese P. Evolution of human influenza A viruses in nature: sequential mutations in the genomes of new H1N1. Cell. 1979;18(1):73-83.

14. Zhdanov VM, Lvov DK, Zakstelskaya LY, Yakhno MA, Isachenko VI, Braude NA, et al. Return of epidemic A1 (H1N1) influenza virus. Lancet. 1978;1(8059):294-5.

15. Yamane N, Arikawa J, Odagiri T, Sukeno N, Ishida N. Isolation of three different influenza A viruses from an individual after probable double infection with H3N2 and H1N1 viruses. Jpn J Med Sci Biol. 1978;31(5-6):431-4.

16. Falchi A, Arena C, Andreoletti L, Jacques J, Leveque N, Blanchon T, et al. Dual infections by influenza A/H3N2 and B viruses and by influenza A/H3N2 and A/H1N1 viruses during winter 2007, Corsica Island, France. J Clin Virol. 2008;41(2):148-51.

17. Kendal AP, Lee DT, Parish HS, Raines D, Noble GR, Dowdle WR. Laboratory-based surveillance of influenza virus in the United States during the winter of 1977--1978. II. Isolation of a mixture of A/Victoria- and A/USSR-like viruses from a single person during an epidemic in Wyoming, USA, January 1978. Am J Epidemiol. 1979;110(4):462-8.

18. Mizuta K, Katsushima N, Ito S, Sanjoh K, Murata T, Abiko C, et al. A rare appearance of influenza A(H1N2) as a reassortant in a community such as Yamagata where A(H1N1) and A(H3N2) cocirculate. Microbiol Immunol. 2003;47(5):359-61.

19. Rith S, Chin S, Sar B, Y P, Horm SV, Ly S, et al. Natural coinfection of influenza A/H3N2 and A/H1N1pdm09 viruses resulting in a reassortant A/H3N2 virus. J Clin Virol. 2015;73:108-11.

20. Liu W, Li ZD, Tang F, Wei MT, Tong YG, Zhang L, et al. Mixed infections of pandemic H1N1 and seasonal H3N2 viruses in 1 outbreak. Clin Infect Dis. 2010;50(10):1359-65.

21. Myers CA, Kasper MR, Yasuda CY, Savuth C, Spiro DJ, Halpin R, et al. Dual infection of novel influenza viruses A/H1N1 and A/H3N2 in a cluster of Cambodian patients. Am J Trop Med Hyg. 2011;85(5):961-3.

22. Frank AL, Taber LH, Wells JM. Individuals infected with two subtypes of influenza A virus in the same season. J Infect Dis. 1983;147(1):120-4.

23. Poon LL, Song T, Rosenfeld R, Lin X, Rogers MB, Zhou B, et al. Quantifying influenza virus diversity and transmission in humans. Nat Genet. 2016;48(2):195-200.

24. Young JF, Palese P. Evolution of human influenza A viruses in nature: recombination contributes to genetic variation of H1N1 strains. Proc Natl Acad Sci U S A. 1979;76(12):6547-51.

25. Chen MJ, La T, Zhao P, Tam JS, Rappaport R, Cheng SM. Genetic and phylogenetic analysis of multi-continent human influenza A(H1N2) reassortant viruses isolated in 2001 through 2003. Virus Res. 2006;122(1-2):200-5.

26. Gregory V, Bennett M, Orkhan MH, Al Hajjar S, Varsano N, Mendelson E, et al. Emergence of influenza A H1N2 reassortant viruses in the human population during 2001. Virology. 2002;300(1):1-7.

27. Dudas G, Bedford T, Lycett S, Rambaut A. Reassortment between influenza B lineages and the emergence of a coadapted PB1-PB2-HA gene complex. Mol Biol Evol. 2015;32(1):162-72.

28. McCullers JA, Wang GC, He S, Webster RG. Reassortment and insertion-deletion are strategies for the evolution of influenza B viruses in nature. J Virol. 1999;73(9):7343-8.

29. Nelson MI, Edelman L, Spiro DJ, Boyne AR, Bera J, Halpin R, et al. Molecular epidemiology of A/H3N2 and A/H1N1 influenza virus during a single epidemic season in the United States. PLoS Pathog. 2008;4(8):e1000133.

30. Phillips PC. Epistasis--the essential role of gene interactions in the structure and evolution of genetic systems. Nat Rev Genet. 2008;9(11):855-67.

31. Essere B, Yver M, Gavazzi C, Terrier O, Isel C, Fournier E, et al. Critical role of segment-specific packaging signals in genetic reassortment of influenza A viruses. Proc Natl Acad Sci U S A. 2013;110(40):E3840-E8.

32. White MC, Steel J, Lowen AC. Heterologous packaging signals on HA, but not NA or NS, limit influenza A virus reassortment. J Virol. 2017;In Press.

33. Cobbin JC, Ong C, Verity E, Gilbertson BP, Rockman SP, Brown LE. Influenza virus PB1 and neuraminidase gene segments can cosegregate during vaccine reassortment driven by interactions in the PB1 coding region. J Virol. 2014;88(16):8971-80.

34. Mitnaul LJ, Matrosovich MN, Castrucci MR, Tuzikov AB, Bovin NV, Kobasa D, et al. Balanced hemagglutinin and neuraminidase activities are critical for efficient replication of influenza A virus. J Virol. 2000;74(13):6015-20.

35. Wagner R, Matrosovich M, Klenk HD. Functional balance between haemagglutinin and neuraminidase in influenza virus infections. Rev Med Virol. 2002;12(3):159-66.

36. Kaverin NV, Gambaryan AS, Bovin NV, Rudneva IA, Shilov AA, Khodova OM, et al. Postreassortment changes in influenza A virus hemagglutinin restoring HA-NA functional match. Virology. 1998;244(2):315-21.

37. Gottschalk A. The influenza virus neuraminidase. Nature. 1958;181(4606):377-8.

38. Gen F, Yamada S, Kato K, Akashi H, Kawaoka Y, Horimoto T. Attenuation of an influenza A virus due to alteration of its hemagglutinin-neuraminidase functional balance in mice. Arch Virol. 2013;158(5):1003-11.

39. Li C, Hatta M, Watanabe S, Neumann G, Kawaoka Y. Compatibility among polymerase subunit proteins is a restricting factor in reassortment between equine H7N7 and human H3N2 influenza viruses. J Virol. 2008;82(23):11880-8.

40. Hara K, Nakazono Y, Kashiwagi T, Hamada N, Watanabe H. Coincorporation of the PB2 and PA polymerase subunits from human H3N2 influenza virus is a critical determinant of the replication of reassortant ribonucleoprotein complexes. J Gen Virol. 2013;94(Pt 11):2406-16.

41. Octaviani CP, Goto H, Kawaoka Y. Reassortment between seasonal H1N1 and pandemic (H1N1) 2009 influenza viruses is restricted by limited compatibility among polymerase subunits. J Virol. 2011;85(16):8449-52.

42. Kim JI, Lee I, Park S, Bae JY, Yoo K, Lemey P, et al. Reassortment compatibility between PB1, PB2, and HA genes of the two influenza B virus lineages in mammalian cells. Sci Rep. 2016;6:27480.

43. Steel J, Lowen AC. Influenza A virus reassortment. Curr Top Microbiol Immunol. 2014;385:377-401.

44. Fonville JM, Marshall N, Tao H, Steel J, Lowen AC. Influenza Virus Reassortment Is Enhanced by Semi-infectious Particles but Can Be Suppressed by Defective Interfering Particles. PLoS Pathog. 2015;11(10):e1005204.

45. Marshall N, Priyamvada L, Ende Z, Steel J, Lowen AC. Influenza virus reassortment occurs with high frequency in the absence of segment mismatch. PLoS Pathog. 2013;9(6):e1003421.

46. Tao H, Steel J, Lowen AC. Intrahost dynamics of influenza virus reassortment. J Virol. 2014;88(13):7485-92.

47. Lakdawala SS, Wu Y, Wawrzusin P, Kabat J, Broadbent AJ, Lamirande EW, et al. Influenza a virus assembly intermediates fuse in the cytoplasm. PLoS Pathog. 2014;10(3):e1003971.

48. Chou YY, Heaton NS, Gao Q, Palese P, Singer R, Lionnet T. Colocalization of different influenza viral RNA segments in the cytoplasm before viral budding as shown by single-molecule sensitivity FISH analysis. PLoS Pathog. 2013;9(5):e1003358.

49. Goto H, Muramoto Y, Noda T, Kawaoka Y. The genome-packaging signal of the influenza A virus genome comprises a genome incorporation signal and a genome-bundling signal. J Virol. 2013;87(21):11316-22.

50. Mehle A, Doudna JA. Adaptive strategies of the influenza virus polymerase for replication in humans. Proc Natl Acad Sci U S A. 2009;106(50):21312-6.

51. Tao H, Li L, White MC, Steel J, Lowen AC. Influenza A virus coinfection through transmission can support high levels of reassortment. J Virol. 2015;89(16):8453-61.

52. Essere B, Yver M, Gavazzi C, Terrier O, Isel C, Fournier E, et al. Critical role of segment-specific packaging signals in genetic reassortment of influenza A viruses. Proc Natl Acad Sci U S A. 2013;110(40):3840-8.

53. Greenbaum BD, Li OT, Poon LL, Levine AJ, Rabadan R. Viral reassortment as an information exchange between viral segments. Proc Natl Acad Sci U S A. 2012;109(9):3341-6.

54. Rabadan R, Levine AJ, Krasnitz M. Non-random reassortment in human influenza A viruses. Influenza Other Respi Viruses. 2008;2(1):9-22.

55. Lubeck MD, Palese P, Schulman JL. Nonrandom association of parental genes in influenza A virus recombinants. Virology. 1979;95(1):269-74.

56. Octaviani CP, Ozawa M, Yamada S, Goto H, Kawaoka Y. High level of genetic compatibility between swine-origin H1N1 and highly pathogenic avian H5N1 influenza viruses. J Virol. 2010;84(20):10918-22.

57. Octaviani CP, Li C, Noda T, Kawaoka Y. Reassortment between seasonal and swine-origin H1N1 influenza viruses generates viruses with enhanced growth capability in cell culture. Virus Res. 2011;156(1-2):147-50.

58. Schrauwen EJ, Herfst S, Chutinimitkul S, Bestebroer TM, Rimmelzwaan GF, Osterhaus AD, et al. Possible increased pathogenicity of pandemic (H1N1) 2009 influenza virus upon reassortment. Emerg Infect Dis. 2011;17(2):200-8.

59. Schrauwen EJ, Bestebroer TM, Rimmelzwaan GF, Osterhaus AD, Fouchier RA, Herfst S. Reassortment between Avian H5N1 and human influenza viruses is mainly restricted to the matrix and neuraminidase gene segments. PLoS One. 2013;8(3):e59889.

60. Chen LM, Davis CT, Zhou H, Cox NJ, Donis RO. Genetic compatibility and virulence of reassortants derived from contemporary avian H5N1 and human H3N2 influenza A viruses. PLoS Pathog. 2008;4(5):e1000072.

61. Varich NL, Gitelman AK, Shilov AA, Smirnov YA, Kaverin NV. Deviation from the random distribution pattern of influenza A virus gene segments in reassortants produced under non-selective conditions. Arch Virol. 2008;153(6):1149-54.

62. Ma W, Lager KM, Lekcharoensuk P, Ulery ES, Janke BH, Solorzano A, et al. Viral reassortment and transmission after coinfection of pigs with classical H1N1 and triple-reassortant H3N2 swine influenza viruses. J Gen Virol. 2010;91(Pt 9):2314-21.

63. Snyder MH, Buckler-White AJ, London WT, Tierney EL, Murphy BR. The avian influenza virus nucleoprotein gene and a specific constellation of avian and human virus polymerase genes each specify attenuation of avian-human influenza A/Pintail/79 reassortant viruses for monkeys. J Virol. 1987;61(9):2857-63.

64. Naffakh N, Massin P, Escriou N, Crescenzo-Chaigne B, van der Werf S. Genetic analysis of the compatibility between polymerase proteins from human and avian strains of influenza A viruses. J Gen Virol. 2000;81(Pt 5):1283-91.

65. Sun Y, Qin K, Wang J, Pu J, Tang Q, Hu Y, et al. High genetic compatibility and increased pathogenicity of reassortants derived from avian H9N2 and pandemic H1N1/2009 influenza viruses. Proc Natl Acad Sci U S A. 2011;108(10):4164-9.

66. Smith GJ, Vijaykrishna D, Bahl J, Lycett SJ, Worobey M, Pybus OG, et al. Origins and evolutionary genomics of the 2009 swine-origin H1N1 influenza A epidemic. Nature. 2009;459(7250):1122-5.

67. Garten RJ, Davis CT, Russell CA, Shu B, Lindstrom S, Balish A, et al. Antigenic and genetic characteristics of swine-origin 2009 A(H1N1) influenza viruses circulating in humans. Science. 2009;325(5937):197-201.

68. Rudneva IA, Kovaleva VP, Varich NL, Farashyan VR, Gubareva LV, Yamnikova SS, et al. Influenza A virus reassortants with surface glycoprotein genes of the avian parent viruses: effects of HA and NA gene combinations on virus aggregation. Arch Virol. 1993;133(3-4):437-50.

69. Rudneva IA, Sklyanskaya EI, Barulina OS, Yamnikova SS, Kovaleva VP, Tsvetkova IV, et al. Phenotypic expression of HA-NA combinations in human-avian influenza A virus reassortants. Arch Virol. 1996;141(6):1091-9.

70. Macken CA, Webby RJ, Bruno WJ. Genotype turnover by reassortment of replication complex genes from avian influenza A virus. J Gen Virol. 2006;87(Pt 10):2803-15.

71. Nelson MI, Detmer SE, Wentworth DE, Tan Y, Schwartzbard A, Halpin RA, et al. Genomic reassortment of influenza A virus in North American swine, 1998-2011. J Gen Virol. 2012;93(Pt 12):2584-9.

72. Lam TT, Zhu H, Wang J, Smith DK, Holmes EC, Webster RG, et al. Reassortment events among swine influenza A viruses in China: implications for the origin of the 2009 influenza pandemic. J Virol. 2011;85(19):10279-85.

73. Li KS, Guan Y, Wang J, Smith GJ, Xu KM, Duan L, et al. Genesis of a highly pathogenic and potentially pandemic H5N1 influenza virus in eastern Asia. Nature. 2004;430(6996):209-13.

74. Neverov AD, Lezhnina KV, Kondrashov AS, Bazykin GA. Intrasubtype reassortments cause adaptive amino acid replacements in H3N2 influenza genes. PLoS Genet. 2014;10(1):e1004037.

75. Rudneva IA, Timofeeva TA, Shilov AA, Kochergin-Nikitsky KS, Varich NL, Ilyushina NA, et al. Effect of gene constellation and postreassortment amino acid change on the phenotypic features of H5 influenza virus reassortants. Arch Virol. 2007;152(6):1139-45.

76. Nelson MI, Vincent AL, Kitikoon P, Holmes EC, Gramer MR. Evolution of novel reassortant A/H3N2 influenza viruses in North American swine and humans, 2009-2011. J Virol. 2012;86(16):8872-8.

77. Centers for Disease C, Prevention. Update: Influenza A (H3N2)v transmission and guidelines - five states, 2011. MMWR Morb Mortal Wkly Rep. 2012;60(51-52):1741-4.

78. Watson SJ, Langat P, Reid SM, Lam TT, Cotten M, Kelly M, et al. Molecular Epidemiology and Evolution of Influenza Viruses Circulating within European Swine between 2009 and 2013. J Virol. 2015;89(19):9920-31.

79. Danzy S, Studdard LR, Manicassamy B, Solorzano A, Marshall N, Garcia-Sastre A, et al. Mutations to PB2 and NP proteins of an avian influenza virus combine to confer efficient growth in primary human respiratory cells. J Virol. 2014;88(22):13436-46.

80. Fodor E, Devenish L, Engelhardt OG, Palese P, Brownlee GG, Garcia-Sastre A. Rescue of influenza A virus from recombinant DNA. J Virol. 1999;73(11):9679-82.

81. Steel J, Lowen AC, Mubareka S, Palese P. Transmission of influenza virus in a mammalian host is increased by PB2 amino acids 627K or 627E/701N. PLoS Pathog. 2009;5(1):e1000252.

82. Chutinimitkul S, Herfst S, Steel J, Lowen AC, Ye J, van Riel D, et al. Virulence-Associated Substitution D222G in the Hemagglutinin of 2009 Pandemic Influenza A(H1N1) Virus Affects Receptor Binding. J Virol. 2010;84(22):11802-13.

83. Xu R, Zhu X, McBride R, Nycholat CM, Yu W, Paulson JC, et al. Functional balance of the hemagglutinin and neuraminidase activities accompanies the emergence of the 2009 H1N1 influenza pandemic. J Virol. 2012;86(17):9221-32.

84. Schwartz SL, Lowen AC. Droplet digital PCR: A novel method for detection of influenza virus defective interfering particles. J Virol Methods. 2016;237:159-65.

85. Tao H, Li L, White MC, Steel J, Lowen AC. Influenza A Virus Coinfection through Transmission Can Support High Levels of Reassortment. J Virol. 2015;89(16):8453-61.

86. Lowen AC, Mubareka S, Tumpey TM, Garcia-Sastre A, Palese P. The guinea pig as a transmission model for human influenza viruses. Proc Natl Acad Sci U S A. 2006;103(26):9988-92.

87. Lowen AC, Mubareka S, Steel J, Palese P. Influenza virus transmission is dependent on relative humidity and temperature. PLoS Pathog. 2007;3(10):1470-6.

Supplemental Information

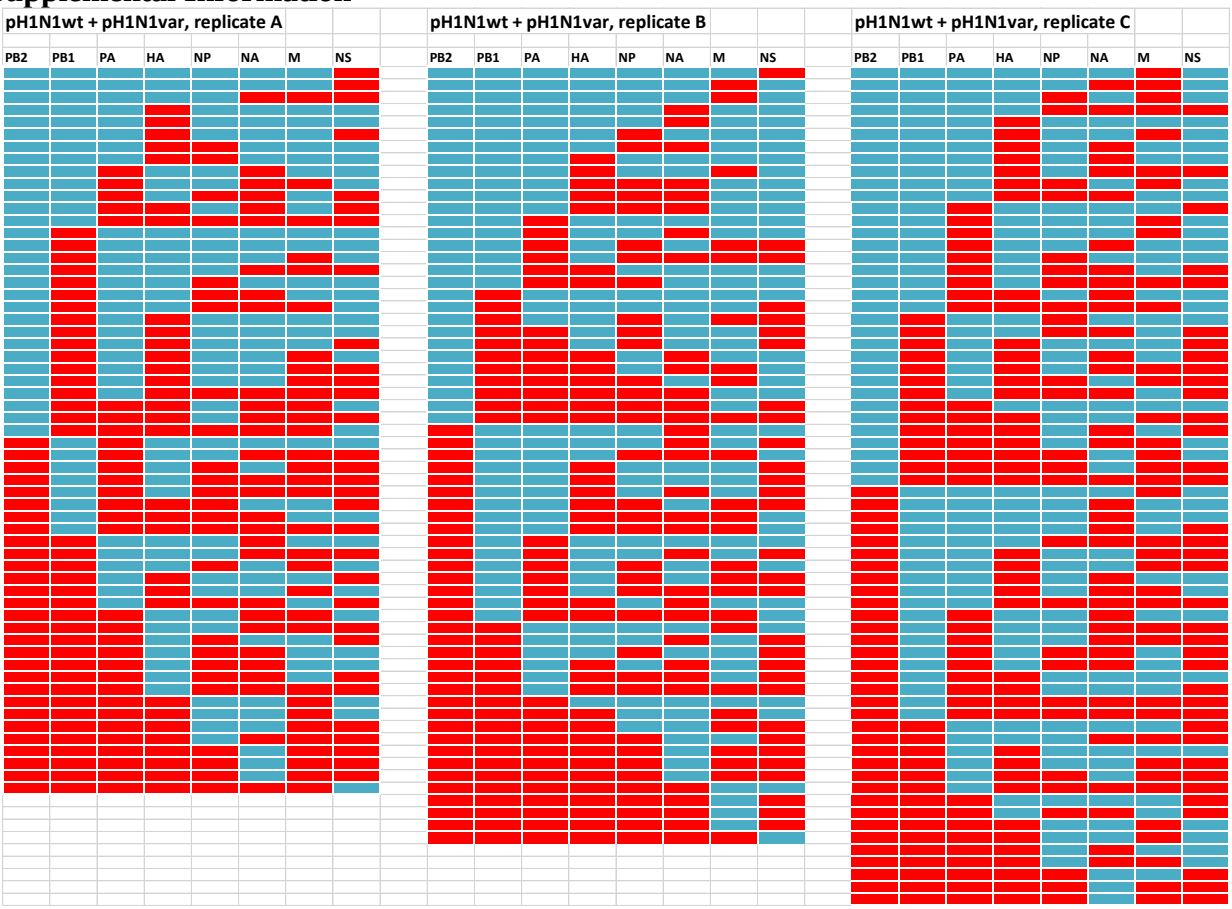

Supplementary Figure 1.

Genotypes of reassortant viruses derived from homologous co-infections performed under single cycle conditions. The genotypes of reassortant viruses sampled from homologous (pH1N1wt + pH1N1var) and heterologous (pH1N1 + H3N2) co-infections are listed in table format. These are the raw data used in the pairwise analysis presented in Figures 3, 4 and 5. Segments were color-coded using the Excel conditional formatting function to allow easy visualization of their origin. Turquoise represents segments derived from pH1N1wt. Red represents segments derived from pH1N1var.

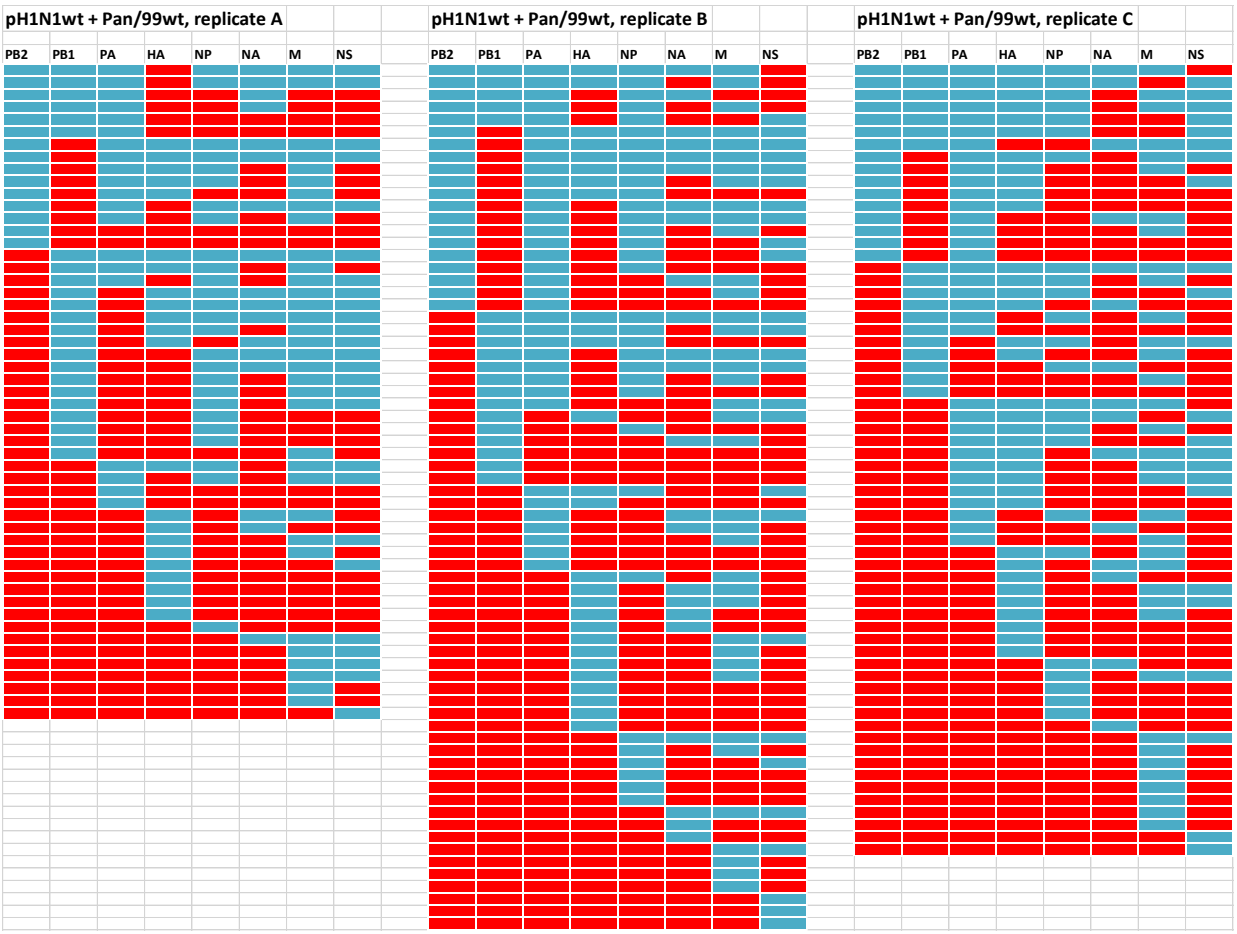

Supplementary Figure 2.

Genotypes of reassortant viruses derived from heterologous co-infections performed under single cycle conditions. Turquoise represents segments derived from pH1N1wt. Red represents segments derived from Pan/99wt.

Supplementary Figure 3.

Genotypes of reassortant viruses derived from homologous co-infections performed under multicycle conditions. Turquoise represents segments derived from pH1N1wt. Red represents segments derived from Pan/99wt.

Chapter III. Collective interactions augment influenza A virus replication in a host-dependent manner

Kara L. Phipps[a], Ketaki Ganti[a], Silvia Carnaccini[b], Miglena Manandhar[c], Nathan T. Jacobs[a], Brett E. Pickett[c], Gene S. Tan[c,d,f] Lucas M. Ferreri [b], Daniel R. Perez [b,e] and Anice C. Lowen[a,d]*

[a]Department of Microbiology and Immunology, Emory University School of Medicine, Atlanta, Georgia, United States of America

[b]Department of Population Health, Poultry Diagnostic and Research Center, University of Georgia, Athens, Georgia, United States of America.

[c]J. Craig Venter Institute, La Jolla, California, United States of America

[d]Emory-UGA Center of Excellence for Influenza Research and Surveillance (CEIRS), Atlanta, Georgia, United States of America

[e]Center of Research on Influenza Pathogenesis (CRIP) CEIRS, New York, New York, United States of America.

[f]Division of Infectious Disease, Department of Medicine, University of California San Diego, La Jolla, CA, United States of America

*Address correspondence: anice.lowen@emory.edu

Abstract

Infection with a single influenza A virus (IAV) is only rarely sufficient to initiate productive infection. Here, we exploit both single-cell approaches and whole-animal systems to show that the extent of IAV reliance on multiple infection varies with virus strain and host species. Influenza A/guinea fowl/HK/WF10/99 (H9N2) [GFHK99] virus exhibits strong dependence on collective interactions in mammalian systems. This reliance focuses viral progeny production within coinfected cells and therefore results in frequent genetic exchange through reassortment. In contrast, GFHK99 virus has greatly reduced dependence on multiple infection in avian systems, indicating a role for host factors in viral collective interactions. Genetic mapping implicated the viral polymerase as a major driver of multiple infection dependence. Mechanistically, quantification of incomplete viral genomes showed that their complementation only partly accounts for the observed reliance on coinfection. Indeed, even when all polymerase components are detected in single-cell mRNA sequencing, robust polymerase activity of GFHK99 virus in mammalian cells is reliant on multiple infection. In sum, IAV collective interactions not only augment reassortment, but can also overcome species-specific barriers to infection. These findings underscore the importance of virus-virus interactions in IAV infection, evolution and emergence.

Introduction

Classically, an infectious unit has been defined as a single virus particle which delivers its genome to a cell, initiates the viral reproductive program, and yields progeny viruses. Increasingly, however, the importance to infection of collective interactions among viruses is being recognized[87-89]. The delivery of multiple virus genomes to a cell allows both antagonistic and mutually beneficial interactions to occur, and these interactions in turn have the potential to shape transmission, pathogenicity, and viral evolutionary pathways.

Recent work has revealed several distinct mechanisms by which multiple viral genomes are co-delivered to a target cell. Diverse taxa including enterovirus, norovirus and rotavirus have all been observed to emerge from cells as groups of particles clustered within extracellular vesicles[90, 91]. Adhesion of virus particles to bacterial cell surfaces has a similar clustering effect and increases coinfection of target cells by poliovirus[92]. The aggregation of free virions was found to yield multi-particle infectious units in the case of vesicular stomatitis virus (VSV)[93, 94]. Various mechanisms of direct cell-to-cell spread also serve to deliver multiple viral genomes to the same cell[95-97]. The implications of multiple infection in these diverse systems are still being explored. In a number of cases, however, collective delivery was demonstrated to increase the efficiency of infection relative to free virus particles[90, 91], or to increase the rate of genetic exchange through recombination[92].

Whether brought about through coordinated infection with physically-linked virions or through independent infection events, the presence of multiple viral genomes within a cell creates the potential for their interaction to alter the course of infection. When distinct variants coinfect, mutually beneficial effects, such as reciprocal compensation for deleterious mutations, can increase overall fitness[98-100]. In the case of IAV, several lines of evidence point to a major role

in infection for multiplicity reactivation, the process by which segmented genomes lacking one or more functional segments complement each other[44, 101-104]. Conversely, negative interactions can also arise in which deleteriously mutated genes act in a dominant negative fashion. Defective interfering particles, which often potently interfere with the production of infectious progeny from a coinfected cell, are the most extreme example of such antagonism[105-107].

Importantly, multiple infection with identical viral genomes can also alter infection outcomes. Such cooperation was documented for VSV and HIV, where rates of transcription and replication were enhanced with increasing multiplicity of infection (MOI)[108, 109]. Similarly, faster kinetics of virus production were seen at high MOI for poliovirus and an H3N2 subtype IAV[104, 110]. In these instances, it is thought that increased copy number of infecting viral genomes provides a kinetic benefit important in the race to establish infection before innate antiviral responses take hold. Indeed, it has been suggested that multiple infection may be particularly relevant for facilitating viral growth under adverse conditions, such as antiviral drug treatment[89, 111].

For IAV, an important adverse condition to consider is that of a novel host environment. IAVs occupy a broad host range, including multiple species of wild waterfowl, poultry, swine, humans and other mammals[112, 113]. Host barriers to infection typically confine a given lineage to circulation in one species or a small number of related species[114, 115]. Spillovers occur occasionally, however, and can seed novel lineages. When a novel IAV lineage is established in humans, the result is a pandemic of major public health consequence[116, 117]. The likelihood of successful cross-species transfer of IAV is determined largely by the presence, absence, and compatibility of host factors on which the virus relies to complete its life cycle, and on the viruses' ability to overcome antiviral defenses in the novel host[118-120].

Owing to the segmented nature of the IAV genome, multiple infection results in viral genetic exchange through reassortment[2, 121]. If coinfecting viral genomes are distinct, reassortment will yield genotypic diversity that may facilitate evolution, including adaptation to a new host[5]. Indeed, reassortment involving human seasonal viruses and IAV adapted to non-human hosts was central to the emergence of the last three pandemic strains[66, 122]. Thus, among the interactions that occur between coinfecting viruses, reassortment is critical to consider for IAV.

Our objective herein was to assess the degree to which IAV relies on the delivery of multiple viral genomes to a cell to ensure production of progeny. In particular, we sought to determine whether this phenotype varies with host species and with virus strain. We therefore examined multiplicity dependence in avian and mammalian cells for two highly divergent avian-origin IAVs, influenza A/mallard/Minnesota/199106/99 (H3N8) [MaMN99] virus and influenza A/guinea fowl/Hong Kong/WF10/99 (H9N2) [GFHK99] virus. While MaMN99 virus is typical of IAV commonly isolated from wild ducks, GFHK99 virus is representative of the G1 lineage of H9N2 viruses prevalent in the poultry of Southeast Asia, Middle East, and North Africa[123, 124]. Results from all virus/cell combinations tested confirm prior reports that cells multiply-infected with IAV produce more viral progeny than singly-infected cells. Importantly, however, the proportion of viral progeny that emerge from coinfected cells varies greatly with virus-host context. The GFHK99 strain exhibits an acute dependence on multiple infection in mammalian cells that is not seen for MaMN99 virus in mammalian cells or for GFHK99 virus in avian cells. The polymerase of the GFHK99 virus drives its host-specific dependence on multiple infection. In line with this finding, both bulk and single-cell measurements of viral RNA showed that polymerase activity in mammalian cells is enhanced with multiple infection. A need for complementation of incomplete viral genomes partially accounts for this cooperative effect.

Importantly, however, single cell data indicate that additional multiplicity-dependent mechanisms support RNA synthesis by the GFHK99 virus in mammalian cells. Thus, our data point to an important role for multiple infection in determining the potential for IAV replication in diverse hosts.

Results

Virus-host interactions dictate degree of multiplicity dependence

To evaluate the extent to which IAV relies on multiple infection for productive infection, we initially used coinfection and reassortment as readouts. Reassortment is a useful measure for coinfection dependence because reassortant viruses must arise from coinfected cells. To ensure accurate quantification of reassortment, coinfections were performed under single-cycle conditions with homologous viruses that differ only by a silent mutation in each segment and the presence of either an HA or HIS epitope tag fused to the HA protein. Such homologous virus pairings were generated in both MaMN99 and GFHK99 strain backgrounds and were named MaMN99 WT / MaMN99 VAR and GFHK99 WT / GFHK99 VAR_1. Tracking of HA and HIS expression by flow cytometry provides a measure of infection that can be compared across cell lines. Quantification of cells expressing one or both epitope tags furthermore gives a means of assessing levels of coinfection across a range of MOIs.

Coinfection and reassortment between homologous viruses of the MaMN99 or GFHK99 strain backgrounds were examined in Madin-Darby canine kidney (MDCK), chicken DF-1 and human A549 cells (**Figure 1, Supplementary Figure 1**). Analysis of MDCK cells infected with the GFHK99 viruses at MOIs ranging from 10 to 0.01 PFU per cell revealed a near linear relationship between total HA^+ cells and dual-HA^+ cells, suggesting that the GFHK99 strain is

strictly dependent on multiple infection for HA expression in these cells (**Figure 1A**). HA production resulting from infection with a single strain was more common for GFHK99 in DF-1 cells or MaMN99 in MDCK cells, indicating a lesser dependence on multiple infection (**Figure 1A**). The more dependent expression of *any* HA protein is on coinfection, the more linear the relationship between the percentages of dual-HA^+ cells and HA^+ cells becomes. Conversely, a more quadratic relationship indicates less dependence on coinfection, as individual particles are more often able to express HA independently. We therefore quantified the degree of linearity from the regression models of each dataset and found that only GFHK99 virus in MDCK cells exhibits appreciable linearity in the relationship between HA+ and dual-HA+ cells (**Figure 1B**).

Genotyping of progeny virus from coinfections similarly revealed that reassortment levels vary by virus strain and cell type. In line with observed levels of coinfection, GFHK99 virus exhibits high levels of reassortment in MDCK cells even at low MOIs, indicating that nearly all progeny virus is produced from WT-VAR_1 coinfected cells (**Figure 1C**). GFHK99 coinfection in A549 cells is also characterized by high levels of reassortment, although less extreme than those seen in MDCK cells (**Supplementary Figure 1**). Compared to GFHK99, MaMN99 viruses infecting MDCK cells show lower levels of reassortment (**Figure 1C**). Moreover, reassortment of GFHK99 viruses is markedly reduced in DF-1 cells compared to that seen in MDCK cells (**Figure 1D**). These results clearly reveal differing degrees of multiplicity dependence for different virus/cell pairings and therefore indicate that multiple infection dependence, rather than solely being an intrinsic property of a virus strain, is determined through virus-host interactions.

That all virus/cell pairings tested show evidence of multiplicity dependence is highlighted by comparison of the experimental reassortment data to a theoretical prediction that assumes infection is perfectly efficient (**Figure 1C, 1D**). This theoretical prediction was published

previously[44] and is derived from a computational model in which the number of viral progeny produced by an infected cell is constant. Because singly- and multiply-infected cells make equivalent numbers progeny, reassortment is predicted to increase only gradually at low levels of infection (low %HA+) where coinfection is relatively rare. By contrast, reassortment observed experimentally reaches high levels much more rapidly. High reassortment indicates that viral progeny production is focused in the proportion of the infected cell population that is multiply infected. Coinfection dependence, therefore, is evident in all virus-cell pairings, but particularly strong for GFHK99 in MDCK cells.

***Strain and host specific phenotypes are also evident* in vivo**

To determine whether host-dependent reliance on multiple infection extended to *in vivo* infection, we performed coinfections with MaMN99 WT and VAR viruses in guinea pigs and GFHK99 WT and VAR_1 viruses in guinea pigs and quail. To ensure use of comparable effective doses for each virus/host pairing, the 50% infectious dose (ID_{50}) of each virus mixture was first determined experimentally in the animal models used. Guinea pigs were then infected intranasally with 10^2 $GPID_{50}$ of either the GFHK99 or MaMN99 WT/VAR mixture and nasal washes were collected daily. Japanese quail were infected with 10^2 QID_{50} of the GFHK99 virus mixture via an oculo-naso-tracheal route and tracheal swabs were collected daily. To evaluate the frequency of reassortment, plaque isolates from these upper respiratory samples were genotyped for each animal on each day. Because multicycle replication *in vivo* allows the propagation of reassortants, analysis of genotypic diversity rather than percent reassortment is more informative for these experiments. Thus, the effective diversity (Hill's N_2) was calculated for each dataset and plotted as a function of time post-inoculation (**Figure 1E, 1F**). The viruses collected from GFHK99 infected guinea

pigs show much higher genotypic diversity throughout the course of infection than viruses isolated from MaMN99 infected guinea pigs (**Figure 1E**) or GFHK99 infected quail (**Figure 1F**). These data indicate that the virus-host interactions which determine dependence on multiple infection in cell culture extend to *in vivo* infection.

Multiple infection enhances viral growth

The abundant reassortment observed with GFHK99 viruses in mammalian systems suggests that multiple infection plays a major role in determining the productivity of an infected cell. We therefore hypothesized that increasing MOI would augment the burst size, or viral output, of infected cells and that the magnitude of this effect would be greater for GFHK99 in MDCK cells than for GFHK99 in DF-1 cells or MaMN99 in MDCK cells. To test this prediction, we infected over a range of MOIs with the same mixtures of GFHK99 WT and VAR_1 or MaMN99 WT and VAR viruses used above and then measured PFU produced per cell under single-cycle conditions. Under non-saturating conditions (determined by flow cytometry to be MOI <1 PFU per cell, as shown in **Supplementary Figure 2**), increasing MOI resulted in accelerated viral growth and higher burst size for all three virus/cell pairings (**Figure 2A-C**). As predicted, however, increasing the MOI of GFHK99 in MDCK cells resulted in a further enhancement of viral amplification (**Figure 2D**). Thus, the benefit conferred by multiple infection was greater for GFHK99 in MDCK cells compared to either MaMN99 in MDCK cells or GFHK99 in DF-1 cells.

We reasoned that the cooperative effect observed might result from i) complementation of incomplete viral genomes or ii) a benefit of increased viral genome copy number per cell. In an effort to differentiate between these possibilities, we measured growth of GFHK99 in MDCK and DF-1 cells infected at a range of MOIs greater than 1 PFU per cell. Because these conditions are

saturating (**Supplementary Figure 2**), incomplete viral genomes are unlikely to be prevalent and any benefit of increasing MOI would be attributable to increasing genome copy numbers per cell. In both cell types, MOIs between 1 and 20 PFU per cell result in similar peak viral titers (**Figure 2E-F**). This saturation of cooperation at higher MOIs suggests diminishing returns from additional genome copies above a certain threshold. Calculation of fold change in viral amplification revealed that burst size was either unchanged or negatively affected by increasing MOI above 1 PFU per cell (**Figure 2G**). Whether this threshold is imposed by a need for complementation or another mechanism sensitive to saturation remained unclear. Overall, however, the increase in viral amplification with increased multiplicity at sub-saturating MOIs strengthened our prior conclusion that viral growth, and particularly productivity of GFHK99 virus in MDCK cells, is enhanced by multiple infection.

The viral polymerase is a major determinant of multiple infection dependence

To identify viral genetic determinants of multiple infection dependence, we mapped segments responsible for the high reassortment phenotype of GFHK99 in MDCK cells. Reverse genetics was used to place one or more genes from GFHK99 into a MaMN99 background. We created a panel of chimeras containing the HA, NP, or the full polymerase complex and NP (3PNP) of GFHK99 virus in the MaMN99 background. We also generated the reciprocal swap of this last genotype in which NS, M, NA and HA segments were derived from GFHK99. These segment groupings were selected for exchange based on their functions in the viral life cycle. For each chimeric genotype, homologous WT and VAR strains were generated to allow tracking of homologous reassortment.

Coinfections with matched WT and VAR strains were performed in MDCK cells and HA expression and reassortment were measured as in **Figure 1**. When levels of dual HA positivity are assessed, most MaMN99:GFHK99 chimeric genotypes cluster together with the parental MaMN99 virus, suggesting a relatively low dependence on multiple infection for HA expression (**Figure 3A-B**). By contrast, the MaMN99:GFHK99 3PNP genotype gives results similar to those of the parental GFHK99 (**Figure 3A-B**). Quantification of reassortment revealed that all chimeric viruses reassort at a higher frequency than MaMN99 parental strains but that the MaMN99:GFHK99 3PNP viruses show the highest reassortment, comparable to that seen for the parental GFHK99 genotype (**Figure 3C-D**). Thus, while other viral genes may make minor contributions, the viral polymerase is the primary genetic determinant of the high reassortment exhibited by GFHK99 in MDCK cells and defines a need for cooperation between coinfecting viruses.

Multiple infection enhances viral RNA replication

Because genetic mapping of the GFHK99 high reassortment phenotype implicated the viral polymerase, we sought to ascertain the effects of multiple infection on polymerase function. We therefore measured GFHK99 WT viral RNA synthesis in the absence and presence of increasing amounts of a homologous coinfecting virus. To evaluate host specificity, we did this analysis in both MDCK and DF-1 cells. The coinfecting virus, GFHK99 VAR_2, was generated in the GFHK99 background to avoid genetic incompatibility and carries silent mutations in each segment that disrupt primer binding sites. Cells were infected with low MOI (0.005 PFU per cell) of GFHK99 WT virus to ensure receipt of a single copy of the virus genome. Concurrently, cells were infected with increasing doses of GFHK99 VAR_2 virus. Digital droplet PCR (ddPCR) with primers specific

for GFHK99 WT cDNA was then used to quantify replication of WT genomes. The results show that, in both cell types, coinfection with low to moderate doses of the VAR_2 virus increases levels of GFHK99 WT vRNA (**Figure 4A**). At the highest doses of VAR_2 virus used, however, a suppressive effect is observed. Importantly, the amount of coinfection required to reach maximal vRNA production differs among cell lines: in MDCK cells 10-fold more VAR_2 virus (1 PFU per cell) is needed than in DF-1 cells (0.1 PFU per cell). The maximal impact of VAR_2 virus on WT vRNA production is also greater in MDCK cells: a ~60-fold enhancement is seen, compared to only ~2-fold in DF-1 cells.

To verify these observations in a more physiologically relevant system, we repeated the experiment in primary human tracheobronchial epithelial (HTBE) cells differentiated at an air-liquid interface. Similar to MDCK cells, these primary human cells exhibit maximal GFHK99 WT RNA production with addition of 1 PFU per cell GFHK99 VAR_2 virus (**Figure 4B**). Peak RNA replication is >10 fold higher in HTBE cells than without coinfecting virus.

Thus, in all three cell types tested, the introduction of coinfecting VAR_2 virus reveals a cooperative effect acting at the level of RNA synthesis. At very high doses of VAR_2 virus, WT RNA levels decline, suggesting competition for a limited resource at these extreme MOIs. Most notably, the magnitude of the cooperative effect and the amount of VAR_2 virus needed to reach maximal WT RNA levels are much greater in mammalian cells than avian cells. These differing outcomes indicate that the multiplicity dependence of GFHK99 polymerase function is modulated by host factors that differ between mammalian and avian hosts.

Multiple infection accelerates viral replication and transcription

To more finely assess the effects of multiplicity on polymerase function in various virus-host combinations, we measured vRNA, mRNA, and cRNA over time following low or high MOI infection (**Figure 5A**). MaMN99 and GFHK99 viruses were examined in MDCK cells and GFHK99 virus in DF-1 cells. To evaluate the activity of the viral polymerase when the encoding genes are supplied as low or single copies, a dose of 0.5 RNA copies per cell was used for infection. Under these low MOI conditions, all three viral RNA species accumulate at a significantly higher rate for GFHK99 in DF-1 cells and MaMN99 in MDCK cells than for GFHK99 in MDCK cells (**Figure 5B**). In defining a high MOI dose, we elected to use HA expressing units, as determined by flow cytometry, rather than genome copy number (**Supplementary Figure 3**). This measure gives a functional readout for polymerase activity, and therefore allows a dose to be chosen that ensures the vast majority of cells carry an active viral polymerase. The high MOI dose used was 3.0 HA expressing units per cell. At this high MOI, accumulation of GFHK99 mRNA, vRNA and cRNA in MDCK cells occurs at a similar rate to that seen for GFHK99 in DF-1 cells or MaMN99 in MDCK cells (**Figure 5C**). Thus, a host-specific defect in GFHK99 polymerase activity that affects synthesis of all three viral RNA species is seen at low MOI. This defect is, however, resolved under conditions where multiple infection is prevalent.

Single cell mRNA sequencing reveals a need for cooperation beyond complementation

An important limitation of working with bulk RNA extracted from a population of cells is the inability to distinguish between i) low, but uniform, RNA synthesis in all cells and ii) robust RNA synthesis in only a minority of cells. To elucidate the basis for cooperation at higher MOIs, it was important to determine which of these scenarios gives rise to the low average viral RNA levels that characterize low MOI infection with GFHK99 in MDCK cells. A highly heterogeneous

picture, with abundant viral RNAs in a minority of cells, would be expected if incomplete viral genomes are common but cells with a complete set of polymerase genes support robust viral RNA synthesis. Conversely, uniformly low levels of viral products would be expected if even complete viral genomes cannot support robust polymerase activity in the context of singular infection.

To evaluate the heterogeneity of viral RNA synthesis at the single cell level, we used single-cell mRNA sequencing. We infected DF-1 or MDCK cells with GFHK99 virus under single-cycle conditions and collected cells at 8 h post-infection for mRNA barcoding on the 10X Genomics Chromium platform prior to sequencing. The relative abundance of mRNA from each viral transcript was calculated by normalizing to the median number of transcripts per cell in that infection. Cells in which at least one viral mRNA molecule was detected were analyzed further. The number of cells that met this criterion ranged between 182 and 478 per infection condition (MOI and cell type combination). We found that the amount of detected GFHK99 viral mRNA varies widely between individual DF-1 cells (**Figure 6A**), which is consistent with previous observations[125]. In contrast, GFHK99 viral mRNA levels are uniformly low in MDCK cells under the relatively low MOI conditions used.

Because only subset of a cell's transcripts is captured and therefore reliably detected[126], the 10X platform does not allow a robust determination of segment presence or absence in a cell. Where viral mRNAs derived from a given segment are detected, however, one can conclude that the corresponding vRNA was present. To evaluate whether low transcript abundance corresponded to the lack of one or more polymerase-encoding segments, we therefore stratified the data based on detection of all four segments necessary to support transcription (PB2, PB1, PA and NP) (**Figure 6A**). Viral transcript levels are markedly increased in DF-1 cells that contained the PB2, PB1, PA, and NP segments compared to those in which one or more of these segments was not

detected. Averaging across all MOIs, a 10-fold increase in transcript abundance was noted in DF-1 cells ($p < 10^{-16}$, linear mixed effects model). In contrast, viral transcription in MDCK cells is consistently low, and the presence of polymerase complex confers no benefit (**Figure 6A**).

Data presented above from bulk samples indicate that multiple infection is needed for efficient GFHK99 transcription in MDCK cells. To measure the impact of coinfecting virus in individual cells, we repeated the single-cell sequencing experiment with the addition of genetically marked variants of GFHK99 virus. For an mRNA sequencing assay, marker mutations proximal to the poly-A tail of the viral transcripts are needed; we therefore generated variant viruses that carry synonymous nucleotide changes near the 5' end of each vRNA, GFHK99 $mVAR_1$ and GFHK99 $mVAR_2$. Cells were inoculated with GFHK99 WT and GFHK99 $mVAR_1$ viruses in a 1:1 ratio and the combined MOI was the same as that used for GFHK99 WT in the first experiment. Coinfection with GFHK99 $mVAR_2$ virus was performed simultaneously and this virus was used at the concentration found to be optimal for WT viral RNA replication in **Figure 4A**; the MOI therefore differed between DF-1 (0.1 PFU per cell) and MDCK (1.0 PFU per cell) cells. After mRNA sequencing, cells in which transcripts from all eight $mVAR_2$ virus segments were detected were analyzed further. Between 131 and 240 cells per infection condition (MOI, cell type, virus strain) met this criterion. The viral transcript levels per cell detected in this second experiment are shown in **Figure 6B** alongside data from the first experiment for comparison. In this figure, GFHK99 WT and GFHK99 $mVAR_1$ mRNAs are plotted separately; the concordance between these two datasets gives an indicator of reproducibility. In comparing the two infections, we observe that total viral transcript abundance is 72% lower in MDCK cells compared to DF-1 cells in the first infection ($p < 10^{-16}$, linear mixed effects model), but this effect is almost entirely mitigated by the presence of $mVAR_2$ virus, as transcript abundance is reduced by only 11% in

MDCK cells in the second infection ($p < 10^{-16}$, linear mixed effects model). This reduction in the disparity between DF-1 and MDCK cell viral transcript abundance resulted from the fact that $mVAR_2$ virus increased transcript abundance by 102% in DF-1 cells, but 545% in MDCK cells ($p < 10^{-16}$, linear mixed effects model) (**Figure 6B)**. These data underscore the significance of viral collective interaction to ensure productive infection in diverse hosts.

Frequency of incomplete GFHK99 genomes in MDCK cells is moderate

Our single-cell sequencing results suggest that the presence of a complete viral genome in the infected cell is not sufficient to support robust transcription of GFHK99 vRNAs. All eight viral gene segments are, however, necessary for productive infection[127] and could play an important role in the reliance of GFHK99 virus on multiple infection in mammalian systems. We therefore sought to quantify the frequency with which fewer than eight vRNAs are replicated in GFHK99 infected MDCK cells. Given the sensitivity limitations of the single-cell mRNA sequencing method, we employed a single-cell assay that we designed previously for this purpose[104]. MDCK cells were coinfected with a low MOI of GFHK99 WT virus and a high MOI of GFHK99 VAR_2 virus. The GFHK99 VAR_2 virus acts to ensure propagation of the WT virus gene segments, even when less than the full WT viral genome is available for transcription and replication. Following inoculation, single cells were sorted into wells which contain a naïve cell monolayer and multicycle replication was allowed for 48 h. To determine which viral gene segments were present in the initially sorted cell, RT-qPCR with primers that differentiate WT and VAR_2 gene segments was applied. As detailed in the Methods, the frequencies of VAR_2 virus infection, WT virus infection, and each distinct WT segment were used to estimate the probability that a cell infected with a single WT virus would contain a given segment. We termed the resultant parameter

Probability Present (P_P). The experimentally determined P_P values vary among the segments, with a range of 0.57 to 0.88 (**Figure 7A**). The product of the eight P_P values gives an estimate of the proportion of singular infections in which all eight segments are available for replication. This estimate is 6.5% for GFHK99 in MDCK cells.

The high reassortment of GFHK99 WT and VAR_1 viruses in MDCK cells indicates that progeny viruses predominantly originate from multiply infected cells in this system. To evaluate whether incomplete viral genomes account for this focusing of GFHK99 virus production within multiply infected cells, we used our previously published computational model of IAV coinfection and reassortment[44]. In this model, the frequency of segment delivery upon replication is governed by eight P_P parameters and an infected cell only produces virus if at least one copy of all eight segments are present. Importantly, in this model the amount of virus produced from productively infected cells is constant – there is no additional benefit to multiple infection. When the eight experimentally determined P_P values for GFHK99 virus in MDCK cells are used to parameterize the model, the theoretical prediction of reassortment frequency is much lower than that observed experimentally for GFHK99 WT and VAR_1 viruses in MDCK cells (**Figure 7B**). This discrepancy indicates that the frequency of missing segments cannot fully account for the high reassortment seen. Thus, the collective interactions on which the GFHK99 virus relies for replication in mammalian systems appears to extend beyond complementation. A full viral genome is necessary, but not sufficient, to support robust replication.

Discussion

Using small genetic tags and a range of molecular tools for their detection, we investigated the determinants of and mechanistic basis for IAV multiplicity dependence. Our data reveal that both

viral and host features dictate the degree to which productive IAV infection relies on cooperation. Thus, multiple infection dependence is a property determined through interaction between the virus and the infected cell, rather than an intrinsic property of the virus. Differences between virus strains and host systems in multiple infection dependence lead to phenotypic differences in the amount of reassortment that occurs upon coinfection. The demonstration of these reassortment differences in mammalian and avian models points to the relevance of viral collective interactions for IAV evolution and emergence. Mechanistically, our data indicate that multiple infection is needed in part for complementation of incomplete viral genomes, but that such complementation is not sufficient to ensure productive infection in all virus-host systems. Rather, we see that the GFHK99 polymerase requires a second form of cooperation to support efficient RNA synthesis in mammalian cells. For this reason, robust infection of GFHK99 virus in mammalian systems is achieved only in the context of high MOI infection. Thus, the data presented reveal that infection efficiency and the need for cooperation varies with virus-host context, and the viral polymerase is a major driver of this phenotype.

An important implication of viral genome segmentation is the potential for replication of incomplete genomes within infected cells[88]. For most segmented viruses of vertebrates, including IAV, each segment encodes at least one essential gene product and a genome lacking one or more functional segments cannot support the production of progeny viruses. Complementation is therefore a major class of collective interaction for viruses with segmented genomes, the relevance of which likely depends on the extent to which delivery and replication of the various genome segments is coordinated for a given virus species[128]. For IAV, we and others have demonstrated that, within singly-infected cells, a subset of segments fails to be replicated or expressed with high frequency[102, 104, 125]. Specifically, for influenza A/Panama/2007/99

(H3N2) virus in MDCK cells, we found that delivery of a single viral genome results in replication of all eight segments only 1.2% of the time[104]. Data reported herein for GFHK99 virus indicate that a somewhat higher proportion of replicated viral genomes are complete – namely, 6.5%. Thus, GFHK99 virus is partially dependent on complementation for productive infection in this cell line. However, the high levels of reassortment seen between GFHK99 WT and VAR_1 viruses in mammalian cells indicate that additional cooperative interactions are at play. This is made clear by the discrepancy between observed GFHK99 virus reassortment and the reassortment levels expected if complementation is the only cooperative effect considered. A necessary but insufficient role for complete viral genomes is further supported by the results of single cell mRNA sequencing of GFHK99 virus infected MDCK cells. Here, viral transcripts are produced at low copy numbers even when all four segments needed to support viral RNA synthesis are confirmed to be present. This outcome is in contrast to that observed for GFHK99 virus in DF-1 cells and to that reported previously for WSN virus in A549 cells, where the heterogeneity in viral transcript levels among cells could be attributed in part to the apparent absence of one or more polymerase complex genes[125]. Notably, however, the restriction of GFHK99 viral transcription in MDCK cells was largely mitigated by the addition of a homologous coinfecting virus. These data point to a model in which the presence of not just complete genomes, but rather multiple copies of the viral genome, are needed to overcome host-specific barriers to GFHK99 infection in mammalian systems.

Insight into the nature of this second cooperative interaction is gleaned from the observation that the amount of viral RNA produced from a constant input of GFHK99 WT viral genomes is significantly increased with the addition of a homologous virus that is genetically tagged to allow independent detection. Because GFHK99 WT virus RNAs can be quantified separately from the coinfecting VAR_2 virus RNAs, we can conclude that the coinfecting virus

functions in *trans* to support GFHK99 WT virus replication. This interaction is likely to occur at the protein level, with increased genome copy number supporting the expression of higher levels of viral polymerase proteins or cofactors. This proposed mechanism is supported by prior work showing that the IAV polymerase can act in *trans* to propagate temperature sensitive (ts) variants at non-permissive temperatures[129].

Our data implicate the viral polymerase in defining an acute reliance on cooperation for efficient viral RNA synthesis and viral progeny production. While our experiments focused on only two avian IAVs, it is well known that avian-adapted IAV polymerases require adaptive changes for efficient replication in mammalian cells[50, 118, 130]. The conformation or composition of the GFHK99 viral polymerase may lead to defects in transcription or replication due to poor interactions with mammalian host factors, such as ANP32A[131]. Low functionality of the viral polymerase complex may furthermore lead to the synthesis of abortive products, such as mini viral RNAs[132]. Thus, the multiplicity dependence of GFHK99 in mammalian systems may be a manifestation of poor adaptation of the viral polymerase to the host cell. Importantly, however, it appears that this lack of adaptation can be at least partially overcome when multiple viral genomes are delivered to the same cell. While MaMN99 virus is also not adapted to mammalian systems, it is only distantly related to GFHK99 virus and is representative of viruses that circulate in a taxonomically and geographically distinct avian population compared to the poultry hosts of GFHK99 virus. It will be important in future studies to delineate further the IAV lineages and host contexts in which an acute need for cooperation exists.

The clear involvement of the polymerase does not exclude the possibility that other virus-host interactions may impact the need for cooperation. In fact, reassortment levels measured for chimeric GFHK99-MaMN99 viruses indicated that other viral components contribute to the high

reassortment phenotype of GFHK99 virus. For example, it has been postulated that the pH of fusion of HA, which dictates when the viral genome is released from endosomes, determines the amount of time that viral gene segments are vulnerable to diffusion or degradation during transit to the nucleus [133]. Because stochastic loss of a subset of gene segments prior to nuclear import would likely be overcome through multiple infection, HA pH of fusion may determine the need for cooperation in some virus-host contexts. The contribution of particular viral proteins to coinfection dependence is relevant for understanding barriers to zoonotic infection and predicting the likelihood of reassortment following zoonoses.

The H9N2 subtype is of particular relevance in the context of zoonotic infection as viruses of this subtype are highly prevalent at the poultry-human interface, sporadic human infections have been reported, and H9N2 viruses share several related genes with H5N1 and H7N9 subtype viruses that have caused hundreds of severe human infections[134-139]. The G1 lineage to which the GFHK99 virus belongs circulates widely in the poultry of Southeast Asia and North Africa and reassorts frequently with other poultry adapted IAVs[123, 124, 140, 141]. The prevalence of reassortment suggests that the internal gene segments – which comprise the six non-HA, non-NA segments – are compatible with other genotypes. Our comparison of reassortment in guinea pigs and quail furthermore indicates that reassortment could be particularly prevalent in the context of zoonotic infection of mammals. This phenotype of high reassortment in mammals is expected to extend to the H5N1 and H7N9 subtype viruses of public health concern, which carry polymerase genes related to those of the GFHK99 virus[137-139]. While reassortment is typically deleterious owing to negative epistasis among heterologous segments[142, 143], a high frequency of reassortment creates greater opportunity for fit genotypes to arise and adapt, and should therefore be considered in assessing the risk of emergence posed by non-human adapted IAVs.

Our work reveals an underappreciated facet of virus-host interactions: the extent to which IAV relies on cooperation with coinfecting viruses is both strain and host dependent. Varied phenotypes of multiplicity dependence occurring in different virus-host contexts likely have important implications for viral fitness and viral evolution. Differences in coinfection dependence are expected to lead to differences in the viral dose required to establish a new infection, which in turn has implications for both the likelihood of transmission and the predominant mode of transmission. For example, transmission among close contacts is associated with the transfer of higher viral loads[144]. Reliance on cooperation is also expected to impact the spatial dynamics of viral spread within an individual[104]. For example, long-distance dispersal of virus within a host is less likely to be productive in a system where the virus is highly dependent on cooperative interactions[145]. Finally, the features which impact coinfection dependence are also likely to impact viral evolution by changing how a virus population samples the available sequence space. As discussed above, multiplicity dependence increases the opportunity for genetic exchange through reassortment, which may in turn slow the accumulation of deleterious mutations and allow coupling of advantageous mutations[146]. A need for cooperation would also be predicted to increase the likelihood that less fit variants are propagated as a result of phenotypic hiding in coinfected cells[147-149]. Thus, host and strain specificity in multiple infection dependence are likely to play an important role in determining the outcomes of IAV infection and evolution in diverse hosts.

Materials and Methods

Cells

Madin-Darby canine kidney (MDCK) cells, a gift from Peter Palese, Icahn School of Medicine at Mount Sinai were used in coinfection experiments, growth curves, and dosage experiments with increasing amounts of GFHK99 VAR_2 virus added. MDCK cells from Daniel Perez at University of Georgia were used for plaque assays as this variant of the MDCK line was found to yield more distinct plaques for the GFHK99 strain. Both MDCK cell lines were maintained in minimal essential medium (MEM; Gibco) supplemented with 10% fetal bovine serum (FBS; Atlanta Biologicals), penicillin (100 IU), and streptomycin (100 µg per mL) (PS; Corning). A549 cells (ATCC CCL-185) were maintained in F-12K nutrient mixture with L-glutamine (Corning) supplemented with 10% FBS and PS. 293T cells (ATCC CRL-3216) and DF-1 cells (ATCC CRL-12203) were maintained in Dulbecco's minimal essential medium (DMEM; Gibco) supplemented with 10% FBS and PS. Human tracheobronchial epithelial (HTBE) cells from a single donor were acquired from Lonza and were amplified and differentiated into air-liquid interface cultures as recommended by Lonza and described by Danzy et al.[79]. All cells were cultured at 37ºC and 5% CO_2 in a humidified incubator.

Viruses

All viruses used in this study were generated through reverse genetics[150]. 293T cells transfected with reverse genetics plasmids 16-24 h prior were injected into the allantoic cavity of 9-11 day old embryonated chicken eggs and incubated at 37ºC for 40-48 h. The resultant egg passage 1 stocks were used in experiments. Defective interfering segment content of PB2, PB1, and PA segments was confirmed to be minimal for each virus stock, following a method described previously[151]. The reverse genetics system for influenza A/guinea fowl/Hong Kong/WF10/99 (H9N2) virus was reported previously[152, 153]. This strain has been referred to as WF10 in previous

publications[152-154] but, for consistency with other strains used in the present manuscript, is referred to herein as GFHK99. A low passage isolate of influenza A/mallard/Minnesota/199106/99 (H3N8) virus, referred to herein as MaMN99, was obtained from David Stallknecht at the University of Georgia[155]. The virus was passaged once eggs and then the eight cDNAs were generated and cloned into the pDP2002 vector[156]. To increase the efficiency of virus recovery for rescues containing polymerase components from the MaMN99 virus, pCAGGS support plasmids encoding PB2, PB1, PA, and NP proteins of the A/WSN/33 (H1N1) strain were supplied.

GFHK99 WT and MaMN99 VAR viruses were engineered to contain a 6XHis epitope tag plus GGGS linker at the N terminus of the HA protein following the signal peptide. GFHK99 VAR_1 and MaMN99 WT viruses contain similarly modified HA genes, with an HA epitope tag plus a GGGS linker inserted at the N terminus of the HA protein[45].

Silent mutations introduced by site directed mutagenesis were used to confer altered melting properties to allow high resolution melt genotyping of WT and VAR_1 segment origin. Mutations introduced in to GFHK99 VAR_1 and MaMN99 VAR viruses are listed in **Supplementary Table 1**. Mutations introduced into the GFHK99 VAR_2 strain were designed to confer unique primer binding sites relative to GFHK99 WT virus for use in digital PCR-based genotyping. The mutations introduced are also listed in **Supplementary Table 1**. Viruses used for single cell mRNA sequencing, GFHK99 $mVAR_1$ and GFHK99 $mVAR_2$, were generated from the GFHK99 WT strain with no HIS tag, following the approach described in Russell et al.[125]. The mutations introduced were designed to be detected where sequence data is available from only the 3' end of each transcript. Site directed mutagenesis was therefore used to place two silent mutations proximal to the stop codon in each viral cDNA. The mutations allow differentiation among the segments of the three strains. All such mutations are reported in **Supplementary Table 1**.

Coinfection in cultured cells for quantification of coinfection and reassortment

MDCK, DF-1, or A549 cells were seeded at a density of 4 x10^5 cells per well in 6-well dishes 24 h before inoculation. Virus inoculum was prepared by combining WT and VAR viruses at high titer in a 1:1 ratio based on PFU titers, and then diluting in PBS to achieve MOIs ranging from 10 to 0.01 PFU per cell. Synchronized infection conditions were used, as follows. Cell monolayers were washed three times with PBS and placed on ice. Chilled virus inoculum was added to each well at a 250 µL volume and incubated at 4°C for 45 minutes with occasional rocking. Inoculum was aspirated and cell monolayer was rinsed three times with cold PBS before addition of warm virus medium. Due to low viral growth of GFHK99 virus in DF-1 cells, acid inactivation of inoculum virus was performed at 1 h post-infection for this cell type. For acid inactivation, media was aspirated and replaced with 500 µL of PBS-HCl, pH 3.00 and incubated 5 min at 37°C. Cells were then washed once with PBS before the addition of virus medium. At 3 h post-infection, virus medium was replaced with ammonium chloride-containing virus medium. GFHK99 virus infected cells were harvested at 12 h post infection due to high amounts of CPE at later time points. Cells infected with MaMN99 virus and MaMN99:GFHK99 chimeric viruses were harvested at 16 h post-infection. Virus medium for each cell line was prepared by supplementing the appropriate media (MDCK, MEM; DF1, DMEM; A549, F12K) with 4.3% bovine serum albumin and penicillin (100 IU), and streptomycin (100 µg per mL). Ammonium chloride-containing virus medium was prepared by the addition of HEPES buffer and NH_4Cl at final concentrations of 50 mM and 20 mM, respectively, to virus media.

Determination of infection levels based on HA surface expression. To enumerate infected cells, surface expression of HIS and HA epitope tags was detected by flow cytometry. This method was previously described in detail[45]. The percentage of cells that were positive for either or both epitope tags is expressed as percentage of cells HA^+. The percentage of cells that were positive for both epitope tags is expressed as percentage of cells dual-HA^+. The relationship between these two parameters was evaluated by plotting % cells dual-HA^+ against % cells HA^+ and regressing the resultant curve as a quadratic polynomial (*% cells dual-HA*$^+$ = β_2*(*% cells HA*$^+$)^2 + β_1*(*% cells HA*$^+$), where β_2 and β_1 are genotype-specific). From the regression models, we then quantified the degree of linearity using the equation $\% \, linearity = \frac{|\beta_1|}{|\beta_1|+|\beta_2|}$.

Animal models and reassortment **in vivo**

Quail eggs obtained from the College of Veterinary Medicine, University of Georgia, were hatched at the Poultry Diagnostic and Research Center, University of Georgia. Two days before virus inoculation, quail sera were confirmed to be seronegative for IAV exposure by NP ELISA (IDEXX, Westbrook, ME). At 3-weeks of age, birds were moved into a HEPA in/out BSL2 facility and each group divided into individual isolator units.

Groups (n=6) of 3-week old Japanese quail (Coturnix Japonica) were used to determine the 50% quail infectious dose of the 1:1 GFHK99 WT and GFHK99 VAR_1 virus mixture. Each quail was inoculated with 500 µL by oculo-naso-tracheal route of virus mixture in PBS, at increasing concentrations of 10^0 to 10^6 $TCID_{50}$ per 500 µL. Tracheal and cloacal swab specimens were collected daily from each bird in brain heart infusion media (BHI). Swab samples were analyzed by $TCID_{50}$ assay and titers of tracheal swabs collected at 4 d post-inoculation were used

to determine the QID_{50} by the Reed and Muench method[157]. Virus was not detected in cloacal swabs. QID_{50} was found to be equivalent to 1 $TCID_{50}$.

To quantify reassortment in quail, samples collected from quail (n=6) infected with the 10^2 $TCID_{50}$ dose of the 1:1 GFHK99 WT and GFHK99 VAR_1 virus mixture were used. These were the same birds as used to determine QID_{50}. Virus shedding kinetics were determined by plaque assay of tracheal swab samples and samples from days 1, 3, and 5 were chosen for genotyping of virus isolates.

Female Hartley strain guinea pigs weighing 250-350 g were obtained from Charles River Laboratories. The $GPID_{50}$ of GFHK99 WT/VAR_1 and MaMN99 WT/VAR virus mixtures were determined as follows. Groups of four guinea pigs were inoculated intranasally with virus mixture in PBS at doses of 10^0 to 10^5 PFU per 300 µL inoculum. Daily nasal washes were collected in 1 mL PBS and titered by plaque assay. Results from day 2 nasal washes were used to determine the $GPID_{50}$ by the Reed and Muench method[157]. The $GPID_{50}$ of GFHK99 virus was found to be 2.1 x 10^3 PFU, while that of MaMN99 virus was determined to be 2.1 x 10^1 PFU.

To evaluate reassortment kinetics in guinea pigs, groups of six animals were infected with 10^2 x $GPID_{50}$ of the aforementioned GFHK99 WT / VAR_1 virus mixture or the MaMN99 WT / VAR virus mixture. Virus inoculum was given intrasnasally in a 300 µL volume of PBS. Nasal washes were performed on days 1-6 post-inoculation and titered for viral shedding by plaque assay. HRM genotyping was performed on samples collected on day 1, 3, and 5 for each guinea pig.

Quantification of reassortment and effective diversity

Reassortment was quantified for *in vitro* coinfection supernatants, guinea pig nasal washes, and quail tracheal swabs as described previously[45]. Briefly, plaque assays were performed in 10 cm

dishes to isolate virus clones. 1 mL serological pipettes were used to collect agar plugs into 160 µL PBS. Using a ZR-96 viral RNA kit (Zymo), RNA was extracted from the agar plugs and eluted in 40 µL nuclease free water (Invitrogen). Reverse transcription was performed using Maxima RT (Thermofisher) according to the manufacturer's protocol. The resulting cDNA was diluted 1:4 in nuclease free water and each cDNA was combined with segment specific primers and Precision Melt Supermix (Bio-Rad) and analyzed by qPCR in a CFX384 Touch real-time PCR detection system (Bio-Rad) designed to amplify a ~100 bp region of each gene segment which contains a single nucleotide change in the VAR virus. The qPCR was followed by high-resolution melt (HRM) analysis to differentiate WT and VAR amplicons[158]. Precision Melt Analysis software (Bio-Rad) was used to determine the parental virus origin of each gene segment based on melting properties of the cDNAs and comparison to WT and VAR controls.

Viral genotypic diversity was quantified as reported previously[159] by calculating Simpson's Index, given by $D = \text{sum}(p_i^2)$, where p_i represents the proportional abundance of each genotype[160]. Simpson's Index accounts for both the raw number of species and variation in abundance of each, and is sensitive to the abundance of dominant species. Because Simpson's Index does not scale linearly, each sample's Simpson's Index value was converted to a corresponding Hill number to derive its effective diversity, $N_2 = 1/D$[161], which is defined as the number of equally abundant species required to generate the observed diversity in a sample community. Because it scales linearly, Hill's N_2 allows a more intuitive comparison between communities (i.e., a community with $N_2 = 10$ species is twice as diverse as one with $N_2 = 5$) and is suitable for statistical analysis by basic linear regression methods[162]. Robust linear models of N_2 vs. time were regressed using the R package robustlmm.

Single-cycle viral growth kinetics

DF-1 or MDCK cells were seeded at $4x10^5$ cells per well in 6 well dishes 24 h prior to infection. GFHK99 WT / VAR_1 virus mixture was serially diluted using PBS. Synchronized infection conditions as described above were used with acid inactivation of inoculum virus and addition of ammonium chloride medium at 3 h post-infection. At each time point, 120 µL supernatant was collected. Viral titers for each sample were assessed by plaque assay in MDCK cells. Each MOI condition was used in 5-6 wells in parallel infections. Three wells served as technical replicates for growth curve sampling while the remaining wells were harvested at 24 h post-infection to enumerate HA expressing cells via flow cytometry. In cases where acid inactivation was inefficient, the replicate was eliminated, and data are plotted in duplicate.

Effect of increasing multiple infection on viral RNA replication

For DF-1 and MDCK cell experiments, 12 well plates were seeded with $3x10^5$ cells per well 24 h prior to infection. For HTBE cells, cells were cultured at an air-liquid interface as previously described[79]. Cell surfaces were rinsed three times with PBS prior to inoculation. Triplicate wells were then mock infected with PBS or inoculated with 0.005 PFU per cell of GFHK99 WT and 0, 0.1, 0.5, 1, 3, and 5 PFU per cell of GFHK99 VAR_2 virus and placed at 37°C. After 55 minutes, inoculum was aspirated, and cells were rinsed three times with PBS and virus medium was added at 500 µL per well. Media was exchanged for ammonium chloride treated media 3 h later. At 12 h post infection, virus media was removed and cells were harvested using RNAprotect Cell Reagent (Qiagen). RNA was extracted using RNAeasy columns (Qiagen). RNA was diluted to 500 ng per µL for MDCK cells and 120 ng per µL for DF-1 cells. A 12 µL volume of this diluted RNA was used in reverse transcription with Maxima RT per protocol instructions. Digital droplet PCR was

performed on the resultant cDNA using a combination of PB2, M, and NS primers specific for the GFHK99 WT virus (final primer concentration of 200 nM) with QX200™ ddPCR™ EvaGreen Supermix (Bio-Rad). WT copy number is determined as cDNA copies per ng of input RNA. WT fold-change was calculated by dividing the copies/ng result obtain in each VAR_2 positive condition by value of copies per ng from the average of the triplicate WT-only samples.

Strand-specific quantification of viral RNA species over time

MOIs used in this experiment were 0.5 RNA copies per cell for the low MOI and 3.0 HA expressing units/cell for the high MOI. Concentrations of virus mixtures in RNA copies per mL were determined by quantifying at least four gene segments by ddPCR and taking the average. HA expressing units per mL was measured by counting HA positive cells via flow cytometry in the relevant cell type. Specifically, cells were infected with serial dilutions of virus under synchronized, single cycle conditions. At 24 h post infection, cells were harvested and flow cytometry was performed as described above, targeting His and HA epitope tags. HA expression units per mL for each virus and cell combination was calculated based on the linear range of $\%HA^+$ cells plotted as a function of volume of virus added to cells[163] (**Supplementary Figure 3**).

Viruses used for this experiment were the same GFHK99 WT/VAR_1 or MaMN99 WT/VAR virus mixtures used to measure reassortment, but in this case each mixture was considered as a single virus population (i.e. the RT ddPCR assay outlined below to quantify viral m/c/vRNA does not differentiate between WT and VAR genotypes).

Twelve well plates were seeded with $2x10^5$ cells per well of MDCK or DF-1 cells and incubated at 37°C for 24 h. Synchronized, single cycle infection conditions were used, as described above. Chilled virus was added at a volume of 125 µL per well. At 0, 1, 2, 4, 6, 8, and 10 h post

infection, virus medium was aspirated and cells were harvested using 400 µL of CELLprotect solution (Qiagen). RNA was extracted from infected cells using the Qiagen RNAeasy Mini kit. Three reverse transcription reactions per sample were set up with three different primers, each containing different nucleotide barcode tags and targeting a distinct species (mRNA, vRNA, and cRNA) of segment 8 (**Supplementary Table 4**). Maxima RT was used according to the manufacturer's instructions and combined with 300 ng MDCK or 150 ng DF-1 RNA.

Absolute copy number of cDNA was determined by ddPCR. Forward and reverse primers for vRNA, mRNA, or cRNA of NS at a total concentration of 200 nM were combined with diluted cDNA and QX200™ ddPCR™ EvaGreen Supermix (Bio-Rad). Primer sequences are given in **Supplementary Table 4**. Thermocycler protocol was as follows: 95ºC for 5 min, [95ºC for 30s, 57ºC for 60s] repeat 40x, 4ºC for 5 min, 90ºC for 5 min, 4ºC hold. Copy number was normalized to RNA input to give final results in units of copy number per ng RNA.

Single-cell mRNA sequencing

For this assay, viruses were titered in DF-1 cells using flow cytometry with anti-NP antibody (Abcam, clone 9G8). DF-1 cells were used because they give allow more sensitive detection of GFHK99 virus infection than MDCK cells. Cells were infected with serial dilutions of virus under synchronized, single-cycle conditions. At 24 h post-infection, cells were harvested and flow cytometry was performed as described above, targeting NP. HA expression units per mL for each virus and cell combination was calculated based on the linear range of % cells NP^+ plotted as a function of volume of virus added to cells[163] (**Supplementary Figure 3**).

To preform single-cell mRNA sequencing, MDCK and DF-1 cells were seeded into 6-well plates at $5x10^5$ cells per well. At 24 h post seeding, MDCK and DF-1 cells from an extra well were

harvested and re-counted to ensure accuracy of cell number for infection. MDCK or DF-1 cells were then infected with a 1:1 ratio of GFHK99 WT virus and GFHK99 $mVAR_1$ virus that amounted to a MOI of 0.02, 0.06, 0.2 or 0.6 NP units per cell. GFHK99 $mVAR_2$ virus was added to MDCK and DF-1 cell infections at MOIs of 1 PFU per cell and 0.1 PFU per cell, respectively. Virus stocks were diluted serially in cold 1X PBS and incubated on ice until use. Before infection, cells were washed three times with cold 1X PBS and placed on ice. To infect, cells were inoculated with a 200 µL volume inoculum (at appropriate concentrations) and placed on ice for 45 minutes, with rocking every 10 minutes. The inoculum was then aspirated and 2 mL of pre-warmed (at 37ºC) virus medium was added. Plates were incubated at 37ºC for 3 h. Afterwards, the virus medium was replaced with 2 mL of pre-warmed virus medium supplemented with HEPES buffer and NH_4Cl at final concentrations of 50 mM and 20 mM, respectively. Plates were placed back into the incubator for an additional 5 h. Subsequently, culture media was aspirated and cells washed once with 1X PBS. Cells were then trypsinized with 200 µL of 0.25% Trypsin EDTA until all cells came off the plate and were mono-dispersed. To each well, 0.5 mL of virus medium was added and replicates were pooled (2 wells per MOI). Cells for each sample were counted. Samples were spun at 150 rcf for 3 minutes and washed with 0.5 mL of 1X PBS/0.04% BSA. Washings were performed two more times. Finally, cells were resuspended with 1X PBS/0.04% BSA to get a final cell count of 7×10^5 cells per mL for each sample. Preparation for single-cell transcriptomic sequencing follows the protocol for 10x Genomics Chromium Single Cell platform.

Analysis of viral transcripts from single cells was performed with the sequencing data from all experiments in R using the CellRanger package (https://github.com/bpickett/Influenza-10X). Briefly, the CellRanger software assigns each read to individual cells and transcripts based on two sets of unique molecular identifiers that are ligated prior to amplification. This approach allows

the quantification of amplification bias at both the cellular and transcript levels. The first step of the analytical workflow was to map the reads to concatenated transcriptomes of IAV with the transcriptomes of dog or chicken to analyze MDCK and DF-1 cell infections, respectively. Protein coding regions for the dog and chicken transcriptomes were identified in the GTF file associated with genome builds CanFam3.1.94 and Gallus gallus-5.0.94, respectively, while IAV coding regions were extracted from the reverse-complement sequences of the GFHK99 strains. For each experiment, all transcripts with non-zero numbers of mapped reads were then normalized to the median number of transcripts per cell to enable cross-experiment comparison. The read counts for all eight unspliced IAV transcripts for each MOI and cell type were subsequently extracted from the complete set and saved in separate files. A quantitative analysis was then performed to compare the number of IAV transcripts that were identified from each of the experimental variables. Unless otherwise stated, data was analyzed using total viral transcripts, derived from all eight vRNA segments. The aligned sequencing data is available on the GEO database with the accession number GSE135553.

Single-cell sorting assay for measurement of P_P values

Segment specific P_P values were determined as previously described for influenza A/Panama/2007/99 (H3N2) virus[104], and as follows. $4x10^5$ MDCK cells were seeded into each well of a 6-well dish. 24 h later, cells were washed 3x with PBS and inoculated with 0.018 PFU per cell of GFHK99 WT virus and 1 PFU per cell of GFHK99 VAR_2 virus in a 250 µL volume of PBS. Virus was allowed to attach at 37ºC for 1 h. Inoculum was then removed and cells were rinsed 3x with PBS and 2 mL of virus medium was added to the well. After 1 h at 37ºC, medium was removed and cells were washed 3x with PBS and harvested by addition of Cell Dissociation

Buffer (Corning). Cells were resuspended in complete medium and washed 3x with 2 mL FACS buffer (2% FBS in PBS). A final resuspension step was performed in PBS containing 1% FBS, 10 mM HEPES, and 0.1% EDTA. Cells were strained through a cell strainer cap (Falcon) and sorted on a BD Aria II cell sorter. Gating was performed to remove debris and multiplets and one event per well was sorted into each well of a 96 well plate containing MDCK monolayers at 30% confluence in 50 µL virus medium supplemented with 1 ug per mL TPCK-treated trypsin. Following the sort, an additional 50 µL of virus medium plus trypsin was added to each well and plates were centrifuged at 1,800 rpm for 2 minutes to promote cell attachment. Plates were incubated at 37^{o}C for 48 h to allow propagation of virus from the sorted cell.

RNA was extracted from infected cells in the 96 well plate using a ZR-96 Viral RNA Kit (Zymo Research) per manufacturer instructions. Extracted RNA was converted to cDNA using universal influenza primers[164] and Maxima RT according to manufacturer instructions. After conversion, cDNA was diluted 1:4 with nuclease-free water and used as template (4 µL per reaction) for segment-specific qPCR using SsoFast EvaGreen Supermix (Bio-Rad) in 10 µL reactions, with 200 nM final primer concentration. Primers employed targeted each segment of GFHK99 WT virus, as well as the PB2 and PB1 segments of GFHK99 VAR_2 virus. Primer sequences are listed in **Supplementary Table 3**.

Given the MOI of GFHK99 WT virus used in the experiments, an appreciable number of wells are expected to receive two or more viral genomes, and so a mathematical adjustment is needed to estimate the probability of each genome segment being delivered by a single virion. Using the relationship between MOI and the fraction of cells infected from Poisson statistics, i.e., $f = 1 - e^{-\mathrm{MOI}}$, the probability of the ith segment being present in a singly infected cell, or $P_{P,i}$ can be calculated from the 96-well plate using the following equation:

$$P_{P,i} = \frac{\mathrm{MOI}_i}{\mathrm{MOI}_{\mathrm{wt}}} = \frac{-\ln(1 - f_i)}{-\ln(1 - f_{\mathrm{wt}})} = \frac{\ln(1 - \frac{C_i}{A})}{\ln(1 - \frac{B}{A})}$$

where A is the number of VAR_2^+ wells, B is the number of WT^+ wells (containing any WT segment), and C_i is the number of wells positive for the WT segment in question. Wells that were negative for VAR_2 virus segments were excluded from analysis.

Acknowledgements

We thank David Stallknecht (University of Georgia) for providing the A/mallard/MN/199106/99 (H3N8) biological isolate. We thank Hui Tao, Shamika Danzy, and Ginger Geiger for technical assistance. This work was funded in part by NIH R01 AI127799 (to ACL and DRP); NIH/NIAID Centers of Excellence in Influenza Research and Surveillance (CEIRS), contract numbers HHSN272201400004C (to ACL) and HHSN272201400008C (to DRP). Additional funds were provided by the Georgia Research Alliance and the Georgia Poultry Federation (to DRP) and NIH/NIAID Genomic Centers for Infectious Diseases (GCID), Award Number U19AI110819.

Figures and tables

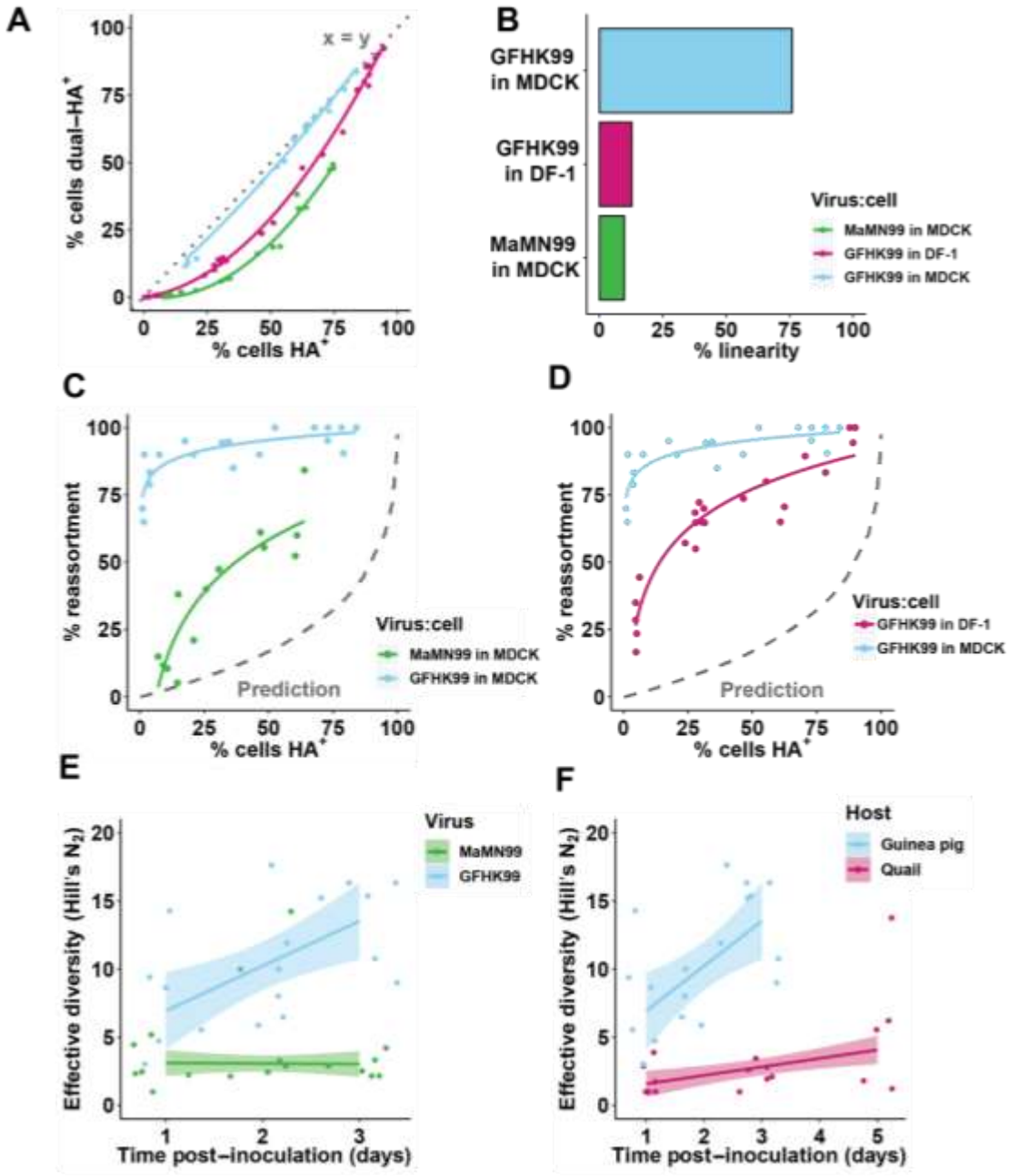

Figure 1. ***Coinfection and reassortment frequencies indicate that IAV multiplicity dependence varies with virus strain and host species.***

A-D) MDCK or DF-1 cells were coinfected with homologous WT and VAR viruses of either GFHK99 or MaMN99 strain backgrounds at a range of MOIs. Following a single cycle of infection, cells were analyzed for HA expression by flow cytometry and plaque clones derived from cell supernatants were genotyped. The relationship between % cells HA positive and % cells dually HA positive (A) varies with strain and cell type, resulting in curves of differing % linearity (B). GFHK99 and MaMN99 viruses exhibit different reassortment levels in MDCK cells, but both show high reassortment relative to a theoretical prediction in which singly infected and multiply infected cells have equivalent burst sizes (C). GFHK99 virus reassortment levels differ in MDCK and DF-1 cells, but reassortment under both conditions remains high relative to the theoretical prediction in which multiple infection confers no advantage (D). In guinea pigs (n=6), GFHK99 WT and VAR_1 viruses exhibit higher reassortment than MaMN99 WT and VAR viruses, as indicated by increased genotypic diversity (E). The GFHK99 WT and VAR_1 viruses exhibit higher reassortment in guinea pigs than in quail (n=5) (F). Guinea pig data shown in panels E and F are the same. Shading represents 95% CI.

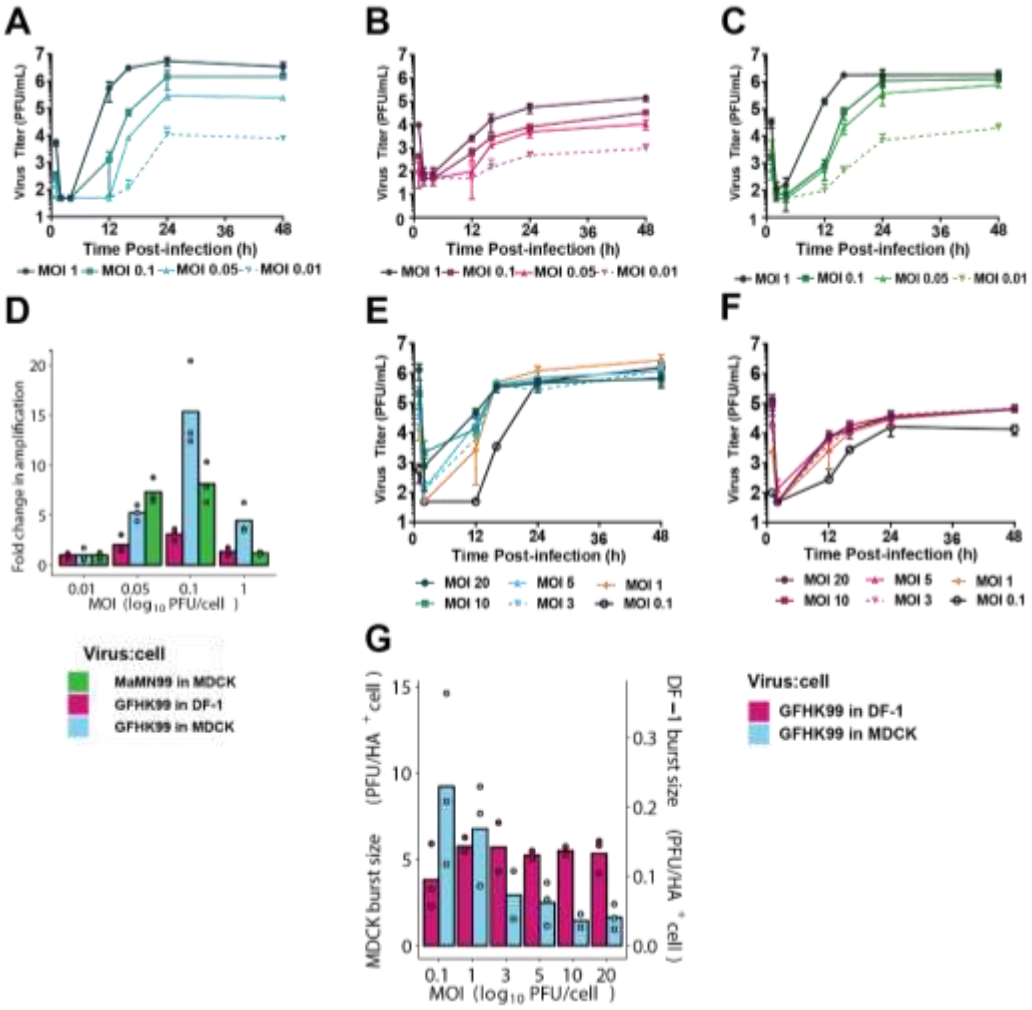

Figure 2. ***Increasing MOI increases viral productivity at sub-saturating, but not saturating MOIs.***

MDCK and DF-1 cells were infected under single cycle conditions at a range of MOIs in triplicate wells for each MOI. A-C, E-F) Viral titers observed at the indicated MOIs are plotted against time post-infection. D) Fold change in amplification (viral input / maximum output) relative to the MOI=0.01 PFU per cell condition is plotted for each virus-cell pairing. G) Burst size, calculated as maximum PFU output / number of HA^+ cells detected by flow cytometry, is plotted for each virus-cell pairing tested in the higher MOI range.

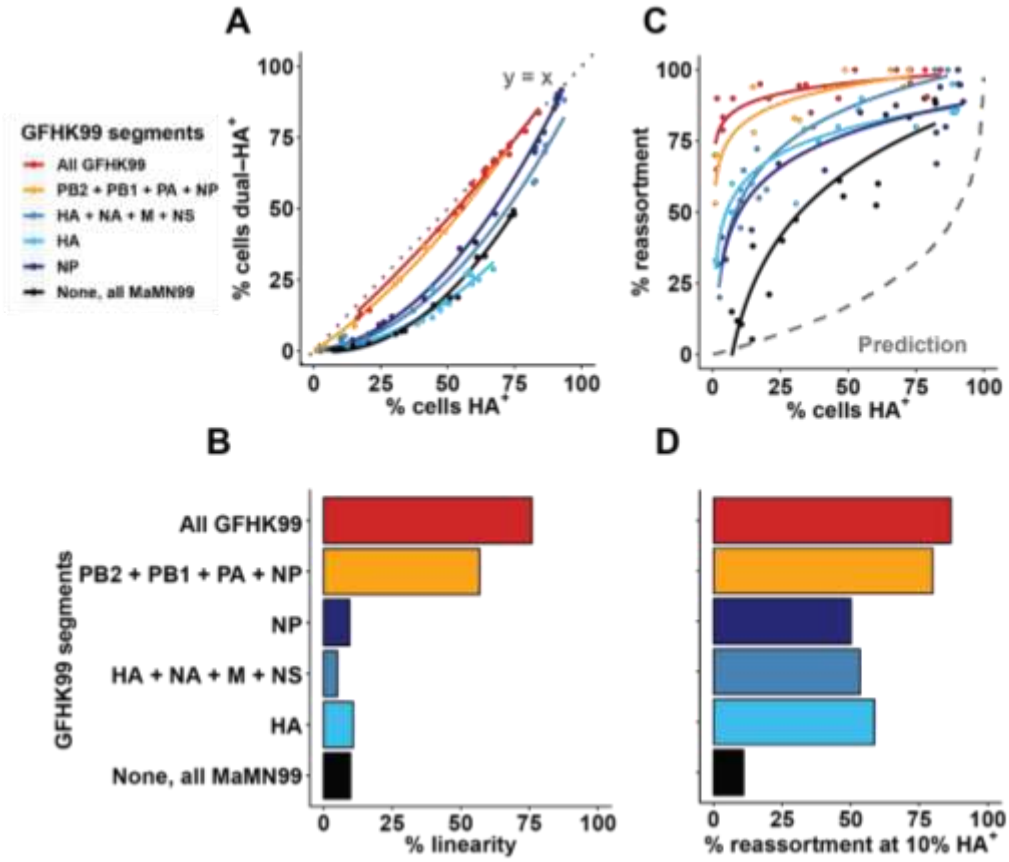

Figure 3. ***Coinfection and reassortment of chimeric viruses reveals a major role for the viral polymerase.***

Reverse genetics was used to place one or more genes from GFHK99 virus into a MaMN99 background. Coinfections with homologous WT and VAR strains were performed in MDCK cells as in Figure 1. The relationship between % cells HA positive and % cells dually HA positive (A) varies with genotype, resulting in curves of differing % linearity (B). Reassortment levels vary with genotype (C), with the chimeric strain carrying GFHK99 PB2, PB1, PA and NP segments exhibiting comparable levels to GFHK99. Experimental results are compared to a theoretical prediction in which singly infected and multiply infected cells have equivalent burst sizes (Prediction). Differences in reassortment levels among the viruses tested are highlighted

by plotting the % reassortment at 10% HA^+ cells, as interpolated from each regression curve (D). Data shown for GFHK99 and MaMN99 viruses are the same as those displayed in Figure 1.

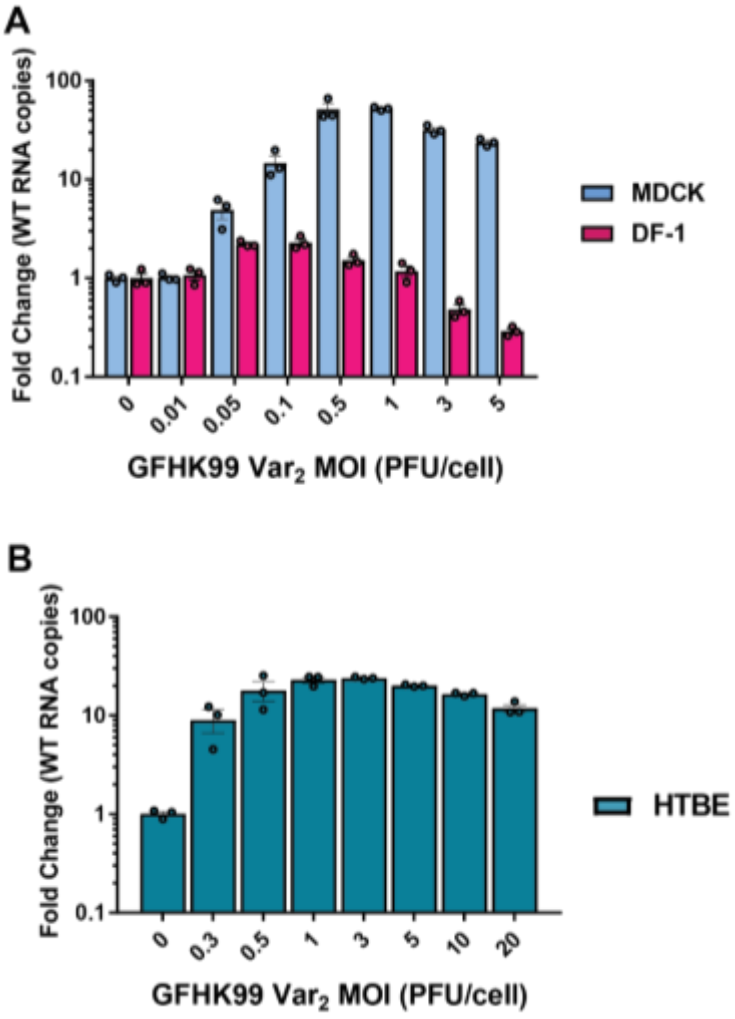

Figure 4. ***Coinfection enhances GFHK99 vRNA synthesis in a dose and host dependent manner.***

Cells were coinfected with 0.005 PFU per cell of GFHK99 WT virus and increasing doses of GFHK99 VAR_2 virus. A) In MDCK and DF-1 cells, the fold change in WT vRNA copy number, relative to that detected in the absence of GFHK99 VAR_2 virus, is plotted for various doses of GFHK99 VAR_2 virus. B) In HTBE cells, the fold change in WT vRNA copy number, relative to that detected in the absence of GFHK99 VAR_2 virus, is plotted for various doses of GFHK99 VAR_2 virus. n=3 cell culture dishes per condition. Error bars represent standard deviation.

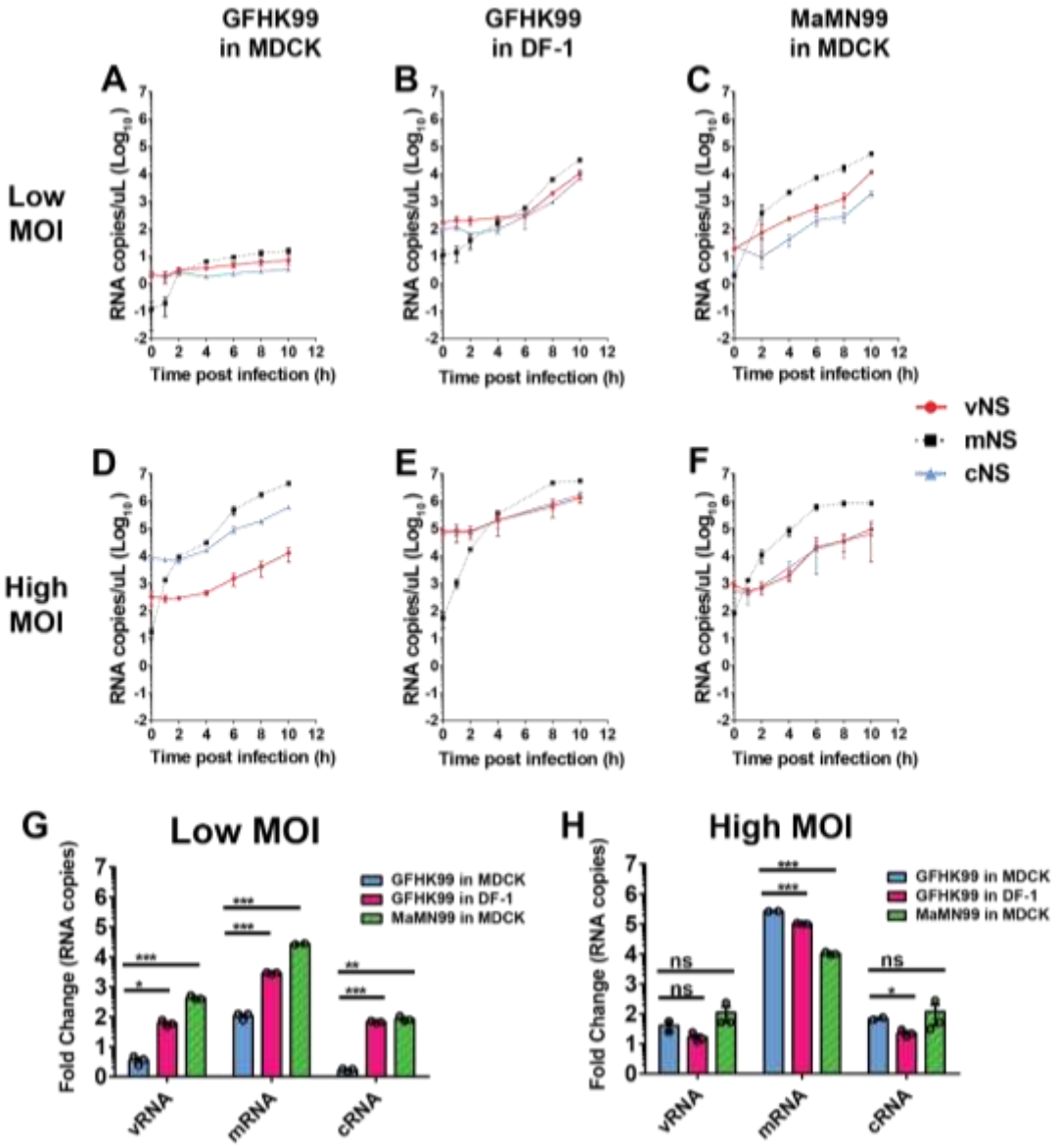

Figure 5. ***High multiplicity of infection is needed for robust GFHK99 polymerase activity in MDCK cells.***

Dishes of MDCK or DF-1 cells (n=3) were infected with GFHK99 or MaMN99 virus at low (0.5 RNA copies per cell) or high (3 HA expressing units per cell) MOI. NS segment vRNA, mRNA, and cRNA were quantified at the indicate time points (A-F). The average fold change from initial (t=0) to peak RNA copy number is plotted for low MOI infections (G) and high

MOI infections (H). Error bars represent standard deviation. Significance was assessed by two-way ANOVA with Dunnett's test for multiple comparisons: *$p < 0.05$, **<0.01, ***<0.001. ns = not significant.

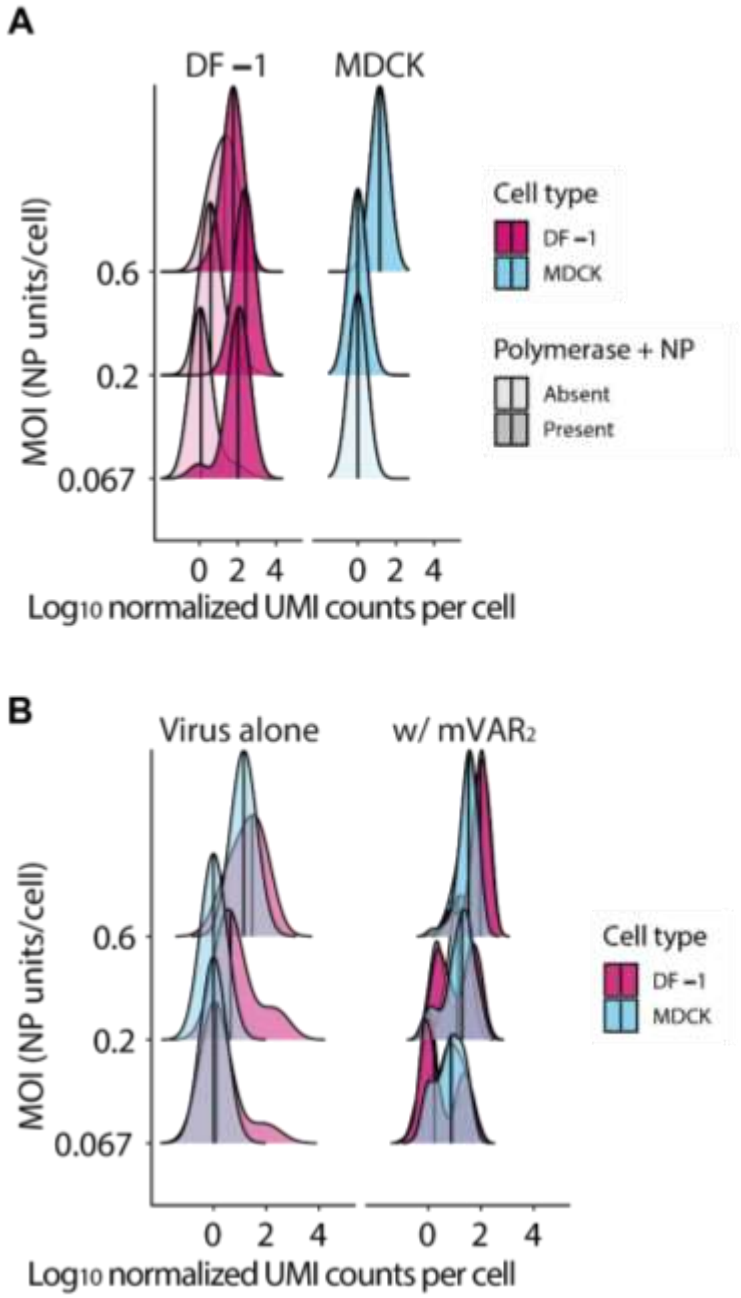

Figure 6. ***GFHK99 viral transcription is uniformly low in MDCK cells in the absence of coinfecting virus.***

(A) DF-1 or MDCK cells were infected with GFHK99 WT virus at three different MOIs (0.67, 0.2, 0.6 NP units per cell), and the transcriptomes of 1,816 individual infected cells were elucidated using the 10X Genomics Chromium platform. Ridge plots show distributions of

log_{10}-transformed viral mRNA abundance, for all eight viral transcripts combined, in individual infected cells. The data are stratified by cell type (MDCK cells in blue, DF-1 cells in pink), MOI, and the presence of polymerase complex (light shading = cells missing PB2, PB1, PA, or NP; dark shading = cells in which PB2, PB1, and PA are all detected). The absence of a dark shaded distribution for MDCK cells at the lowest MOI is due to the absence of any cells in which all four of these segments were detected. (B) DF-1 or MDCK cells were infected and sequenced as in (A), but the inocula contained a 1:1 mixture of GFHK99 WT and GFHK99 $mVAR_1$ viruses at three different total MOIs (0.67, 0.2, 0.6 NP units per cell) and a constant amount of GFHK99 $mVAR_2$ virus (0.1 PFU per cell in DF-1 cells, 1.0 PFU per cell in MDCK cells). Left facet shows data from (A), and right facet shows data from WT/$mVAR_1$ coinoculations with $mVAR_2$ virus, with WT and $mVAR_1$ transcript abundances partitioned into separate distributions in each infection. Vertical lines denote the median of each distribution. UMI = unique molecular identifier.

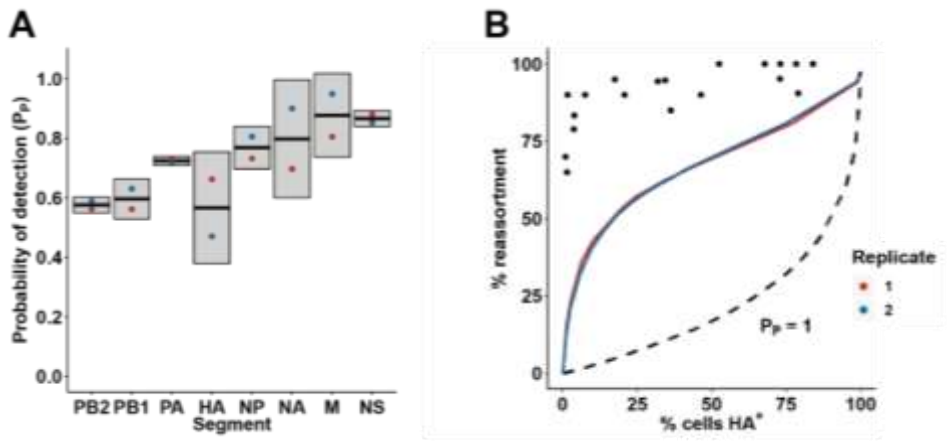

Figure 7. ***Incomplete GFHK99 virus genomes are present in MDCK cells but not sufficiently abundant to account for observed reassortment.***

Incomplete viral genomes were quantified experimentally by a single-cell based assay which relies on the amplification of incomplete viral genomes of GFHK99 WT virus (0.018 PFU per cell) by a genetically similar coinfecing virus, GFHK99 VAR_2. Based on the rate of detection of GFHK99 WT virus segments in this assay, the probability that a given segment would be present and replicated in a singly infected MDCK cell is reported as P_P. A) Summary of experimental P_P data. n = 2 biological replicates, shown in blue and red. Shading represents 95% CI. B) Experimentally obtained P_P values in A were used to parameterize a computational model[44]. Levels of reassortment predicted using the experimentally determined parameters are shown in red and blue. Levels of reassortment predicted if P_P=1.0 are shown with the dashed line. Observed reassortment of GFHK99 WT and VAR viruses in MDCK cells are shown with black circles. Observed data are the same as those plotted in Figure 1.

References

1. Desselberger, U., et al., *Biochemical evidence that "new" influenza virus strains in nature may arise by recombination (reassortment).* Proc Natl Acad Sci U S A, 1978. **75**(7): p. 3341-5.

2. Scholtissek, C., *Molecular evolution of influenza viruses.* Virus Genes, 1995. **11**(2-3): p. 209-15.

3. Taubenberger, J.K. and J.C. Kash, *Influenza Virus Evolution, Host Adaptation, and Pandemic Formation.* Cell Host & Microbe, 2010. **7**(6): p. 440-451.

4. Schrauwen, E.J. and R.A. Fouchier, *Host adaptation and transmission of influenza A viruses in mammals.* Emerg Microbes Infect, 2014. **3**(2): p. e9.

5. Ma, E.J., et al., *Reticulate evolution is favored in influenza niche switching.* Proc Natl Acad Sci U S A, 2016. **113**(19): p. 5335-9.

6. Holmes, E.C., et al., *Whole-genome analysis of human influenza A virus reveals multiple persistent lineages and reassortment among recent H3N2 viruses.* PLoS Biol, 2005. **3**(9): p. e300.

7. Nelson, M.I., et al., *The origin and global emergence of adamantane resistant A/H3N2 influenza viruses.* Virology, 2009. **388**(2): p. 270-8.

8. Nelson, M.I., et al., *Multiple reassortment events in the evolutionary history of H1N1 influenza A virus since 1918.* PLoS Pathog, 2008. **4**(2): p. e1000012.

9. Rambaut, A., et al., *The genomic and epidemiological dynamics of human influenza A virus.* Nature, 2008. **453**(7195): p. 615-9.

10. Simonsen, L., et al., *The genesis and spread of reassortment human influenza A/H3N2 viruses conferring adamantane resistance.* Mol Biol Evol, 2007. **24**(8): p. 1811-20.

11. Westgeest, K.B., et al., *Genome-wide Analysis of Reassortment and Evolution of Human Influenza A(H3N2) Viruses Circulating between 1968 and 2011.* Journal of Virology, 2014. **88**(5): p. 2844-57.

12. Ince, W.L., et al., *Reassortment complements spontaneous mutation in influenza A virus NP and M1 genes to accelerate adaptation to a new host.* J Virol, 2013. **87**(8): p. 4330-8.

13. Young, J.F., U. Desselberger, and P. Palese, *Evolution of human influenza A viruses in nature: sequential mutations in the genomes of new H1N1.* Cell, 1979. **18**(1): p. 73-83.

14. Zhdanov, V.M., et al., *Return of epidemic A1 (H1N1) influenza virus.* Lancet, 1978. **1**(8059): p. 294-5.

15. Yamane, N., et al., *Isolation of three different influenza A viruses from an individual after probable double infection with H3N2 and H1N1 viruses.* Jpn J Med Sci Biol, 1978. **31**(5-6): p. 431-4.

16. Falchi, A., et al., *Dual infections by influenza A/H3N2 and B viruses and by influenza A/H3N2 and A/H1N1 viruses during winter 2007, Corsica Island, France.* J Clin Virol, 2008. **41**(2): p. 148-51.

17. Kendal, A.P., et al., *Laboratory-based surveillance of influenza virus in the United States during the winter of 1977--1978. II. Isolation of a mixture of A/Victoria- and A/USSR-like viruses from a single person during an epidemic in Wyoming, USA, January 1978.* Am J Epidemiol, 1979. **110**(4): p. 462-8.

18. Mizuta, K., et al., *A rare appearance of influenza A(H1N2) as a reassortant in a community such as Yamagata where A(H1N1) and A(H3N2) co-circulate.* Microbiol Immunol, 2003. **47**(5): p. 359-61.

19. Rith, S., et al., *Natural co-infection of influenza A/H3N2 and A/H1N1pdm09 viruses resulting in a reassortant A/H3N2 virus.* J Clin Virol, 2015. **73**: p. 108-111.

20. Liu, W., et al., *Mixed infections of pandemic H1N1 and seasonal H3N2 viruses in 1 outbreak.* Clin Infect Dis, 2010. **50**(10): p. 1359-65.

21. Myers, C.A., et al., *Dual infection of novel influenza viruses A/H1N1 and A/H3N2 in a cluster of Cambodian patients.* Am J Trop Med Hyg, 2011. **85**(5): p. 961-3.

22. Frank, A.L., L.H. Taber, and J.M. Wells, *Individuals infected with two subtypes of influenza A virus in the same season.* J Infect Dis, 1983. **147**(1): p. 120-4.

23. Poon, L.L., et al., *Quantifying influenza virus diversity and transmission in humans.* Nat Genet, 2016. **48**(2): p. 195-200.

24. Young, J.F. and P. Palese, *Evolution of human influenza A viruses in nature: recombination contributes to genetic variation of H1N1 strains.* Proc Natl Acad Sci U S A, 1979. **76**(12): p. 6547-51.

25. Chen, M.J., et al., *Genetic and phylogenetic analysis of multi-continent human influenza A(H1N2) reassortant viruses isolated in 2001 through 2003.* Virus Res, 2006. **122**(1-2): p. 200-5.

26. Gregory, V., et al., *Emergence of influenza A H1N2 reassortant viruses in the human population during 2001.* Virology, 2002. **300**(1): p. 1-7.

27. Dudas, G., et al., *Reassortment between influenza B lineages and the emergence of a coadapted PB1-PB2-HA gene complex.* Mol Biol Evol, 2015. **32**(1): p. 162-72.

28. McCullers, J.A., et al., *Reassortment and insertion-deletion are strategies for the evolution of influenza B viruses in nature.* J Virol, 1999. **73**(9): p. 7343-8.

29. Nelson, M.I., et al., *Molecular epidemiology of A/H3N2 and A/H1N1 influenza virus during a single epidemic season in the United States.* PLoS Pathog, 2008. **4**(8): p. e1000133.

30. Phillips, P.C., *Epistasis--the essential role of gene interactions in the structure and evolution of genetic systems.* Nat Rev Genet, 2008. **9**(11): p. 855-67.

31. Essere, B., et al., *Critical role of segment-specific packaging signals in genetic reassortment of influenza A viruses.* Proceedings of the National Academy of Sciences of the United States of America, 2013. **110**(40): p. E3840-E3848.

32. White, M.C., J. Steel, and A.C. Lowen, *Heterologous packaging signals on HA, but not NA or NS, limit influenza A virus reassortment.* J Virol, 2017. **In Press**.

33. Cobbin, J.C., et al., *Influenza virus PB1 and neuraminidase gene segments can cosegregate during vaccine reassortment driven by interactions in the PB1 coding region.* J Virol, 2014. **88**(16): p. 8971-80.

34. Mitnaul, L.J., et al., *Balanced hemagglutinin and neuraminidase activities are critical for efficient replication of influenza A virus.* J Virol, 2000. **74**(13): p. 6015-20.

35. Wagner, R., M. Matrosovich, and H.D. Klenk, *Functional balance between haemagglutinin and neuraminidase in influenza virus infections.* Rev Med Virol, 2002. **12**(3): p. 159-66.

36. Kaverin, N.V., et al., *Postreassortment changes in influenza A virus hemagglutinin restoring HA-NA functional match.* Virology, 1998. **244**(2): p. 315-21.

37. Gottschalk, A., *The influenza virus neuraminidase.* Nature, 1958. **181**(4606): p. 377-8.

38. Gen, F., et al., *Attenuation of an influenza A virus due to alteration of its hemagglutinin-neuraminidase functional balance in mice.* Arch Virol, 2013. **158**(5): p. 1003-11.

39. Li, C., et al., *Compatibility among polymerase subunit proteins is a restricting factor in reassortment between equine H7N7 and human H3N2 influenza viruses.* J Virol, 2008. **82**(23): p. 11880-8.

40. Hara, K., et al., *Co-incorporation of the PB2 and PA polymerase subunits from human H3N2 influenza virus is a critical determinant of the replication of reassortant ribonucleoprotein complexes.* J Gen Virol, 2013. **94**(Pt 11): p. 2406-16.

41. Octaviani, C.P., H. Goto, and Y. Kawaoka, *Reassortment between seasonal H1N1 and pandemic (H1N1) 2009 influenza viruses is restricted by limited compatibility among polymerase subunits.* J Virol, 2011. **85**(16): p. 8449-52.

42. Kim, J.I., et al., *Reassortment compatibility between PB1, PB2, and HA genes of the two influenza B virus lineages in mammalian cells.* Sci Rep, 2016. **6**: p. 27480.

43. Steel, J. and A.C. Lowen, *Influenza A virus reassortment.* Curr Top Microbiol Immunol, 2014. **385**: p. 377-401.

44. Fonville, J.M., et al., *Influenza Virus Reassortment Is Enhanced by Semi-infectious Particles but Can Be Suppressed by Defective Interfering Particles.* PLoS Pathog, 2015. **11**(10): p. e1005204.

45. Marshall, N., et al., *Influenza virus reassortment occurs with high frequency in the absence of segment mismatch.* PLoS Pathog, 2013. **9**(6): p. e1003421.

46. Tao, H., J. Steel, and A.C. Lowen, *Intrahost dynamics of influenza virus reassortment.* J Virol, 2014. **88**(13): p. 7485-92.

47. Lakdawala, S.S., et al., *Influenza a virus assembly intermediates fuse in the cytoplasm.* PLoS Pathog, 2014. **10**(3): p. e1003971.

48. Chou, Y.Y., et al., *Colocalization of different influenza viral RNA segments in the cytoplasm before viral budding as shown by single-molecule sensitivity FISH analysis.* PLoS Pathog, 2013. **9**(5): p. e1003358.

49. Goto, H., et al., *The genome-packaging signal of the influenza A virus genome comprises a genome incorporation signal and a genome-bundling signal.* J Virol, 2013. **87**(21): p. 11316-22.

50. Mehle, A. and J.A. Doudna, *Adaptive strategies of the influenza virus polymerase for replication in humans.* Proc Natl Acad Sci U S A, 2009. **106**(50): p. 21312-6.

51. Tao, H., et al., *Influenza A virus co-infection through transmission can support high levels of reassortment.* J Virol, 2015. **89**(16): p. 8453-61.

52. Essere, B., et al., *Critical role of segment-specific packaging signals in genetic reassortment of influenza A viruses.* Proc Natl Acad Sci U S A, 2013. **110**(40): p. 3840-8.

53. Greenbaum, B.D., et al., *Viral reassortment as an information exchange between viral segments.* Proc Natl Acad Sci U S A, 2012. **109**(9): p. 3341-6.

54. Rabadan, R., A.J. Levine, and M. Krasnitz, *Non-random reassortment in human influenza A viruses.* Influenza Other Respi Viruses, 2008. **2**(1): p. 9-22.

55. Lubeck, M.D., P. Palese, and J.L. Schulman, *Nonrandom association of parental genes in influenza A virus recombinants.* Virology, 1979. **95**(1): p. 269-74.

56. Octaviani, C.P., et al., *High level of genetic compatibility between swine-origin H1N1 and highly pathogenic avian H5N1 influenza viruses.* J Virol, 2010. **84**(20): p. 10918-22.

57. Octaviani, C.P., et al., *Reassortment between seasonal and swine-origin H1N1 influenza viruses generates viruses with enhanced growth capability in cell culture.* Virus Res, 2011. **156**(1-2): p. 147-50.

58. Schrauwen, E.J., et al., *Possible increased pathogenicity of pandemic (H1N1) 2009 influenza virus upon reassortment.* Emerg Infect Dis, 2011. **17**(2): p. 200-8.

59. Schrauwen, E.J., et al., *Reassortment between Avian H5N1 and human influenza viruses is mainly restricted to the matrix and neuraminidase gene segments.* PLoS One, 2013. **8**(3): p. e59889.

60. Chen, L.M., et al., *Genetic compatibility and virulence of reassortants derived from contemporary avian H5N1 and human H3N2 influenza A viruses.* PLoS Pathog, 2008. **4**(5): p. e1000072.

61. Varich, N.L., et al., *Deviation from the random distribution pattern of influenza A virus gene segments in reassortants produced under non-selective conditions.* Arch Virol, 2008. **153**(6): p. 1149-54.

62. Ma, W., et al., *Viral reassortment and transmission after co-infection of pigs with classical H1N1 and triple-reassortant H3N2 swine influenza viruses.* J Gen Virol, 2010. **91**(Pt 9): p. 2314-21.

63. Snyder, M.H., et al., *The avian influenza virus nucleoprotein gene and a specific constellation of avian and human virus polymerase genes each specify attenuation of avian-human influenza A/Pintail/79 reassortant viruses for monkeys.* J Virol, 1987. **61**(9): p. 2857-63.

64. Naffakh, N., et al., *Genetic analysis of the compatibility between polymerase proteins from human and avian strains of influenza A viruses.* J Gen Virol, 2000. **81**(Pt 5): p. 1283-91.

65. Sun, Y., et al., *High genetic compatibility and increased pathogenicity of reassortants derived from avian H9N2 and pandemic H1N1/2009 influenza viruses.* Proc Natl Acad Sci U S A, 2011. **108**(10): p. 4164-9.

66. Smith, G.J., et al., *Origins and evolutionary genomics of the 2009 swine-origin H1N1 influenza A epidemic.* Nature, 2009. **459**(7250): p. 1122-5.

67. Garten, R.J., et al., *Antigenic and genetic characteristics of swine-origin 2009 A(H1N1) influenza viruses circulating in humans.* Science, 2009. **325**(5937): p. 197-201.

68. Rudneva, I.A., et al., *Influenza A virus reassortants with surface glycoprotein genes of the avian parent viruses: effects of HA and NA gene combinations on virus aggregation.* Arch Virol, 1993. **133**(3-4): p. 437-50.

69. Rudneva, I.A., et al., *Phenotypic expression of HA-NA combinations in human-avian influenza A virus reassortants.* Arch Virol, 1996. **141**(6): p. 1091-9.

70. Macken, C.A., R.J. Webby, and W.J. Bruno, *Genotype turnover by reassortment of replication complex genes from avian influenza A virus.* J Gen Virol, 2006. **87**(Pt 10): p. 2803-15.

71. Nelson, M.I., et al., *Genomic reassortment of influenza A virus in North American swine, 1998-2011.* J Gen Virol, 2012. **93**(Pt 12): p. 2584-9.

72. Lam, T.T., et al., *Reassortment events among swine influenza A viruses in China: implications for the origin of the 2009 influenza pandemic.* J Virol, 2011. **85**(19): p. 10279-85.

73. Li, K.S., et al., *Genesis of a highly pathogenic and potentially pandemic H5N1 influenza virus in eastern Asia.* Nature, 2004. **430**(6996): p. 209-13.

74. Neverov, A.D., et al., *Intrasubtype reassortments cause adaptive amino acid replacements in H3N2 influenza genes.* PLoS Genet, 2014. **10**(1): p. e1004037.

75. Rudneva, I.A., et al., *Effect of gene constellation and postreassortment amino acid change on the phenotypic features of H5 influenza virus reassortants.* Arch Virol, 2007. **152**(6): p. 1139-45.

76. Nelson, M.I., et al., *Evolution of novel reassortant A/H3N2 influenza viruses in North American swine and humans, 2009-2011.* J Virol, 2012. **86**(16): p. 8872-8.

77. Centers for Disease, C. and Prevention, *Update: Influenza A (H3N2)v transmission and guidelines - five states, 2011.* MMWR Morb Mortal Wkly Rep, 2012. **60**(51-52): p. 1741-4.

78. Watson, S.J., et al., *Molecular Epidemiology and Evolution of Influenza Viruses Circulating within European Swine between 2009 and 2013.* J Virol, 2015. **89**(19): p. 9920-31.

79. Danzy, S., et al., *Mutations to PB2 and NP proteins of an avian influenza virus combine to confer efficient growth in primary human respiratory cells.* J Virol, 2014. **88**(22): p. 13436-46.

80. Fodor, E., et al., *Rescue of influenza A virus from recombinant DNA.* J Virol, 1999. **73**(11): p. 9679-82.

81. Chutinimitkul, S., et al., *Virulence-Associated Substitution D222G in the Hemagglutinin of 2009 Pandemic Influenza A(H1N1) Virus Affects Receptor Binding.* Journal of Virology, 2010. **84**(22): p. 11802-11813.

82. Xu, R., et al., *Functional balance of the hemagglutinin and neuraminidase activities accompanies the emergence of the 2009 H1N1 influenza pandemic.* J Virol, 2012. **86**(17): p. 9221-32.

83. Schwartz, S.L. and A.C. Lowen, *Droplet digital PCR: A novel method for detection of influenza virus defective interfering particles.* Journal of Virological Methods, 2016. **237**: p. 159-165.

84. Tao, H., et al., *Influenza A Virus Coinfection through Transmission Can Support High Levels of Reassortment.* J Virol, 2015. **89**(16): p. 8453-61.

85. Lowen, A.C., et al., *The guinea pig as a transmission model for human influenza viruses.* Proc Natl Acad Sci U S A, 2006. **103**(26): p. 9988-92.

86. Lowen, A.C., et al., *Influenza virus transmission is dependent on relative humidity and temperature.* PLoS Pathog, 2007. **3**(10): p. 1470-6.

87. Leeks, A., R. Sanjuan, and S.A. West, *The evolution of collective infectious units in viruses.* Virus Res, 2019. **265**: p. 94-101.

88. Brooke, C.B., *Population Diversity and Collective Interactions during Influenza Virus Infection.* J Virol, 2017. **91**(22).

89. Sanjuan, R., *Collective Infectious Units in Viruses.* Trends Microbiol, 2017. **25**(5): p. 402-412.

90. Santiana, M., et al., *Vesicle-Cloaked Virus Clusters Are Optimal Units for Inter-organismal Viral Transmission.* Cell Host Microbe, 2018. **24**(2): p. 208-220 e8.

91. Chen, Y.H., et al., *Phosphatidylserine vesicles enable efficient en bloc transmission of enteroviruses.* Cell, 2015. **160**(4): p. 619-630.

92. Erickson, A.K., et al., *Bacteria Facilitate Enteric Virus Co-infection of Mammalian Cells and Promote Genetic Recombination.* Cell Host Microbe, 2018. **23**(1): p. 77-88 e5.

93. Andreu-Moreno, I. and R. Sanjuan, *Collective Infection of Cells by Viral Aggregates Promotes Early Viral Proliferation and Reveals a Cellular-Level Allee Effect.* Curr Biol, 2018. **28**(20): p. 3212-3219.e4.

94. Cuevas, J.M., M. Duran-Moreno, and R. Sanjuan, *Multi-virion infectious units arise from free viral particles in an enveloped virus.* Nat Microbiol, 2017. **2**: p. 17078.

95. Cifuentes-Munoz, N., R.E. Dutch, and R. Cattaneo, *Direct cell-to-cell transmission of respiratory viruses: The fast lanes.* PLoS Pathog, 2018. **14**(6): p. e1007015.

96. Lawrence, D.M., et al., *Measles virus spread between neurons requires cell contact but not CD46 expression, syncytium formation, or extracellular virus production.* J Virol, 2000. **74**(4): p. 1908-18.

97. McDonald, D., et al., *Recruitment of HIV and its receptors to dendritic cell-T cell junctions.* Science, 2003. **300**(5623): p. 1295-7.

98. Shirogane, Y., S. Watanabe, and Y. Yanagi, *Cooperation between different RNA virus genomes produces a new phenotype.* Nat Commun, 2012. **3**: p. 1235.

99. Ciota, A.T., et al., *Cooperative interactions in the West Nile virus mutant swarm.* BMC Evol Biol, 2012. **12**: p. 58.

100. Xue, K.S., et al., *Cooperation between distinct viral variants promotes growth of H3N2 influenza in cell culture.* Elife, 2016. **5**: p. e13974.

101. Brooke, C.B., et al., *Influenza A virus nucleoprotein selectively decreases neuraminidase gene-segment packaging while enhancing viral fitness and transmissibility.* Proc Natl Acad Sci U S A, 2014. **111**(47): p. 16854-9.

102. Brooke, C.B., et al., *Most influenza a virions fail to express at least one essential viral protein.* J Virol, 2013. **87**(6): p. 3155-62.

103. Sun, J. and C.B. Brooke, *Influenza A Virus Superinfection Potential Is Regulated by Viral Genomic Heterogeneity.* MBio, 2018. **9**(5).

104. Jacobs, N.T., et al., *Incomplete influenza A virus genomes occur frequently but are readiliy complemented during localized viral spread.* Nature Communications, 2019.

105. Nayak, D.P., *Defective interfering influenza viruses.* Annu Rev Microbiol, 1980. **34**: p. 619-44.

106. Von Magnus, P., *Incomplete forms of influenza virus.* Adv Virus Res, 1954. **2**: p. 59-79.

107. Brooke, C.B., *Biological activities of 'noninfectious' influenza A virus particles.* Future Virol, 2014. **9**(1): p. 41-51.

108. Timm, C., A. Gupta, and J. Yin, *Robust kinetics of an RNA virus: Transcription rates are set by genome levels.* Biotechnol Bioeng, 2015. **112**(8): p. 1655-62.

109. Boulle, M., et al., *HIV Cell-to-Cell Spread Results in Earlier Onset of Viral Gene Expression by Multiple Infections per Cell.* PLoS Pathog, 2016. **12**(11): p. e1005964.

110. Sanjuán, R. and M.-I. Thoulouze, *Why viruses sometimes disperse in groups?(†).* Virus evolution, 2019. **5**(1): p. vez014-vez014.

111. Sigal, A., et al., *Cell-to-cell spread of HIV permits ongoing replication despite antiretroviral therapy.* Nature, 2011. **477**(7362): p. 95-8.

112. Webster, R.G., et al., *Influenza viruses from avian and porcine sources and their possible role in the origin of human pandemic strains.* Dev Biol Stand, 1977. **39**: p. 461-8.

113. Wright, P.F., G. Neumann, and Y. Kawaoka, *Orthomyxoviruses*, in *Fields Virology*, D.M.H. Knipe, P. M., Editor. 2006, Lippincott-Raven: Philidelphia. p. 1691-1740.

114. Webster, R.G., et al., *Evolution and ecology of influenza A viruses.* Microbiol Rev, 1992. **56**(1): p. 152-79.

115. Webster, R.G., K.F. Shortridge, and Y. Kawaoka, *Influenza: interspecies transmission and emergence of new pandemics.* FEMS Immunol Med Microbiol, 1997. **18**(4): p. 275-9.

116. Taubenberger, J.K. and D.M. Morens, *1918 Influenza: the mother of all pandemics.* Emerg Infect Dis, 2006. **12**(1): p. 15-22.

117. Viboud, C., et al., *Preliminary Estimates of Mortality and Years of Life Lost Associated with the 2009 A/H1N1 Pandemic in the US and Comparison with Past Influenza Seasons.* PLoS Curr, 2010: p. RRN1153.

118. Long, J.S., et al., *Host and viral determinants of influenza A virus species specificity.* Nat Rev Microbiol, 2019. **17**(2): p. 67-81.

119. Rajsbaum, R., et al., *Species-specific inhibition of RIG-I ubiquitination and IFN induction by the influenza A virus NS1 protein.* PLoS Pathog, 2012. **8**(11): p. e1003059.

120. Manz, B., et al., *Pandemic influenza A viruses escape from restriction by human MxA through adaptive mutations in the nucleoprotein.* PLoS Pathog, 2013. **9**(3): p. e1003279.

121. Lowen, A.C., *Constraints, Drivers, and Implications of Influenza A Virus Reassortment.* Annu Rev Virol, 2017. **4**(1): p. 105-121.

122. Kilbourne, E.D., *Influenza pandemics of the 20th century.* Emerg Infect Dis, 2006. **12**(1): p. 9-14.

123. Kayed, A.S., et al., *Surveillance for avian influenza viruses in wild birds at live bird markets, Egypt, 2014-2016.* Influenza Other Respir Viruses, 2019. **13**(4): p. 407-414.

124. Xu, K.M., et al., *The genesis and evolution of H9N2 influenza viruses in poultry from southern China, 2000 to 2005.* J Virol, 2007. **81**(19): p. 10389-401.

125. Russell, A.B., C. Trapnell, and J.D. Bloom, *Extreme heterogeneity of influenza virus infection in single cells.* Elife, 2018. **7**.

126. Zheng, G.X., et al., *Massively parallel digital transcriptional profiling of single cells.* Nat Commun, 2017. **8**: p. 14049.

127. Palese, P. and M.L. Shaw, *Orthomyxoviridae*, in *Fields Virology*, D.M.H. Knipe, P. M., Editor. 2013, Lippincott-Raven: Philidelphia. p. 1151-1185.

128. Lowen, A.C., *It's in the mix: Reassortment of segmented viral genomes.* PLoS Pathog, 2018. **14**(9): p. e1007200.

129. Krystal, M., et al., *Expression of the three influenza virus polymerase proteins in a single cell allows growth complementation of viral mutants.* Proc Natl Acad Sci U S A, 1986. **83**(8): p. 2709-13.

130. Naffakh, N., et al., *Host restriction of avian influenza viruses at the level of the ribonucleoproteins.* Annu Rev Microbiol, 2008. **62**: p. 403-24.

131. Long, J.S., et al., *Species difference in ANP32A underlies influenza A virus polymerase host restriction.* Nature, 2016. **529**(7584): p. 101-4.

132. Te Velthuis, A.J.W., et al., *Mini viral RNAs act as innate immune agonists during influenza virus infection.* Nat Microbiol, 2018. **3**(11): p. 1234-1242.

133. Schelker, M., et al., *Viral RNA Degradation and Diffusion Act as a Bottleneck for the Influenza A Virus Infection Efficiency*. PLOS Computational Biology, 2016. **12**(10): p. e1005075.

134. Butt, K.M., et al., *Human infection with an avian H9N2 influenza A virus in Hong Kong in 2003.* J Clin Microbiol, 2005. **43**(11): p. 5760-7.

135. Peiris, M., et al., *Human infection with influenza H9N2.* Lancet, 1999. **354**(9182): p. 916-7.

136. Guan, Y., et al., *H9N2 influenza viruses possessing H5N1-like internal genomes continue to circulate in poultry in southeastern China.* J Virol, 2000. **74**(20): p. 9372-80.

137. Guan, Y., et al., *Molecular characterization of H9N2 influenza viruses: were they the donors of the "internal" genes of H5N1 viruses in Hong Kong?* Proc Natl Acad Sci U S A, 1999. **96**(16): p. 9363-7.

138. Lam, T.T., et al., *The genesis and source of the H7N9 influenza viruses causing human infections in China.* Nature, 2013. **502**(7470): p. 241-4.

139. Wu, A., et al., *Sequential Reassortments Underlie Diverse Influenza H7N9 Genotypes in China.* Cell Host Microbe, 2013. **4**(14): p. 446-52.

140. Gu, M., et al., *Current situation of H9N2 subtype avian influenza in China.* Veterinary research, 2017. **48**(1): p. 49-49.

141. Pusch, E.A. and D.L. Suarez, *The Multifaceted Zoonotic Risk of H9N2 Avian Influenza.* Veterinary sciences, 2018. **5**(4): p. 82.

142. White, M.C. and A.C. Lowen, *Implications of segment mismatch for influenza A virus evolution.* J Gen Virol, 2018. **99**(1): p. 3-16.

143. Villa, M. and M. Lassig, *Fitness cost of reassortment in human influenza.* PLoS Pathog, 2017. **13**(11): p. e1006685.

144. Varble, A., et al., *Influenza A virus transmission bottlenecks are defined by infection route and recipient host.* Cell Host Microbe, 2014. **16**(5): p. 691-700.

145. Gallagher, M.E., et al., *Causes and Consequences of Spatial Within-Host Viral Spread.* Viruses, 2018. **10**(11).

146. Chao, L., T. Tran, and C. Matthews, *Muller's Ratchet and the Advantage of Sex in the Rna Virus 6.* Evolution, 1992. **46**(2): p. 289-299.

147. Froissart, R., et al., *Co-infection weakens selection against epistatic mutations in RNA viruses.* Genetics, 2004. **168**(1): p. 9-19.

148. Novella, I.S., D.D. Reissig, and C.O. Wilke, *Density-dependent selection in vesicular stomatitis virus.* J Virol, 2004. **78**(11): p. 5799-804.

149. Wilke, C.O. and I.S. Novella, *Phenotypic mixing and hiding may contribute to memory in viral quasispecies.* BMC Microbiol, 2003. **3**: p. 11.

150. Hoffmann, E., et al., *A DNA transfection system for generation of influenza A virus from eight plasmids.* 2000. **97**(11): p. 6108-6113.

151. Schwartz, S.L. and A.C. Lowen, *Droplet digital PCR: A novel method for detection of influenza virus defective interfering particles.* J Virol Methods, 2016. **237**: p. 159-165.

152. Perez, D.R., et al., *Land-based birds as potential disseminators of avian mammalian reassortant influenza A viruses.* Avian Dis, 2003. **47**(3 Suppl): p. 1114-7.

153. Song, H., G.R. Nieto, and D.R. Perez, *A new generation of modified live-attenuated avian influenza viruses using a two-strategy combination as potential vaccine candidates.* J Virol, 2007. **81**(17): p. 9238-48.

154. Sorrell, E.M., et al., *Minimal molecular constraints for respiratory droplet transmission of an avian-human H9N2 influenza A virus.* Proc Natl Acad Sci U S A, 2009. **106**(18): p. 7565-70.

155. Brown, J.D., et al., *Intestinal excretion of a wild bird-origin H3N8 low pathogenic avian influenza virus in mallards (Anas Platyrhynchos).* J Wildl Dis, 2012. **48**(4): p. 991-8.

156. Chen, H., et al., *Partial and full PCR-based reverse genetics strategy for influenza viruses.* PLoS One, 2012. **7**(9): p. e46378.

157. Reed, L.J. and H. Muench, *A SIMPLE METHOD OF ESTIMATING FIFTY PER CENT ENDPOINTS12.* American Journal of Epidemiology, 1938. **27**(3): p. 493-497.

158. Wittwer, C.T., et al., *High-resolution genotyping by amplicon melting analysis using LCGreen.* Clin Chem, 2003. **49**(6 Pt 1): p. 853-60.

159. Richard, M., et al., *Influenza A virus reassortment is limited by anatomical compartmentalization following co-infection via distinct routes.* J Virol, 2017.

160. Simpson, E.H., *Measurement of diversity.* Nature, 1949. **163**: p. 688-688.

161. Hill, M.O., *Diversity and evenness: a unifying notation and its consequences.* Ecology, 1973. **54**: p. 427-432.

162. Jost, L., *Entropy and diversity.* Oikos, 2006. **113**: p. 363-375.

163. Drayman, N., et al., *Rapid method for SV40 titration.* J Virol Methods, 2010. **164**(1-2): p. 145-7.

164. Zhou, B., et al., *Single-reaction genomic amplification accelerates sequencing and vaccine production for classical and Swine origin human influenza a viruses.* J Virol, 2009. **83**(19): p. 10309-13.

Supplementary information

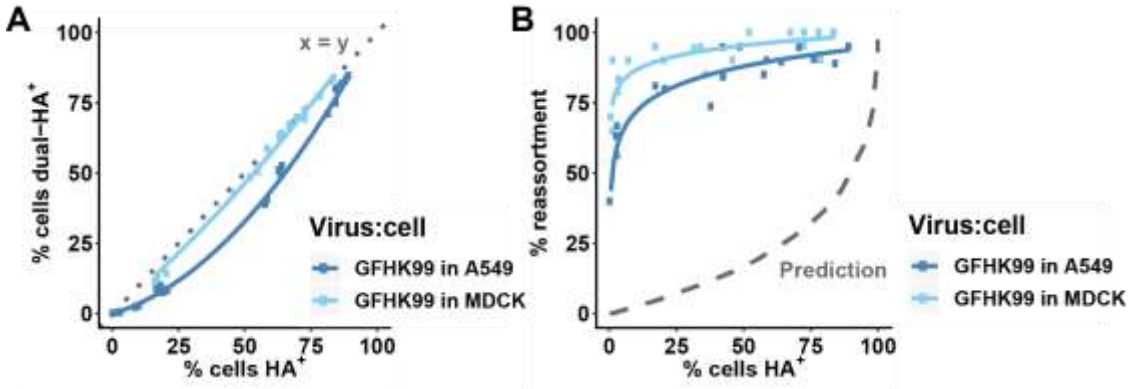

Supplementary Figure 1. ***Co-infection and reassortment of GFHK99 viruses in a human cell line.***

Synchronized, single cycle co-infections were performed for a 1:1 mixture of GFHK99 virus in A549 cells. A) HA expression and B) reassortment was measured as described in Figure 1.

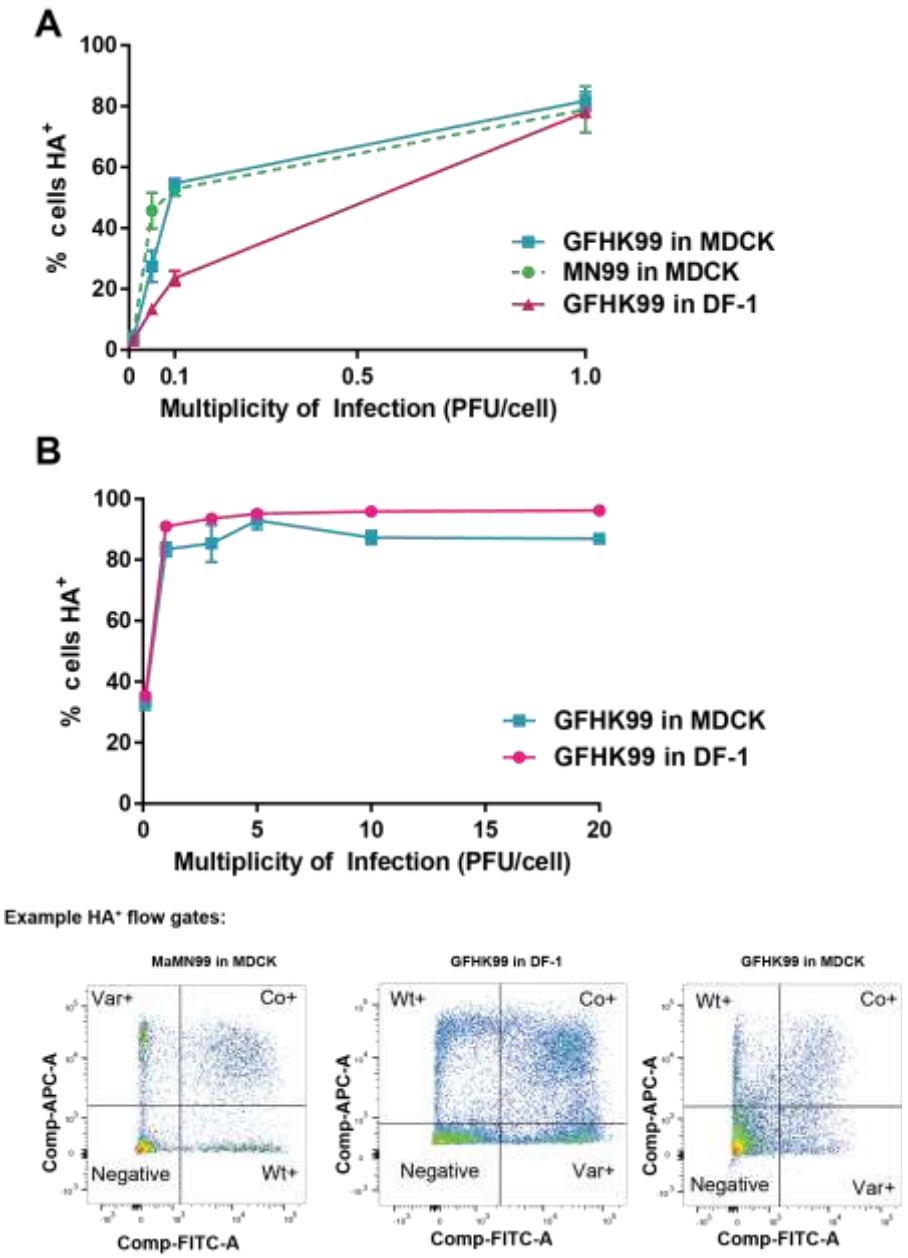

Supplementary Figure 2. ***Flow cytometry of HA expression represents infection level across MOIs for single cycle growth assays.***

Triplicate or duplicate wells of cells were harvested 24 h post infection and stained to detect surface expression of HA and HIS epitope tags. Panel A) corresponds to Figure 2 A-C and

Panel B) corresponds to Figure 2 D-E. Flow gating was performed by exluding cell debris and multiplet cells. Quandrant gates were used to quantify each population.

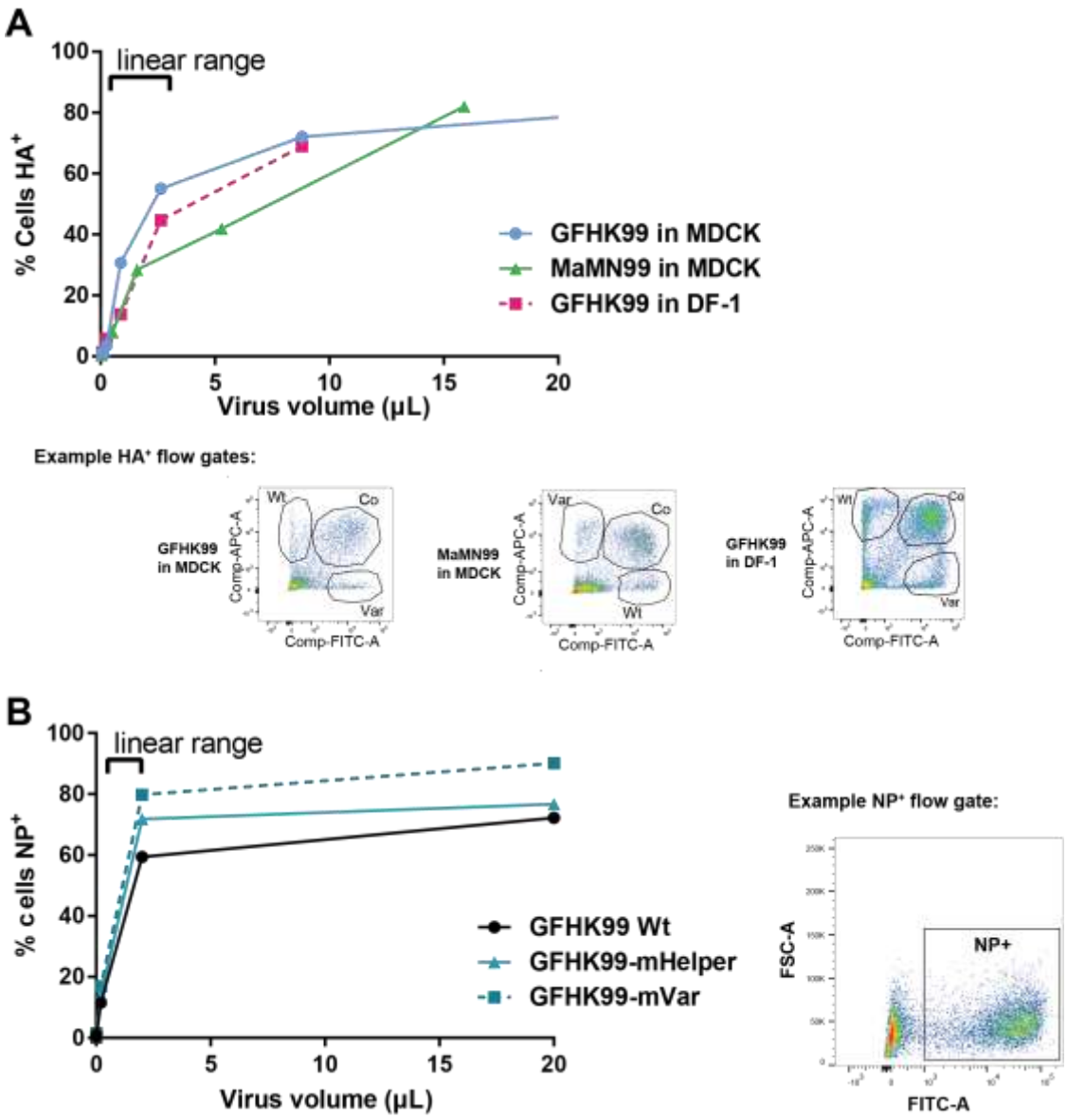

Supplementary Figure 3. ***Titration of virus stocks for HA expressing units and NP expressing units by flow cytometry.***

A) The doses to be used in RNA kinetics studies shown in Figure 6 were determined via flow titration of HA expressing units in relevant cell lines. GFHK99 and MaMN99 virus mixtures were titrated in MDCK and DF-1 cell lines to calculate HA expressing units/mL in each virus-cell line combination. Serial dilutions of virus were used to infect cells under synchronized,

single cycle conditions. Cells were harvested at 24 h post infection and stained for epitope tags. Data points of percent cells positive within the linear range were used to calculate the viral titer. B) GFHK99 viruses used in mRNA sequencing experiments were titered in DF-1 cells. Previous experiments indicated DF-1 cells were more permissive to infection and thus should give a more sensitive measurement of virus present. As the virus strains used did not contain epitope tags, virus detection was accomplished through cell permeabilization and detection of the viral NP protein. Data points within the linear range were used to calculate viral titers. Examples of flow cytometry gates show selection of HA epitope tag or internal NP expressing singlets following gating to exclude cell debris and doublets.

Table 1. ***Genotypes of viruses used in this study***

	PB2	PB1	PA	HA	NP	NA	M	NS
MaMN99 Var	G399A	G573A	G402A	A344G	A414G	G548A	A433G	A458G
GFHK99 Var$_1$	A285G	A420G	A426G	T341C	T327C	T295C	A349G	T329C
GFHK99 Var$_2$	300G, 303T, 306C, 459C, 461A, 467T	282C, 285C, 288G, 420G, 426C, 432T	351G, 354T, 357T, 501G, 504T, 507T	338G, 351C, 344C, 432G, 435A, 438T	345G, 351A, 354G, 485C, 488A, 494A	424G, 430A, 433A, 583G, 586C, 589C	340A, 343G, 349G, 439A, 442T, 445G	386T, 389A, 392G, 479G, 482C, 488G
GFHK99 mVar$_1$	A2151G, C2164T	A2193G, A2185C	C2064A, A2061G	T1574C, G1589A	G1442A, T1411C	C1315T, G1300A	A818C, G815A	A694C, G690A
GFHK99 mVar$_2$	A2127G, A2124G	C2175T, T2184C	C2017T, A2019G	G1553A, G1556A	G1383A, A1374G	A1255C, A1240C	C809T, T806C	A681G, C678T

Table 2. ***Primers for the differentiation of Wt and Var$_1$ by HRM***

MaMN99[1] Primers	
MN99 PB2 337 F	CCGACAACAAGCACAGTTCA
MN99 PB2 420 R	GCCAAAGGTCCCATGTTTTA
MN99 PB1 522 F	CCTCAAGGACGTGATGGAAT
MN99 PB1 622 R	CCATTTTCTTGGTCATGTTGTC
MN99 PA 379 F	GAAATTGGAGTGACACGGAGA
MN99 PA 461 R	TGAATGTGTGTCTTCTCGGATT
MN99 HA 322 F	AAACCTGGGACCTTTATGTGG
MN99 HA 402 R	TGAGCGATGCATAGTCTGGT
MN99 NP 378 F	CGACAAAGAAGAGATCAGAAGGA
MN99 NP 457 R	TCATCAAATGGGTGAGACCA
MN99 NA 522 F	TACCAGGCAAGGTTTGAAGC
MN99 NA 605 R	GCCCGTTACTCCAATTGTCA
MN99 M 404 F	TGCATGGGCCTCATATACAA
MN99 M 493 R	ATCAGCAATCTGCTCACACG
MN99 NS 389 F	GGCCATTATGGACAAGAGGA
MN99 NS 483 R	CGTCTGTGAAAGCCCTCAGT
GFHK99[2] Primers	
WF10 PB2 240 F	TGAGCAAGGCCAAACTCTTT
WF10 PB2 320 R	CACGTTACAGCCAGAGGTGA
WF10 PB1 362 F	TTGTCCAGCAAACGAGAGTG
WF10 PB1 441 R	AGCCGGCTGGTTTCTATTC
WF10 PA 386 F	GTGTGACACGGAGGGAAGTT
WF10 PA 461 R	TGGATATGTGTTTTCTCGGATTT
WF10 HA 278 F	CCCTTCTTGTGACCTGCTGT
WF10 HA 364 R	CCAGGGTAACACGTTCCATT
WF10 NP 279 F	CCTAGAGGAACATCCCAGTGC
WF10 NP 369 R	CAGCTCTCTCACCCATTTCC
WF10 NA 270 F	ATTGGTCAAAACCGCAATGT
WF10 NA 346 R	GCCTGCAGAAAGCCTAATTG
WF10 M 291 F	ACCCAAACAACATGGACAGG
WF10 M 373 R	TGCAACTTCCTTTGCTCCAT
WF10 NS 265 F	CTATCGCTTCAATGCCTGCT
WF10 NS 357 R	CTTTCTGCTTGGGAATGAGC

[1] A/mallard/Minnesota/199106/99[H3N8], also referred to as “MN99”
[2]A/guinea fowl/Hong Kong/WF10/99 [H9N2], also referred to as “WF10”

Table 3. ***Primers for the differentiation of Wt and Var$_2$ by PCR***

GFHK99 Wt Virus Primers	
WF10wt PB2 286F	GACAGGGTAATGGTATCACCT
WF10wt PB2 480R	GGCCAGGGTTCATGTCAACCCT
WF10wt PB1 266F	GGTATGCACAAACAGATTGTGTAT
WF10wt PB1 440R	CCGGCTGGTTTCTATTCAAT
WF10wt PA 337F	TCTTCCGGACCTATACGACTA
WF10wt PA 521R	CTTCATCAAGGGTGTAGTCAG
WF10wt NP 336F	GAAGGAGAGACGGGAAATG
WF10wt NP 505R	GGCTCTTGTTCTCTGGTATG
WF10wt HA 323F	CGTCGAAAGATCATCAGCTGTA
WF10wt HA 451R	CAGGTTGTGTCTGGGAAGATT
WF10wt NA 413F	CTTGGGCAGGGAACCACTTTG
WF10wt NA 601R	CCCAGTGACACAAACATGTAAC
WF10wt M 328F	GAAGCTGAAGAGGGAAATGACA
WF10wt M 457R	AAGAGCCACTTCTGTGGTC
WF10wt NS 374F	CATTAGAGTGGACCAGGCA
WF10wt NS 499R	CCCACTATTGCTCCTTCATCT
GFHK99 Var$_2$ Virus Primers	
WF10help PB2 286F	GACAGGGTAATGGTgTCtCCc
WF10help PB2 480R	GGCCAGGGTTCATaTCAACtCg
WF10help PB1 266F	GGTATGCACAAACAGAcTGcGTgT
WF10help PB1 440R	CCGGCTGaTTTCTgTTCAAc
WF10help M 331F	GCTGAAGAGAGAGATGACG
WF10help M 459R	CAAGAGCCACTTCCGTAGTTA
WF10help NS 373F	GCATTAGAGTGGATCAAGCG
WF10help NS 496R	ACTATTGCCCCTTCGTCC

Table 4. ***Primers for identification of strand specific RNA species***

MaMN99 Reverse Transcription and PCR Primers	
MN99 NS 552F	GGCCGTCATGGTGGCGAAT AATGCAATTGGAATCCTCAT
MN99 NS mRNAtag_dTR 13	CCAGATCGTTCGAGTCGT TTT TTT TTT TTT TTT AGTACTAAATAAG
MN99 NS cRNAtag_dTR 25	GCTAGCTTCAGCTAGGCATC AGTAGAAACAAGGGTGTTTTTTAG
MN99 NS 795F	CTTGCAGGCATTGCAAC
MN99 NS 643R	CGGACTCCCCAAGCGAATCTC
GFHK99 Reverse Transcription and PCR Primers	
WF10 vRNA NS 520F	GGCCGTCATGGTGGCGAAT CCCTTCCAGGACATACTGAC
WF10 NS mRNAtag_dTR 13	CCAGATCGTTCGAGTCGTTTTTTTTTTTTTTTTATCATTAAATAAG
WF10 NS cRNAtag_dTR 25	GCTAGCTTCAGCTAGGCATC AGTAGAAACAAGGGTGTTTTTTATC
WF10 NS 592R	TCATTCCATTCAAGTCCTCCGATGAG
WF10 NS 791F	CCTTTATGCAAGCCTTACAAC
MaMN99 and GFHK99 Tagged PCR Primers	
vRNA	GGCCGTCATGGTGGCGAAT
cRNA	GCTAGCTTCAGCTAGGCATC
mRNA	CCAGATCGTTCGAGTCGT

Chapter IV. Discussion

The second chapter of this dissertation investigated the molecular determinants of reassortment potential between representative strains of pandemic H1N1 (pH1N1) and human seasonal H3N2 subtypes. Since 1977, human IAVs of H1N1 and H3N2 subtypes have co-circulated with relatively few documented cases of co-infection and intersubtype reassortment [1-3]. Through this study we sought to better understand the constraints acting on their genetic exchange by evaluating the potential for viruses of the currently circulating pH1N1 and seasonal H3N2 lineages to reassort under experimental conditions. Results of heterologous co-infections with A/NL/602/2009 (pH1N1) and A/Panama/2007/99 (H3N2) were compared to those obtained following co-infection with homologous, genetically tagged pH1N1 viruses as a control. Heterologous and homologous co-infections produced similar levels of reassortment and genotype diversity. However, analysis of genotype patterns revealed that homologous reassortment was random while heterologous reassortment was biased. In particular, pairwise analysis of segments incorporated into pH1N1/H3N2 reassortant viruses under single cycle growth conditions identified a strong preference for genotypes containing homologous PB2 and PA segments, a general preference for the H3N2 NA, and a preference for the H3N2 PB2 except when paired with the pH1N1 PA or NP. The pH1N1 M segment was also favored in many genotype combinations. Analysis of genotypes resulting from heterologous, multicycle co-infections corroborated these findings and revealed an additional general preference for the H3N2 HA. Segment compatibility was further investigated by measuring chimeric polymerase activity and growth of selected reassortants in human tracheobronchial epithelial cells. In guinea pigs inoculated with a mixture of viruses derived from pH1N1/H3N2 co-infection, parental H3N2 viruses dominated but reassortant genotypes also infected and transmitted to cagemates.

These results indicate that intrinsic barriers to reassortment between H3N2 and pH1N1 viruses are present, but limited. If selective forces permit, intersubtypic reassortment in humans could give rise to epidemiologically significant IAVs.

Compatibility of viral genes from alternate backgrounds is affected by RNA and protein mismatch, though the specific contribution of each was not measured in this study. RNA packaging signals on the viral genes direct assembly into virions, and the production of reassortant progeny can be restricted at this step. IAVs and IBVs cocirculate in humans and contain the same number of genomic segments with conserved functions, however, reassortment events between these types have never been detected [3]. Indeed, incorporation of the IBV HA segment into an IAV background, or vice versa, was not observed in experimental coinfection [4]. However, by incorporating IAV packaging signal regions of the HA and NA genes of IBV, inter-type reassortant viruses were able to be generated. This finding suggests that RNA compatibility exerts greater constraints on reassortment frequency by acting at the stage of virion production. The compatibility of the incorporated proteins is likely important for subsequent infection and viral fitness. Indeed, studies employing engineered virus strains of the same backgrounds used in the second chapter of this study, demonstrated that grafting the packaging signal of the pH1N1 HA segment onto the HA segment of H3N2 led to disfavored incorporation of this segment when compared to a control which contained similarly engineered H3N2 HA packaging signals [5]. Though not directly addressed in this work, compatibility at the RNA level should be also considered when assessing reassortment potential between IAV strains [5-10].

Reassortment potential is difficult to assay comprehensively. Even when excluding epidemiological factors and differences among host backgrounds, predicting the full scope of

compatibility and fitness of reassortant genotypes is complex, if not impossible. The complexity of higher order epistatic interactions among the eight gene segments prohibit exhaustive studies. The approach used here enables detection of epistasis between two genes. Epidemiological information regarding circulating IAV genotypes should be mined for insights into gene compatibility. Whole genome sequencing is becoming more commonly utilized, and phylogenetic analysis of the full genome sequence could enable the identification of reassortant genotypes which have achieved sustained transmission in the population studied [11, 12]. Indeed, phylogenetic studies considering multiple genes have been able to detect epistatic interactions and may show promise for future predictions of compatible gene combinations which could be carefully investigated by molecular characterization [11, 13-16].

Deep mutational scanning (DMS) approaches have proved very informative for predicting the fitness effects of amino acid changes in a single gene [17, 18]. In these studies, a large number of unique mutants are generated and subjected to a selection pressure. Sequencing following selection enables the identification of advantageous mutations [17-23]. This method has not yet been used to identify adaptive mutations which would enhance reassortment potential. To reduce the number of potential outcomes, mutations which confer compatibility of one gene in a particular genetic background could be identified. Specifically, DMS could be performed using a library of mutants in a single gene and supplied with the remaining seven IAV segments. Here, the selection pressure is compatibility with a heterologous background. This approach could be further refined by reducing the library to mutants which contain variance in specific sites known to be important for adaptation. This strategy would reduce complexity and enable more thorough experimentation with increased power and sensitivity. For example, a number of studies have been published detailing residues which are important for viral

polymerase function [24-26]. By limiting DMS approaches to a subset of mutants within these locations, it may be possible to reduce the number of potential subunit partners to make the interrogation of compatible polymerase gene combinations for a particular background more practical. Additionally, a functional readout for selection, such as the production of a fluorescent viral protein, could identify cells containing compatible polymerase units, and these cells could be sorted and the containing RNA sequenced to identify the compatible viral polymerase units present. Together, phylogenetic and molecular approaches could be used to more fully flesh out what interactions lead to segment mismatch among diverse IAVs.

The third chapter of this work investigates the degree to which IAVs exhibit a dependence on co-infection for productive infection. This study reveals that both viral features and the host background impact the degree of reliance on multiplicity for virus production. For the first time it is described that co-infection dependence is a property determined during infection through interactions between the virus and the infected host cell, rather than an intrinsic, conserved property of the virus. The observed differences in co-infection dependence led to a phenotypic difference in the amount of reassortment observed within avian and mammalian animal models and established relevance for co-infection dependence in the case of infection of an animal host. Increasing MOI and the opportunity for cooperative virus-virus interactions resulted in faster virus and RNA production kinetics and elevated overall viral productivity in infected cells. Single cell studies revealed that, while genetic complementation certainly plays a role in co-infection dependence, additional cooperative interactions boosted transcription in infected cells. This study reveals that infection efficiency and the need for cooperative actions varies with virus-host context, and the viral polymerase is an important driver of the underlying need for cooperation.

Further studies are needed to determine the underlying mechanism of coinfection dependence seen with the GFHK99 virus in MDCK cells. The identification of GFHK99 viral genes amplified from a singly infected MDCK cell predicts much lower reassortment values than observed. The discrepancy between experimental and predicted reassortment levels of GFHK99 in MDCK cells suggests that viral genomes are more incomplete than the single-cell assay reports. The conditions of viral propagation are very different between these two assays. The helper virus in the single cell sorting assay is able to provide not only missing genes, but much more time for amplification - 48 h compared to 12 h for the *in vitro* reassortment assay - and is provided viral proteins from the helper virus, as well as viral genes themselves. It is possible with poor polymerase activity and kinetic delay at low MOI, as observed in other experiments, the viral gene templates could be present, but too scarce to contribute to infection. To investigate whether kinetic delay in viral RNA production is responsible for the coinfection dependence seen with GFHK99 in MDCK cells, the reassortment assay and replication measurements should be taken at a later time. These assays should be performed under single cycle conditions in order to assess the presence of genes upon initial infection. Another explanation for the prevalence of complete viral genomes measured by the single cell assay would be that the viral genes are present but non-functional due to lethal mutations. The quantification of viral genes by qPCR relies on the presence of viral RNA, but does not give information about the quality of its sequence. The prevalence of lethal mutations may be assayed by detecting the frequency of the loss of function of a fluorescent reporter gene. This approach has been previously utilized for quantifying the frequency of lethal mutations of an IAV [27]. Te Velthuis et al. reports the production of nonfunctional, mini viral RNAs (mvRNAs) by the viral polymerase [28]. The prevalence of mvRNAs is shown to be impacted by the presence of host adaptive signatures on

the viral polymerase and suggests that poor interaction with host factors may lead to the production of nonfunctional RNAs. To investigate if mvRNAs may contribute to the difference in coinfection dependence between GFHK99 in different host environments, we will infect both MDCK and DF-1 cells with the GFHK99 virus and measure the size and prevalence of RNAs produced by primer extension and assessment of band size by gel electrophoresis. If mvRNAs contribute to the host dependent phenotype, greater amounts of these non-standard RNAs will be detected in MDCK cells when compared to DF-1 cells.

H9N2 avian influenza viruses related to the GFHK99 strain described in chapter three are of particular concern due to their widespread circulation and the frequent contribution of internal genes to other avian influenza viruses of greater virulence [29-32]. Thus, the propensity of the H9N2 viral polymerase to establish infection in mammals is of epidemiological significance. Additionally, studying this protein complex more closely could provide information regarding the mechanisms which play a major role in determining coinfection and cooperation dependence of other IAVs. For these reasons, subsequent studies will focus on assessing coinfection dependence in 1) specific mutants and 2) past and contemporary H9N2 viruses. The mutations to be tested in the GFHK99 background include PB2 E627K, PB2 D9N, and PB1 V43I. When lysine is placed at the PB2 627 position in avian IAVs, it improves interaction with mammalian ANP32A and facilitates robust polymerase activity [33, 34]. The D9N mutation in PB1 can augment the production of mini viral RNAs and may have a role in reducing polymerase processivity and eliciting a heightened immune response [28]. The V43I change to PB1 confers increased fidelity [35]. The effect of coinfection dependence will be assayed by measuring the viral RNA replication of the mutant “test” virus given varying coinfection doses of a genetically tagged variant virus of the same genetic background. Comparison of the fold change in RNA

replication levels of the test virus template at the various doses will give insight as to which property or properties may influence coinfection dependence and will serve as an initial screen for mechanisms and strains which should be tested further by other assays. We will employ the same experimental technique with wildtype and variant pairs generated from the panel of H9N2 isolates. We will test an early H9N2 isolate, A/duck/Hong Kong/448/1978, a poultry isolate shortly following its introduction, A/quail/Hong Kong/1988, and a recent isolate from the same G1 lineage as GFHK99, A/chicken/Tunisia/12/2010. The use of these viruses will give insight as to whether the coinfection dependence seen with GFHK99 is generalizable to H9N2 viruses. Additionally, if the phenotype was developed following introduction to poultry, it may have relevance as an adaptive feature and could be investigated further by testing of other poultry viruses of other subtypes. The more recent 2010 isolate will address whether more contemporary G1 lineages viruses have retained the phenotype. Together, targeted mutations and the use of representative strains will reveal further information about the mechanism and epidemiology underlying the observed phenotype of coinfection dependence of GFHK99.

Both studies detailed in this work indicate that the viral polymerase is important in determining the frequency of reassortment and the fitness of reassortant viruses. In chapter two, we found that incompatibilities between the heterologous seasonal strains used in our studies showed the strongest pairwise relationships and the greatest fitness differences. Indeed, the phenotype of polymerase segment compatibility driving successful viruses in nature has been demonstrated by studies of IBV epidemiology [16, 36]. Specifically, multiple reassortment events have been observed for the distinct Victoria and Yamagata lineages of IBV. Phylogenetic data indicate that the IBV polymerase segments of the same lineage assort together, while the remaining five segments reassort randomly [16]. Molecular characterization of the chimeric

polymerase trimers derived from the two IBV lineages revealed fitness defects in viral polymerases which derived their components from heterologous lineages [36]. Thus, these molecular and epidemiological data together support functional compatibility of polymerase proteins as an important constraint of diversity produced through reassortment and the potential for such interactions to be identified on a population level. This finding and others have indicated that a phylogenetics powered approach could detect epistasis among circulating IAVs [13, 14, 37].

The viral strain and host differences observed with co-infection dependence indicate that the infectious dose and stringency of the transmission bottleneck could also vary with strain and species. The transmission of reassortant pH1N1/H3N2 viruses between guinea pigs indicates that the propagation of less fit genotypes may be achieved through collective spread with variants of higher fitness. Saira et al. suggest that IAV defective interfering particles, which lack one or more functional viral RNAs, may be transmissible and propagated in a subsequent host [38]. If indeed, less fit variants are transmitted and propagated by coinfection with virions contributing more fit viral components, a comparison of the transmission efficiency of the variant strain alone may not provide an accurate assessment if a variant can transmit in a population in nature. Additionally, as a variant is able to persist in a population, it may undergo mutation to acquire compensatory mutations or reassortment to produce a more fit genotype [39]. Indeed, such an event occurred in the seasonal H1N1 lineage. Initial detection of IAVs which contained a mutation which conferred resistance to the drug, oseltamivir, occurred in 1999. This specific mutation carried a fitness cost and did not become dominant in the population until 2007, when a compensatory mutation was acquired [40, 41]. In this case, a less fit variant was maintained in the viral population until the beneficial mutation could be attained. This finding supports that the

transmission and propagation of less fit or even nonfunctional variants does occur and is significant in natural infection of IAV. The frequency of minor variants present in a host and in a population should be evaluated using sequencing methods, such as deep sequencing, which could identify the presence of variants and the frequency of which variants are present in an IAV infected host [12, 42]. While the transmission of a group of strain variants is an established idea, the observed differences in coinfection dependence among hosts indicate that the processes which impact viral diversity, such as reassortment, may differ with host species and virus strain. In addition to host species differences in diversity of variants and spread, other factors, such as immune pressure should be investigated. For instance, animals raised for consumption, such as poultry and swine, are often present in large numbers of naïve members and may likely exert less immune pressure and thus support greater circulation and adaptation of diverse variants in their populations.

In its entirety, this work focuses on the factors and conditions which facilitate and constrain IAV diversification through collective interactions. Though reassortment is a means for increasing genetic diversity, its potential for producing genetic diversity is limited by the frequency with which it occurs and the fitness of the genotypes produced. The techniques and data analyses employed in the study of reassortment among homologous and heterologous human seasonal IAVs in chapter two highlighted the importance of functional segment mismatch. Clearly, interactions among segments can limit the number of viable genotypes arising from a coinfection. Though important functional mismatches, namely HA/NA balance and viral polymerase activity [7], have been identified in this study and others, predicting compatibility among, or even between IAV genes is often prohibitively complex [39]. More studies are needed to improve our capacity to detect and model epistatic interactions. The third

chapter of this work reveals that collective interactions among coinfecting viruses can enhance reassortment frequency and viral replication, and that the dependence of the virus on this cooperative interaction is determined through virus-host interactions. The mechanism underlying the need for collective interactions, and its epidemiological relevance will be explored in future studies. Both studies underline the importance of the viral polymerase for determining reassortment frequency and the fitness of reassortant viruses. The evolutionary implications of frequent collective interactions and host dependence should be further considered. Limitations to the transmission of viruses, including reassortant viruses, with fitness defects may be overcome due to collective interactions with more fit strains or variants in the transmitting population, particularly if the bottleneck for transmission is wide.

References

1. Ellis, J.S., et al., *Influenza AH1N2 viruses, United Kingdom, 2001-02 influenza season.* Emerg Infect Dis, 2003. **9**(3): p. 304-10.
2. Mizuta, K., et al., *A rare appearance of influenza A(H1N2) as a reassortant in a community such as Yamagata where A(H1N1) and A(H3N2) co-circulate.* Microbiol Immunol, 2003. **47**(5): p. 359-61.
3. Xu, X., et al., *Reassortment and evolution of current human influenza A and B viruses.* Virus Res, 2004. **103**(1-2): p. 55-60.
4. Baker, S.F., et al., *Influenza A and B virus intertypic reassortment through compatible viral packaging signals.* J Virol, 2014. **88**(18): p. 10778-91.
5. White, M.C., J. Steel, and A.C. Lowen, *Heterologous Packaging Signals on Segment 4, but Not Segment 6 or Segment 8, Limit Influenza A Virus Reassortment.* J Virol, 2017. **91**(11).
6. White, M.C., et al., *H5N8 and H7N9 packaging signals constrain HA reassortment with a seasonal H3N2 influenza A virus.* Proc Natl Acad Sci U S A, 2019.
7. White, M.C. and A.C. Lowen, *Implications of segment mismatch for influenza A virus evolution.* J Gen Virol, 2018. **99**(1): p. 3-16.
8. Nakatsu, S., et al., *Complete and Incomplete Genome Packaging of Influenza A and B Viruses.* MBio, 2016. **7**(5).
9. Brooke, C.B., et al., *Influenza A virus nucleoprotein selectively decreases neuraminidase gene-segment packaging while enhancing viral fitness and transmissibility.* Proc Natl Acad Sci U S A, 2014. **111**(47): p. 16854-9.
10. Gerber, M., et al., *Selective packaging of the influenza A genome and consequences for genetic reassortment.* Trends Microbiol, 2014. **22**(8): p. 446-55.
11. Morris, D.H., et al., *Predictive Modeling of Influenza Shows the Promise of Applied Evolutionary Biology.* Trends Microbiol, 2018. **26**(2): p. 102-118.
12. Barbezange, C., et al., *Seasonal Genetic Drift of Human Influenza A Virus Quasispecies Revealed by Deep Sequencing.* Front Microbiol, 2018. **9**: p. 2596.
13. Neverov, A.D., et al., *Coordinated Evolution of Influenza A Surface Proteins.* PLoS Genet, 2015. **11**(8): p. e1005404.
14. Fisher, K.J., S. Kryazhimskiy, and G.I. Lang, *Detecting genetic interactions using parallel evolution in experimental populations.* Philos Trans R Soc Lond B Biol Sci, 2019. **374**(1777): p. 20180237.
15. Rambaut, A., et al., *The genomic and epidemiological dynamics of human influenza A virus.* Nature, 2008. **453**(7195): p. 615-9.
16. Dudas, G., et al., *Reassortment between influenza B lineages and the emergence of a coadapted PB1-PB2-HA gene complex.* Mol Biol Evol, 2015. **32**(1): p. 162-72.
17. Doud, M.B. and J.D. Bloom, *Accurate Measurement of the Effects of All Amino-Acid Mutations on Influenza Hemagglutinin.* Viruses, 2016. **8**(6).
18. Lee, J.M., et al., *Deep mutational scanning of hemagglutinin helps predict evolutionary fates of human H3N2 influenza variants.* Proc Natl Acad Sci U S A, 2018. **115**(35): p. E8276-e8285.
19. Hom, N., et al., *Deep Mutational Scan of the Highly Conserved Influenza A Virus M1 Matrix Protein Reveals Substantial Intrinsic Mutational Tolerance.* J Virol, 2019. **93**(13).
20. Setoh, Y.X., et al., *Determinants of Zika virus host tropism uncovered by deep mutational scanning.* Nat Microbiol, 2019. **4**(5): p. 876-887.
21. Dingens, A.S., et al., *Comprehensive Mapping of HIV-1 Escape from a Broadly Neutralizing Antibody.* Cell Host Microbe, 2017. **21**(6): p. 777-787.e4.
22. Bloom, J.D., *Identification of positive selection in genes is greatly improved by using experimentally informed site-specific models.* Biol Direct, 2017. **12**(1): p. 1.

23. Fowler, D.M. and S. Fields, *Deep mutational scanning: a new style of protein science.* Nat Methods, 2014. **11**(8): p. 801-7.
24. Manz, B., et al., *Multiple Natural Substitutions in Avian Influenza A Virus PB2 Facilitate Efficient Replication in Human Cells.* J Virol, 2016. **90**(13): p. 5928-5938.
25. Danzy, S., et al., *Mutations to PB2 and NP proteins of an avian influenza virus combine to confer efficient growth in primary human respiratory cells.* J Virol, 2014. **88**(22): p. 13436-46.
26. Sediri, H., et al., *Adaptive mutation PB2 D701N promotes nuclear import of influenza vRNPs in mammalian cells.* Eur J Cell Biol, 2015. **94**(7-9): p. 368-74.
27. Pauly, M.D., M.C. Procario, and A.S. Lauring, *A novel twelve class fluctuation test reveals higher than expected mutation rates for influenza A viruses.* Elife, 2017. **6**.
28. Te Velthuis, A.J.W., et al., *Mini viral RNAs act as innate immune agonists during influenza virus infection.* Nat Microbiol, 2018. **3**(11): p. 1234-1242.
29. Choi, Y.K., et al., *Continuing evolution of H9N2 influenza viruses in Southeastern China.* J Virol, 2004. **78**(16): p. 8609-14.
30. Gu, M., et al., *Current situation of H9N2 subtype avian influenza in China.* Veterinary research, 2017. **48**(1): p. 49-49.
31. Guan, Y., et al., *Molecular characterization of H9N2 influenza viruses: were they the donors of the "internal" genes of H5N1 viruses in Hong Kong?* Proc Natl Acad Sci U S A, 1999. **96**(16): p. 9363-7.
32. Lam, T.T., et al., *The genesis and source of the H7N9 influenza viruses causing human infections in China.* Nature, 2013. **502**(7470): p. 241-4.
33. Long, J.S., et al., *Species difference in ANP32A underlies influenza A virus polymerase host restriction.* Nature, 2016. **529**(7584): p. 101-4.
34. Staller, E., et al., *ANP32 proteins are essential for influenza virus replication in human cells.* J Virol, 2019.
35. Cheung, P.P., et al., *Generation and characterization of influenza A viruses with altered polymerase fidelity.* Nat Commun, 2014. **5**: p. 4794.
36. Kim, J.I., et al., *Reassortment compatibility between PB1, PB2, and HA genes of the two influenza B virus lineages in mammalian cells.* Sci Rep, 2016. **6**: p. 27480.
37. Dolan, P.T., Z.J. Whitfield, and R. Andino, *Mapping the Evolutionary Potential of RNA Viruses.* Cell Host Microbe, 2018. **23**(4): p. 435-446.
38. Saira, K., et al., *Sequence analysis of in vivo defective interfering-like RNA of influenza A H1N1 pandemic virus.* Journal of virology, 2013. **87**(14): p. 8064-8074.
39. Lyons, D.M. and A.S. Lauring, *Mutation and Epistasis in Influenza Virus Evolution.* Viruses, 2018. **10**(8).
40. Duan, S., et al., *Epistatic interactions between neuraminidase mutations facilitated the emergence of the oseltamivir-resistant H1N1 influenza viruses.* Nat Commun, 2014. **5**: p. 5029.
41. Bloom, J.D., L.I. Gong, and D. Baltimore, *Permissive secondary mutations enable the evolution of influenza oseltamivir resistance.* Science, 2010. **328**(5983): p. 1272-5.
42. Diaz-Munoz, S.L., *Uncovering Virus-Virus Interactions by Unifying Approaches and Harnessing High-Throughput Tools.* mSystems, 2019. **4**(3).